UNIVERSITY OF
KWAZULU-NATAL

INYUVESI
YAKWAZULU-NATALI

Fusaric Acid Induces Oxidative Stress and Apoptosis in Human Oesophageal Cancer Cells

By

Nikita Devnarain

B. Sc. B. Med. Sc. (Hons) (UKZN)

Submitted in fulfilment of the requirements for the degree of MMedSci. in the Discipline of

Medical Biochemistry and Chemical Pathology

School of Laboratory Medicine and Medical Sciences

College of Health Sciences

Durban

2016

DECLARATION

I, Miss N Devnarain, declare as follows:

1. That the work described in this dissertation contains the original work by the author and has not been submitted in any form to UKZN or other tertiary institution for purposes of obtaining an academic qualification, whether by myself or any other party. The use of work by others has been duly acknowledged in the text.

2. That my contribution to the project was as follows:
   I have personally conducted all assays in the laboratory regarding this project. Analysis and interpretation of all raw data, capturing of images and presentation of all data were conducted by myself. Apart from this dissertation, I also composed a manuscript reporting this data for publication purposes.

3. That the contribution of others to the project were as follows:
   - Under the supervision of Prof Anil A. Chuturgoon, I was given constructive criticism and guidance with writing as well as presenting this study. Not only did Prof Anil A. Chuturgoon contribute significantly to the idea of this study, he also provided intellectual assistance and edited the dissertation, as well as the manuscript.

   - Dr Charlette Tiloke and Dr Savania Nagiah were co-supervisors of this study. They approved all experiments in advance and data post lab work. They assisted me writing up and editing of this dissertation. They also helped me compose the manuscript reporting this study for publication purposes and assisted me with presenting the work at conferences.

Signed  Date 14 February 2017

DEDICATION

I would like to dedicate this thesis to those special in my life whom I've loved, and lost. To my **Father**, Rajen Subesh Devnarain (30/12/1960 – 29/08/2015); my **Dada**, Aniruth Andy Devnarain (28/11/1948 - 05/04/2015); my **Brother**, Rishi Raj Devnarain (23/07/1978 - 04/03/2011); and my **Uncle**, Ishwarlal Maharaj (22/07/1948 - 07/10/2015). You all gave me support, courage and blessings my entire life. As I remind myself of how proud you'll always were of me, I gain the strength to go on, to make a name for myself… I miss you all dearly, and will cherish your memories and carry your blessings always.

Jai Durga Maa

ACKNOWLEDGEMENTS

My Mother

Having you for a mother was the best beginning life could've given me. I couldn't have gotten this far in life, having achieved so much, without your love and unfailing support. My passion to study became yours. You gave me motivation to go further as you nurtured me through my late nights of studying. You've sacrificed a lot for me to gain my accomplishments, and no matter where I go in life, I will never forget that. I love you, ma.

Professor Anil A. Chuturgoon

Einstein said, 'It is the supreme art of the teacher to awaken joy in creative expression and knowledge'. I want to thank you, Prof, for all the wisdom, guidance and knowledge you've bestowed upon me throughout these years. I would also like to thank you for the opportunities you've given to me and the motivation to make my discoveries in the lab known to the world. Thank you for inspiring me and making me a confident scientist.

Dr Charlette Tiloke

I am so grateful to you for everything you have taught me, all your guidance, supervision and patience over these two years. Thank you for consistently reminding me that it would all be worth it in the end.

Dr Savania Nagiah

Thank you for always reminding me that it's only human to make mistakes, and thank you more for correcting me and letting me find myself in the lab.

Ms Rene B. Myburg

I could never thank you enough for being my pillar of strength, but most of all, more like family. I will never forget that you taught me to love science for what it is.

Shaylen

You've had more faith in me than I've had in myself. Thank you for being my best friend, and thank you even more for handling the perks that came with it. You understood when I had a bad day in the lab and listened without judgement… you were my number one fan at the beginning and end of every achievement. Thank you from the bottom of my nerdy heart.

Med Sci Medical Biochemistry Masters Class of 2015/2016

I could never have asked for a better class of intellectually gifted and amazing friends to share my studying career with. I would like to thank you for all the laughter and for sharing the responsibilities of all the rewarding, as well as the tough times. Miss Letitia Shunmugam, Miss Pritika Ramharack, Mr Naeem Sheik Abdul, Miss Terisha Ghazi, Miss Denelle Moodley, Miss Shanel Dhani and Miss Taskeen Dockrat, you guys are like the acrylamide in my gels…dangerous to mental health, but who've stuck with me and made my postgraduate years unforgettable. I will always cherish the memories we've made, as they say…friends who eat together (and western blot together), stay together.

Friends and loved ones

To my sisters, and the rest of my family and friends, I want to thank you for the support.

Department of Medical Biochemistry

I would like to thank everyone in our department for their assistance, patience and support over the years. Especially, Miss Samantha M. Anderson for all your technical assistance.

University of KwaZulu-Natal College of Health Sciences and National Research Foundation

Thank you for financially supporting me and providing laboratory expenses as a postgraduate student.

PUBLICATION

Devnarain, Nikita, Charlette Tiloke, Savania Nagiah, and Anil A. Chuturgoon. (2017). Fusaric acid induces oxidative stress and apoptosis in human cancerous oesophageal SNO cells. *Toxicon* 126: 4-11. http://dx.doi.org/10.1016/j.toxicon.2016.12.006 (Appendix H).

PRESENTATIONS

Fusaric Acid Induces Oxidative Stress and Apoptosis in Human Oesophageal Cancer Cells.

N. Devnarain, C. Tiloke, S. Nagiah and A.A. Chuturgoon.

UKZN School of Laboratory Medicine and Medical Science Research Day (August 2016), Durban, South Africa.

Fusaric Acid Induces Oxidative Stress and Apoptosis in Human Oesophageal Cancer Cells.

N. Devnarain, C. Tiloke, S. Nagiah and A.A. Chuturgoon.

UKZN College of Health Science Research Symposium (September 2016), Durban, South Africa.

TABLE OF CONTENTS

LIST OF ABBREVIATIONS

Ab	Antibody
ADP	Adenosine diphosphate
AIF	Apoptosis inducing factor
Apaf-1	Apoptotic-protease-activating-factor-1
APS	Ammonium persulphate
ATP	Adenosine triphosphate
Bax	Bcl-2-associated X
BCA	Bicinchoninic acid
Bcl-2	B-cell lymphoma/leukemia-2
BH	Bcl-2 homology
BHT	Butylated hydroxytoluene
Bid	BH3 interacting-domain death agonist
BIR	Baculovirus inhibitor of apoptosis repeat
BSA	Bovine serum albumin
Ca (Ca^{2+})	Calcium
CAT	Catalase
CCM	Complete culture medium
Cd (Cd^{2+})	Cadmium
c-IAP	Cellular inhibitor of apoptosis protein
CO_2	Carbon dioxide
CoQ	Coenzyme Q
Cu (Cu^{2+})	Copper (Cupric ion)
dH_2O	De-ionised water
DISC	Death inducing signalling complex
DMSO	Dimethyl sulphoxide
DNA	Deoxymethylribose nucleic acid
ds	Double stranded
ECL	Enhanced chemiluminescence
EDTA	Ethylenediaminetetraacetic acid
ELISA	Enzyme-linked immunosorbent assay
EMEM	Eagle's minimum essential medium

ER	Endoplasmic reticulum
ETC	Electron transport chain
FA	Fusaric acid (5-n-butyl-pyridine-2-carboxylic acid)
FADD	Fas associated protein with death domain
$FADH_2$	Flavin adenine dinucleotide hydroquinone
FasL	Fas ligand
FCS	Foetal calf serum
GERD	Gastroesophageal reflux disease
GPx	Glutathione peroxidase
GSH	Reduced glutathione
GSSG	Oxidised glutathione
GST	GSH-S-transferase
H^+	Hydrogen ion/ proton
H_2O_2	Hydrogen peroxide
H_3PO_4	Phosphoric acid
HCl	Hydrochloric acid
$HO_2^{\bullet}$	Hydroperoxyl radical
HOCl	Hypochlorous acid
HRP	Horseradish peroxidase
IAP	Inhibitor of apoptosis protein
IBM	IAP-binding motif
IC_{50}	Median Inhibition Concentration
IMM	Inner mitochondrial membrane
IMS	Intermembrane space
INT	Iodonitrotetrazolium
kDa	Kilodalton
LDH	Lactate dehydrogenase
LMPA	Low melting point agarose
MDA	Malondialdehyde
mt	Mitochondrial
MPTP	Mitochondrial permeability transition pore
MTT	3-(4,5-Dimethyl-2-thiazolyl)-2,5-diphenyl-2H-tetrazolium bromide

NaCl	Sodium chloride
NAD (NAD^+)	Nicotinamide adenine dinucleotide
NADH	Nicotinamide adenine dinucleotide hydride (reduced)
NADPH	Nicotinamide adenine dinucleotide phosphate (reduced)
NaOH	Sodium hydroxide
Ni (Ni^{2+})	Nickel
NIAP	Normal-molecular-weight IAP
$^{\bullet}OH$	Hydroxyl radical
$O_2^{\bullet-}$	Primary superoxide anion radical
OC	Oesophageal cancer
OD	Optical density
OMM	Outer mitochondrial membrane
PA	Picolinic acid
PARP-1	Poly (ADP-ribose) polymerase-1
Pb (Pb^{2+})	Lead
PBS	Phosphate buffer saline
PFA	Paraformaldehyde
PSF	Penicillin-streptomycin-fungizone
RBD	Relative band density
RLU	Relative light unit
RNS	Reactive nitrogen species
$RO_2^{\bullet}$	Peroxyl radical
ROS	Reactive oxygen species
RT	Room temperature
SCC	Squamous cell carcinoma
SCGE	Single cell gel electrophoresis
SD	Standard deviation
SDS-PAGE	Sodium dodecyl sulphate - polyacrylamide gel electrophoresis
Smac/DIABLO	Second mitochondria-derived activator of caspases/DIABLO
SNO	Spindle-shaped N-cadherin (+) CD45 (-) osteoblastic
SOD	Superoxide dismutase
TBA	Thiobarbituric Acid

TBARS	Thiobarbituric Acid Reactive Substances
TCA	Tricarboxylic acid
TEMED	Tetramethylene diamine
TNF-α	Tumour necrosis factor-α
TNF-R1	Tumour necrosis factor receptor-1
TRAIL-R	Tumour necrosis factor related apoptosis inducing ligand receptors
TTBS	Tris-buffered saline containing 0.5% Tween20
VDAC	Voltage-dependent anion channel
XIAP	X-linked mammalian inhibitor of apoptosis protein
Zn (Zn^{2+})	Zinc

LIST OF FIGURES

LIST OF TABLES

ABSTRACT

Background/Aims: The incidence of oesophageal cancer (OC) is a worldwide problem and is incremental among black South African males. The high prevalence of OC may be due to the consumption of maize as a staple, often contaminated with mycotoxins. Fusaric acid (FA), a neglected mycotoxin, was first isolated from *Fusarium heterosporum* and a major contaminant of maize. FA is known to disrupt mitochondrial energy metabolism, chelate divalent metal cations, induce cell death in plants, and has been suggested as an aetiological agent of OC. However, the mechanism by which FA causes cytotoxicity in oesophageal cells has not been conclusively elucidated. This study investigated FA-induced cytotoxicity and apoptotic induction in the SNO OC cell line.

Methods: SNO cells were treated with a range of FA concentrations (0-500 µg/ml) over 24 h and an IC_{50} was obtained using the MTT assay. The cells were assayed for oxidative stress and membrane damage (TBARS, LDH cytotoxicity and glutathione), apoptotic induction (ATP levels, caspase-8, -9, -3/7 activities) (Luminometry), single strand DNA and nuclear fragmentation (Comet and Hoechst assay). Additionally, relative expression of pro- and anti-apoptotic proteins were determined using Western Blotting.

Results: An IC_{50} of 78.81 µg/ml FA was obtained. Significant antioxidant (glutathione) depletion (1.62-fold, $p < 0.0001$) was consistent with a concomitant increase in reactive oxygen species (ROS)-induced lipid peroxidation (1.23-fold, $p < 0.05$) and extracellular LDH levels (1.15-fold, $p < 0.005$). FA induced apoptosis by significantly increasing Bax expression (1.08-fold, $p < 0.05$) and caspase-8, -9 and -3/7 activities ($p < 0.05$) whilst decreasing ATP levels (1.16-fold, $p < 0.05$) and Bcl-2 expression (1.24-fold, $p < 0.05$). Further, FA significantly increased comet tail lengths ($p < 0.0001$), PARP-1 cleavage (1.53-fold, $p < 0.05$) and late stage apoptotic body formation in SNO cells.

Conclusion: FA induced oxidative stress by increasing the level of ROS-induced lipid peroxidation resulting in membrane damage and concomitantly reducing antioxidant response, Disruption of mitochondrial activity was associated with low ATP levels. Collectively, these events triggered the caspase-cascade which compromised DNA integrity and averted its repair, leading to cell death via intrinsic and extrinsic apoptosis. Taken together, FA is a cytotoxic agent to human oesophageal SNO cells.

CHAPTER 1

1.1 Introduction

Oesophageal cancer (OC) is a globally prominent disease and ranks as the sixth most common cause of cancer-related deaths worldwide and the second most prevalent cancer among black South African men (Siegel *et al.*, 2016). The increasing incidence of OC may be attributed to a number of aetiological factors including dietary deficiencies (low consumption of fruits and vegetables), drinking very hot liquids, family history, age, achalasia, poor oral hygiene, having gastroesophageal reflux disease (GERD) and tylosis (Bravi *et al.*, 2012, Dar *et al.*, 2013, Ballo and Millikan, 2015). These factors also include an increase in cancer-causing behaviours, particularly excessive smoking, alcohol consumption and consumption of foods contaminated with fungi (Nedělník, 2002, Ballo and Millikan, 2015).

Since the oesophagus is the second organ in the digestive tract, the oesophagus becomes highly susceptible to exposure to contaminated food which may be carcinogenic. Maize, the staple food of many developing countries, including South Africa, is susceptible to fungal contamination, that produce carcinogenic mycotoxins such as fumonisin B_1 (Mqoco and Marais, 2010). In South Africa, rural populations rely on subsistence farming. The harvested crops are poorly stored and are susceptible to fungal contamination and proliferation. Contaminated maize is normally ground into flour and used as a staple. However, heavily contaminated maize is used to prepare traditional home made beer. This beer is consumed mainly by South African black men, further exposing them to a potent mycotoxin cocktail that contains alcohol. It has been shown that home brewed beers contain many carcinogens (Cousin *et al*., 2005) and this may explain the high incidence of OC in black South African men residing in rural areas.

Mycotoxin contamination of maize is a global problem (Surai *et al.*, 2008). Over the past decade, mycotoxins have been implicated as cytotoxic agents in certain types of cancers (Wang *et al.*, 2007, Oda *et al.*, 2010). Mycotoxins are fungal metabolites known to elicit various effects in humans. Fusaric acid (FA, 5-butylpicolinic acid), isolated from the fungus *Fusarium heterosporum,* is referred to as a 'neglected' mycotoxin since there is limited literature regarding the effects of FA on animals and humans (Nedělník, 2002).

Fusaric acid contains a butyl aliphatic side chain which accentuates its lipophilic properties to freely penetrate cell membranes and cause membrane damage (Fernández-Pol, 1998). Since FA is a metabolite of picolinic acid and tryptophan, FA contains a pyridine ring which allows chelation of divalent metal cations. Chelation would disrupt cellular processes which require those cations (Gäumann, 1958). Being a weak acid, FA is able to carry protons across the inner mitochondrial (mt) membrane thus destroying the proton gradient across the membrane. This process is termed "uncoupling" and hence FA is known as an oxidative phosphorylation uncoupler (Bachmann, 1956).

Membrane disruption and the inhibition of oxidative phosphorylation by FA (Telles-Pupulin *et al.*, 1998) will contribute to a highly oxidative environment (Sies, 1985, Sies, 2015), which if sustained results in cell death (Circu and Aw, 2010). Prior studies have demonstrated suppressive effects of FA on cell survival rates, and DNA damage promoting effects in laryngeal cancer (Hep2) and squamous epithelial cells (Ye *et al.*, 2013, Stack *et al.*, 2014), however cytotoxicity and cell death were observed in hepatocellular carcinoma ($HepG_2$) cells (Sheik Abdul *et al.*, 2016). Several studies also showed that FA caused cell death and oxidative

stress in plants (Jiao *et al.*, 2014, Singh and Upadhyay, 2014). In this study, we investigated the cytotoxic effects of FA in the SNO cell line after 24 hour (h) acute exposure.

1.2 Aim & Objectives

The ***null hypothesis*** of this study states that FA has no effect on SNO cells subsequent to acute exposure (24 h).

The ***aim*** of this study was:

> To determine the cytotoxic effects of FA on the SNO cell line by measuring expression and activities of various cellular molecules following an acute exposure period (24 h).

The ***objectives*** of this study were to investigate the effects of FA after 24 h in SNO cells on:

- Cellular viability and metabolic activity using the MTT assay.
- Oxidative capacity of the cell using the TBARS assay to determine the extent of reactive oxygen species (ROS)-induced lipid peroxidation [malondialdehyde (MDA) generation] and GSH assay to determine the antioxidant response.
- Cell and mt membrane integrity using the lactate dehydrogenase (LDH) cytotoxicity detection assay and quantification of intracellular ATP levels (determine the activity of the ATPase complex).
- The induction/inhibition of the apoptotic pathway using western blotting to determine expression of pro- and anti-apoptotic proteins (Bax, Smac/DIABLO, Bcl-2) and measuring caspase-3/7, -8 and -9 activities.
- DNA integrity and cellular and nuclear morphology using the Hoechst staining assay, the comet assay, and western blotting to measure the expression of the activated fragment of the DNA repair enzyme, Poly (ADP-ribose) polymerase-1 (PARP-1).

Experimental approach:

> The human oesophageal cancer SNO cell line was utilised as a toxicity model to investigate the effects of FA. Cells were exposed to various concentrations of FA over a 24 h period to determine metabolic output and cell viability. This yielded a concentration of FA that produced half the maximum inhibition (IC_{50}). This concentration was used to test the effects of FA on various molecular features of the cell.

1.3 Literature Review

1.3.1 Cancer

Carcinogens cause normal cells to mutate, leading to uncontrollable proliferation of these abnormal cells which evade programmed cell death i.e. apoptosis. This uncontrolled cell growth is known as cancer. Cancer cells may be benign (inactive) or malignant (active) (Evan and Vousden, 2001). Cancer causing agents are represented in Figure 1.1.

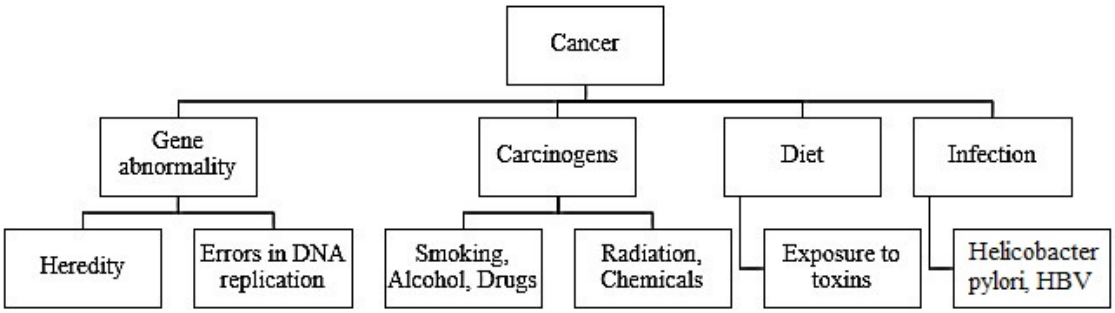

Figure 1.1: Cancer causing agents. Cancer can evolve due to various factors, which include abnormalities in gene material, carcinogen exposure, dietary exposure to toxins including mycotoxins, and infections due to viruses, bacteria and parasites (Prepared by Author).

Carcinogenesis is the process which a normal cell undergoes to ultimately become a cancer cell. There are three stages associated with carcinogenesis: initiation, promotion and progression (Pitot, 1993). Initiation occurs due to irreversible gene mutation: transition, deletion or transversion. Promotion involves reversible alterations in gene expression. This stage does not involve structural alterations of DNA, but rather promoter-receptor interactions which modify downstream gene expression. Progression involves malignant cell proliferation and irreversible chromosomal instability. This stage is characterised by an ongoing development of chromosomal abnormalities leading to independent characteristics, such as metastatic growth, invasion and anaplasia (loss of cellular orientation and differentiation) (Pitot, 1993).

The main types of genes affected by variations induced by carcinogenesis are tumour suppressor genes, cellular oncogenes and proto-oncogenes. Mutation of tumour suppressor genes, such as DNA repair gene p53, results in change in or loss of function so that its tumour supressing activity is altered. Cellular oncogenes are mutated or overexpressed genes in cancer cells. Proto-oncogenes are the normal genes as compared to oncogenes which stimulate cell cycle and regulate proliferation (Oliveira *et al.*, 2007).

The distinguishing characteristics of cancer include: evasion of immune destruction and suppressors of tumours; stimulation of metastasis, angiogenesis, invasion and infinite ability to replicate; sustained signals for division; apoptotic resistance and enhanced energy production. Inflammation aggravates these hallmarks, eventually compromising genome stability and encouraging genetic variation. These hallmarks promote cancer cell survival, among other factors, which include decreased cell adhesion and thereby decreased communication between cells, and protease secretion such as serine proteases and metalloproteases (Hanahan and Weinberg, 2011).

Treatments for cancer include radiation and chemotherapy, as well as surgical removal of tumours. Chemotherapy involves introducing chemicals to the bloodstream to target tumours that have metastasised (migration of cancer cells to new sites in the body). Radiation therapy involves using laser beams to target tumours. These treatments are harsh and have serious side effects which include destruction of normal cells, suppression of the immune system, nausea, fatigue, loss of hair, damage to skin and drug resistance (Gerber, 2008).

1.3.1.1 Oesophageal cancer

Oesophageal cancer remains one of the most deadly cancers worldwide. It is the 8th most common cancer throughout the world, and the 6th most prevalent cause of cancer-related deaths worldwide. Oesophageal cancer is also the 2nd most frequent cancer among South African men, being 8 times more common in men than women. Oesophageal cancer has a low 5 year survival rate of only 10% and is also one of the least studied cancers (Ballo and Millikan, 2015).

Oesophageal cancers have poor prognosis with early local invasion to the lymphatic system. Early symptoms of oesophageal cancer (weight loss and dysphagia) generally go unnoticed, hence, oesophageal cancer is generally diagnosed at an advanced stage. Other symptoms include retrosternal pains, food/saliva regurgitation, blood loss causing anaemia, coughing and pneumonias (Ballo and Millikan, 2015).

The two main types of oesophageal cancer include adenocarcinoma from Barrett's oesophagus and squamous cell carcinoma (SCC). The risk factors for SCC include smoking, foods containing N-nitroso compounds, alcohol abuse, achalasia, drinking hot liquids, history of corrosive childhood oesophageal injury and tylosis. A risk factor for adenocarcinoma is intestinal metaplasia due to established gastroesophageal reflux disease (GERD). The oesophagus is highly susceptible to the effects of toxins due to maximum exposure via ingestion of toxin-contaminated foodstuffs (Ballo and Millikan, 2015).

Oesophageal cancer is treated mainly via surgical removal. Other treatments include: neoadjuvant (preoperative) chemotherapy which involves shrinkage of the primary tumour and killing of the micrometastases in local and systemic nodes; radiation therapy; and palliative therapy to improve symptoms and comfort while reducing illness and hospital stay (laser therapy, stenting, oesophageal dilations and brachytherapy) (Shahbaz Sarwar *et al.*, 2010, Ballo and Millikan, 2015).

1.3.1.2 SNO cell line

SNO (spindle-shaped N-cadherin (+) CD45 (-) osteoblastic) cells are human oesophageal epithelial carcinoma cells. The SNO cell line was initially derived from a well-differentiated squamous cell carcinoma (6.5 cm in length, metastatic to lymph nodes) explanted from a 62-year old Zulu African male (Patient S. N.) in July 1972. SNO cells are non-keratinising cells that express a variety of apoptotic genes which code for many proteins. These cells grow as an adherent monolayer and rapidly invade surrounding tissue since the oesophageal outer surface lacks a serous membrane. Hence, SNO cells are suitable as a transfection host and a good model for toxicity testing (Bey *et al.*, 1976).

1.3.2 Mycotoxins

At least 300 mycotoxins exist in nature and are naturally produced as secondary metabolites by fungi. The most economically significant types of fungi that produce mycotoxins are *Fusarium*, *Penicillium* and *Aspergillus*. Mycotoxins are low molecular mass molecules that can be highly toxic even at very low concentrations. Some can interfere with membrane integrity, as this cytotoxic effect aids their mycological pathogenicity, or for self-defence purposes (Surai *et al.*, 2008).

The toxicity of mycotoxins in humans depends on various factors, including the membrane-active properties, type, level and duration of exposure of the mycotoxin. Host factors such as age, gender, health, dietary status and genetics of exposed individual; and other mycotoxin interactions also determine toxicity (Omar, 2013). Different mycotoxins may affect various cellular processes, e.g. nucleic acid synthesis, protein synthesis, lipid synthesis, DNA adduct formation, pro-apoptotic activity and alteration of gene expression. Essentially, molecular mechanisms of mycotoxin associated toxicity include alteration of membrane structure and induction of apoptosis, oxidative stress and lipid peroxidation which result in functional alterations in growth, development and reproduction (Surai *et al.*, 2008).

A major mode of mycotoxin toxicity is via ingestion of agricultural produce that has been contaminated with fungi producing mycotoxins (Pal *et al.*, 2015). Mycotoxin contamination of grain is influenced by moisture levels (ought to be <15%) and stress due to drought. *Fusarium* mycotoxins contaminate most cereal grains (Surai *et al.*, 2008).

1.3.2.1 Fusaric acid

Fusaric acid (5-n-butyl-pyridine-2-carboxylic acid) (FA) is a mycotoxin produced by *Fusarium heterosporum* and other *Fusarium* species. This mycotoxin was initially discovered by Yabuta *et al*. (Yabuta *et al.*, 1937) as a low to moderately toxic mycotoxin that is found in maize, wheat, oats, rye and barley. FA is synergistic with other mycotoxins including Fumonisin B_1, and can enhance the global toxic effects of other mycotoxins. FA was reported to have a mean concentration of 643 µg/kg in feed samples (Streit *et al.*, 2013) and may perhaps be amongst the most extensively distributed mycotoxins produced by *Fusarium* species in agricultural commodities (Bacon *et al.*, 1996).

Fusaric acid is a metabolite of picolinic acid (PA), which is catabolised from L-tryptophan and contains a pyridine ring. This feature allows PA to affect the synthesis of nicotinamide adenine dinucleotide (NAD^+) since PA is an isomer of nicotinic acid, and allows it to chelate divalent metal cations such as zinc (Zn^{2+}), nickel (Ni^{2+}), lead (Pb^{2+}) and cadmium (Cd^{2+}). The pyridine ring along with its substituent carboxyl group is also present in FA, and maintains its chelation properties. However, FA contains a lipophilic butyl aliphatic side chain in position five which PA lacks (Fernández-Pol, 1998, Ogata *et al.*, 2001).

Picolinic acid synthesis occurs via the kynurenine pathway which involves the catabolism of tryptophan to produce NAD, PA and kynurenic acid. PA elicits several effects in the human body. It has especially been involved in antimicrobial activity and improved immune function. PA has shown to positively affect normal, healthy cells, and induce apoptosis of microbacterial-infected cells, reduce viral replication and has also been effective in killing lymphoma cells in rats. Cytotoxicity of PA is attributable to its activity as a chelating agent (Fernández-Pol, 1998, Ogata *et al.*, 2001, Grant *et al.*, 2009).

Since FA is a weak acid, it functions as a proton (H^+) carrier and can affect the polarity of membranes by dissipating the mt membrane proton gradient and uncoupling the electron transport chain from oxidative phosphorylation. The effect of FA on mt membranes in particular compromises ATP production. FA inhibits succinate dehydrogenase and α-ketoglutarate dehydrogenase in the Krebs TCA cycle, which require H^+ ions to form $FADH_2$ and NADH, respectively. It also inhibits oxidative phosphorylation via direct inhibition of ATPase or via inhibition of the ADP/ATP transport system. In this way, FA inhibits mt energy metabolism, leading to reduced cell viability and cell death. Since FA inhibits mt energy metabolism, all cell processes that are dependent on ATP are compromised (Telles-Pupulin *et al.*, 1998).

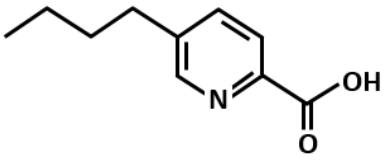

Figure 1.2: Fusaric Acid. Molecular structure of FA showing the butyl group (4C), pyridine ring (C_5H_5N) and carboxyl group (COOH) (Prepared by Author).

The pyridine ring of FA (Figure 1.2) allows it to form chelate rings by sequestering divalent metal cations between the N atom of the pyridine ring and the carboxyl radical in the α-position, creating a five-membered direct link (Gäumann, 1958). The pyridine ring of FA also inhibits oxidative phosphorylation (Bachmann, 1956) and induces DNA damage via chelation of divalent metal cations from catalytic DNA-associated metalloproteins, preventing DNA repair and synthesis (Stack *et al.*, 2004). The n-butyl aliphatic side chain in the β-position of FA accentuates its lipophilic properties, increasing its permeability to allow effortless penetration through cell membranes (Fernández-Pol, 1998). The lipophilic tail of FA also impairs cytochrome *c* oxidase activity, thereby uncoupling the electron transport chain (ETC) from ATP synthesis (Gäumann, 1958).

Many of the metal cations chelated by FA are cofactors of enzymes required for normal cellular processes, FA thereby inhibits the functioning of certain enzymes via deprivation of these cations (Fernández-Pol, 1998). Furthermore, divalent cations contribute to membrane integrity by stabilising the ordered state of membranes. Divalent cations react with negatively charged phospholipids in membranes which are essential for natural processes such as signal transduction (Träuble and Eibl, 1974). Divalent ions also inhibit permeability changes in membranes by blocking leakage at the site of lesion formation subsequent to binding of toxins to cells. Calcium (Ca^{2+}) and Zn^{2+} are heavily involved in this inhibition and are known membrane protective agents. FA thereby disrupts membranes and prevents normal processes from occurring by chelating divalent cations (Bashford *et al.*, 1986).

FA has many primary and secondary effects in the human host. FA inhibits tyrosine hydroxylase and dopamine β-hydroxylase, which result in elevated levels of serum melatonin, tyrosine, dopamine and 5-hydroxytrypamine. FA induces peripheral arteriolar dilation which causes peripheral vascular resistance and consequential antihypertensive effects (Voss *et al.*, 1999).

1.3.3 Oxidative stress

Oxidative stress was first described by Sies as "an imbalance between oxidants and antioxidants in favour of the oxidants, leading to a disruption of redox signalling and control and/or molecular damage" (Sies, 1985). Oxidants (a class of free radicals), are highly reactive species which contain one or more unpaired valence electrons and are capable of independent existence. The free valence electrons "steal" their electrons from neighbouring molecules, causing oxidation to cellular macromolecules. Oxidation causes structural and functional alterations to nucleic acids, proteins, carbohydrates and DNA which result in lipid peroxidation, oxidation of amino acids in proteins, DNA mutations and loss of enzyme function via oxidation of cofactors. Free radicals comprise of ROS and reactive nitrogen species (RNS). Normal, healthy cells neutralise toxic levels of ROS through decomposition via antioxidants (Kelly, 2003, Ježek and Hlavatá, 2005).

1.3.3.1 Reactive oxygen species (ROS)

ROS are chemically reactive molecules or ions that form due to incomplete one-electron reduction of oxygen (Pan *et al.*, 2009). Intermediates of ROS include singlet oxygen, hydrogen peroxide (H_2O_2), hypochlorous acid (HOCl), fatty acid hydroperoxides, reactive aldehydes, hydroperoxyl radical ($HO_2^{\bullet}$), primary superoxide anion radical ($O_2^{\bullet-}$), hydroxyl radical ($^{\bullet}OH$), peroxyl radical ($RO_2^{\bullet}$), carbonate radical ($CO_3^{\bullet-}$) and alkoxyl radical ($RO^{\bullet}$) (Ježek and Hlavatá, 2005, Pan *et al.*, 2009).

ROS are natural by-products of various natural cellular processes, especially respiration in mitochondria. They are necessary for normal physiological functions to occur, such as apoptosis, cell signalling and cellular immunity (Ježek and Hlavatá, 2005). Other processes include one-carbon oxygen reduction during the process of aerobic respiration which yield hydroxyl and superoxide radicals; activated phagocytes produce HOCl and $O_2^{\bullet-}$ (oxidative burst), certain cells and vascular endothelium produce nitric oxide. ROS are also by-products of biochemical processes such as the arachidonic acid cascade activation and catecholamine oxidation produce electrons which are capable of reducing molecular oxygen to superoxide anion (Betteridge, 2000). Exogenous sources of ROS include pollutants, smoke, drugs, toxins and radiation, like gamma rays, which form hydroxyl radicals from the separation of water (Betteridge, 2000, Pan *et al.*, 2009).

Free radical attack on lipid components of the cell leads to lipid peroxidation (oxidation of polyunsaturated fatty acids in lipids). Some free radicals, such as the hydroxyl radical, can react with a hydrogen atom (H) from the methylene bridge (CH_2) of fatty acids, resulting in a carbon with an unpaired electron (CH). Polyunsaturated fatty acids are highly susceptible to free radical attack due to the presence of the double bond in the methylene bridge which weakens the C-H bond at the neighbouring carbon atom. The resultant radical becomes rearranged forming a conjugated diene, which has the capacity to conjugate with oxygen to produce a peroxyl radical. This peroxyl radical forms a free radical chain reaction mechanism by interacting with an adjacent H. This reaction goes on until substrate consumption occurs, or termination via an antioxidant like vitamin E which breaks the chain reaction. Extensive lipid peroxidation of cell membranes alters membrane fluidity, causes increased permeability, decreased membrane potential, and ultimately rupture of the membrane (Betteridge, 2000).

Free radicals oxidise DNA to form single-/double-strand breaks and mutations (Betteridge, 2000). A major free radical that causes biomolecule damage is the hydroxyl radical. When the

hydroxyl radical is produced near DNA, it interacts with nucleotide bases of DNA causing the addition of new DNA bases resulting in variation of oxidation products, for example, guanine is converted to C8-hydroxyguanine (8-OHGua) or its oxidised nucleoside form 7,8-dihydro-8-oxo-2`-deoxyguanosine (8-oxodG) (Kasai, 1997). Another product of oxidative DNA damage is thymine glycol (5,6-dihydroxydihydrothymine), an oxidative mutagen produced via ionising radiation or chemical oxidation (Cathcart *et al.*, 1984). Along with nuclear DNA, mt DNA is highly susceptible to oxidative damage by free radicals. This is due to the close proximity of mt DNA to the ETC in the mitochondria since ROS are abundantly produced in the ETC, and mt DNA contain fewer introns and lack histones which serve to protect against and repair oxidative base lesions (Circu and Aw, 2010). Along with reduced protection, reduced fidelity of replication by mt-specific DNA polymerase γ contribute to faster accumulation of mt DNA mutations than nuclear DNA (Qian *et al.*, 2014).

Free radicals cause protein damage via crosslinking or conjugation of carbonyl groups to amino acid residues to from carbonyl derivatives or fragmentation. Carbonyl derivatives make the protein prone to proteolysis (Dalle-Donne *et al.*, 2003). The R groups of amino acid residues of proteins, especially methionine and cysteine residues are susceptible to ROS/RNS oxidation (Stadtman, 2004).

1.3.3.2 Antioxidant response

Due to the potential of ROS-associated toxicity in tissue, cells have developed protective antioxidant defence mechanisms. Antioxidants were described by Gutteridge (1995) as "any substance that, when present at low concentrations, compared with those of the oxidisable substrate, considerably delays or inhibits oxidation of the substrate" (Gutteridge, 1995).

Antioxidant defences are categorised as cellular (catalase (CAT), dismutase and peroxidase enzymes), extracellular and membrane mechanisms (Gutteridge, 1995). Superoxide dismutase (SOD) (localised in the cytoplasm contains copper (Cu) and Zn, whilst SOD localised in the mitochondria contains manganese) catalyses the detoxification of superoxide radical to hydrogen peroxide and oxygen (Gutteridge, 1995).

$$2O_2^{\bullet-} + 2H^+ \rightarrow H_2O_2 + O_2$$

This hydrogen peroxide is a weak oxidant which has the ability to diffuse rapidly across membranes, and is capable of being converted to hydroxyl radicals in the presence of transition metal ions (Gutteridge, 1995).

$$Fe^{2+} + H_2O_2 \rightarrow Fe^{3+} + {}^{\bullet}OH + OH^-$$

Hydrogen peroxide can be detoxified by two antioxidant systems, glutathione peroxidase (GPx) and CAT. GPx is found in the cytoplasm and mitochondria and detoxifies hydrogen peroxide by oxidising GSH (Gutteridge, 1995).

$$2GSH + H_2O_2 \xrightarrow{GPx} GSSG + 2H_2O$$

High concentrations of CAT which are found in peroxisomes in several tissues can detoxify hydrogen peroxide (Gutteridge, 1995).

$$2H_2O_2 \rightarrow O_2 + 2H_2O$$

Non-enzymatic antioxidants such as β-carotene, coenzyme Q and α-tocopherol (vitamin E) are highly effective within the lipid components of cell membranes (Gutteridge, 1995). Other non-enzymatic antioxidants include ascorbic acid (vitamin C), GSH and flavonoids. GSH (L-γ-glutamyl-L-cysteinyl-glycine) is an important thiol antioxidant and cellular redox buffer. GSH is the reduced form, while GSSG (glutathione disulphide) is the oxidised form (Gutteridge, 1995).

$$ROOH + 2GSH \xrightarrow{GPx} 2ROH + GSSG$$

GSH is localised in the cytoplasm, nuclei and mitochondria. Synthesis of GSH occurs in the cytoplasm via glutamate–cysteine ligase and glutathione synthetase, and it is transported into the mitochondria via inner membrane carrier proteins, dicarboxylate and 2-oxoglutarate carrier proteins, against a concentration gradient. The GSH/GSSG ratio can be used to measure the level of oxidative stress in an organism (Circu and Aw, 2008).

The major protective roles of GSH against oxidative stress include: (a) GSH serves as a cofactor for many detoxifying enzymes against free radicals, such as GPx and GSH transferase; (b) GSH contributes to the transport of amino acids through the cell membrane; (c) GSH directly scavenges singlet oxygen and hydroxyl radicals - GPx catalyses detoxification of lipid peroxides and hydrogen peroxide; (d) GSH can regenerate inactive vitamins C and E back to their active forms - GSH reduces tocopherol radical of Vitamin E to ascorbic acid (Masella *et al.*, 2005).

1.3.3.3 Mitochondrial ROS

The mitochondrion is the principle source of cellular energy (ATP) and is the metabolic hub of the cell. However, it is also the major source of endogenous ROS. A proton (H^+) electrochemical potential gradient exists within the inner mt membrane (IMM) due to the flow of electrons from reducing equivalents, such as NADH and $FADH_2$, through complexes of the ETC and is used to drive ATP synthesis. Enzymatic electron transport along the ETC coupled with a proton gradient across the IMM which drives the ATPase to generate ATP is termed oxidative phosphorylation. Oxidative phosphorylation does not have the capacity to contain electron flow specifically for ATP production, hence, some electrons escape the ETC and interact with oxygen to produce $O_2^{\bullet -}$ (Ježek and Hlavatá, 2005).

As mentioned, during aerobic metabolism in the mitochondria, superoxide anion is produced in specific sites in complexes I, II and III from premature one-electron reduction of oxygen and is catalysed by SOD to form hydrogen peroxide in the mitochondria and cytoplasm (Figure 1.3) (Hamanaka and Chandel, 2010).

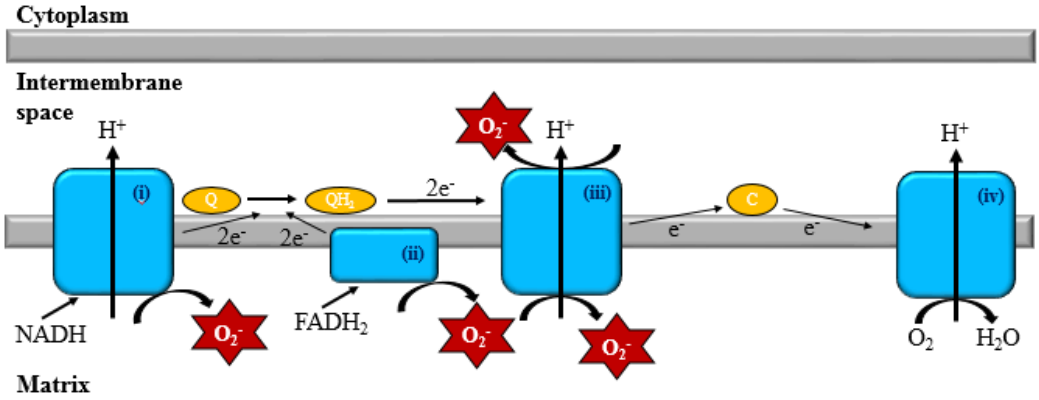

Figure 1.3: Mitochondrial ETC generates ROS. Electron transfer between complexes within the ETC give off ROS as a by-product (Prepared by Author).

Complexes I and II of the mitochondria reduce coenzyme Q (CoQ) using electrons donated from NADH and $FADH_2$. CoQ transports the electrons to complex III. The electrons are then transferred from complex III to cytochrome *c*. Cytochrome *c* donates electrons to complex IV to allow the reduction of molecular oxygen to water. The flow of electrons between complexes I, III, and IV generate a H^+ electrochemical potential gradient, which produces free energy that is used to phosphorylate ADP at ATP synthase. Superoxide is produced at complexes I, II, and III due to incomplete reduction of oxygen. Complexes I and II generate superoxide specifically into the mt matrix, while complex III generates superoxide into the matrix and intermembrane space (IMS) (Figure 1.3) (Hamanaka and Chandel, 2010).

1.3.4 Apoptosis

The term "apoptosis" was first used by Kerr *et al*. to describe programmed cell death due to intrinsically regulated mechanism for suicide (Kerr *et al.*, 1972). Apoptosis is essential for maintenance of tissue homeostasis, immune function, growth and development. It allows for the rapid removal of redundant, senescent, damaged, genetically mutated, or virus infected cells. For example, histogenic cell death of neurons during brain development, phylogenic cell death of the tail of the vertebra during foetal development, morphogenic cell death of mesenchyme between fingers and toes and programmed cell death of damaged precancerous cells (Fan *et al.*, 2005).

Apoptosis is characterised by several distinct and sequential morphological features which are due to the activation of caspases (cysteine aspartate proteases). These include cell shrinkage, internucleosomal DNA fragmentation, nuclear and cytoplasmic condensation, membrane "blebbing", apoptotic body formation, rapid phagocytosis and degradation by adjacent cells (Figure 1.4). Even though fragmentation and condensation occur, the apoptotic bodies that form are bound by intact membranes enclosing fragments of functional cellular components of different sizes (Kerr *et al.*, 1972).

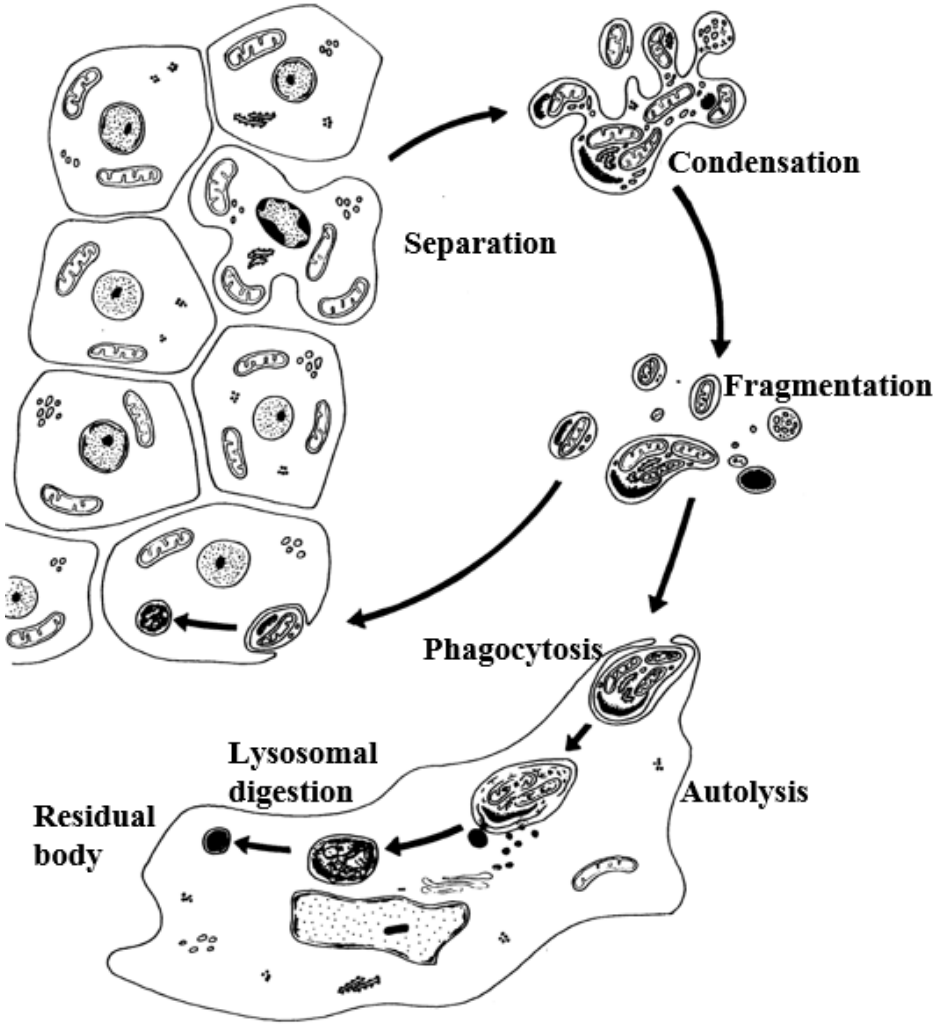

Figure 1.4: Series of events that occur throughout apoptosis. Cells separate from each other and undergo a series of events involving cellular shrinkage and fragmentation leading to phagocytosis of apoptotic bodies and lysosomal digestion (Image adapted from Kerr et al., 1972).

Another type of cell death, called necrosis, has distinct morphological characteristics different to that of apoptosis (Edinger and Thompson, 2004). There are several variations between the two types of cell death, tabulated in Table 1.1 below

Table 1.1: Distinction between morphological and biochemical characteristics of apoptosis vs necrosis (Adapted from Edinger and Thompson, 2004)**.**

Apoptosis	**Necrosis**
Affects scattered, individual cells	Affects neighbouring cells, hence tissues and organs
Physiological response to cell suicide mechanism which requires ATP (regulated)	Pathological response to physical damage or toxic insult which resulted in serious depletion of ATP
Organised fragmentation of chromosomal DNA into 200 base pair fragments	Random degradation of DNA
Cytoplasmic condensation	Vacuolation of cytoplasm
Membrane blebbing and apoptotic body formation with maintained cell membrane integrity	Membrane blebbing followed disintegration of cell membrane
Absence of inflammation around lysed cell since phagocytes recognise and remove apoptotic bodies	Induction of inflammation around lysed cell due to leakage of pro-inflammatory molecules and cellular components.
Cell shrinkage due to extrusion of water	Cell swelling due to swelling of organs (cellular oedema)

Apoptosis can occur via the extrinsic or intrinsic pathway, the endpoint of which is the activation of several proteases and endonucleases to degrade specific cellular proteins and other constituents. Apoptosis can also occur via caspase-independent pathways which don't require caspase activity (Fan *et al.*, 2005).

1.3.4.1 Caspases

Caspases belong to the interleukin-1β-converting enzyme family of proteases. All caspases have consistent properties: cysteine proteases that are specific to aspartate residues; exist as inactive precursors (zymogens) called pro-caspases; have a conservative active site consisting of five residues (QACXG); caspase activation requires the extremely diverse structure of the N-terminal in pro-caspases; all caspases have the capacity to auto-activate and activate other caspases (Fan *et al.*, 2005).

Caspases are involved in the caspase-cascade system and are regulated by numerous molecules, for example, B-cell lymphoma/leukemia-2 (Bcl-2) family proteins, inhibitor of apoptosis (IAP) proteins, Ca^{2+} and calpain. Caspases are categorised according to their involvement in inducing, transducing and amplifying intracellular apoptotic signals and according to their substrate specificity (Fan *et al.*, 2005). The first subfamily of caspases include the initiator caspases, caspase-2, -8, -9 and -10. Caspase-2, -8 and -10 are involved in the initiation of the extrinsic apoptotic pathway. Caspase-9 is involved in the induction of the intrinsic apoptotic pathway (Fan *et al.*, 2005).

1.3.4.2 Intrinsic apoptotic pathway: mitochondrial-mediated

The intrinsic apoptotic pathway, also known as the mt pathway, can be triggered by various signals. These include oxidative stress and ROS production, chemotherapy, growth factor

withdrawal, toxins, ceramide, DNA damage, endoplasmic reticulum stress, ultraviolet and γ-irradiation, and growth factor deprivation trigger the intrinsic pathway. This occurs via Bax (Bcl-2-associated X) activation, a pro-apoptotic protein of the bcl-2 superfamily, which form oligomers on the outer mt membrane (OMM) resulting in altered mt polarity, permeability and mt dysfunction. The anti-apoptotic proteins of the Bcl-2 superfamily, Bcl-2 or Bcl-XL, have the capacity to inhibit the pro-apoptotic activity of Bak and Bax. Dysfunction of the mitochondrion results in the release of several apoptotic proteins stored within the IMS of mitochondria into the cytoplasm, such as, second mitochondria derived activator of caspases/direct IAP binding protein with low pI (Smac/DIABLO) and cytochrome *c*. Smac/DIABLO allows for caspase activation by binding and inhibiting the activity of XIAP. Cytochrome *c* binds to the adaptor protein, adaptor apoptosis associated factor 1 (Apaf-1). Cytochrome *c*-bound Apaf-1 recruits pro-caspase-9 (inactive) to form an ATP-requiring apoptosome, which cleaves and activates pro-caspase-9 to produce active initiator caspase-9. Thereafter, caspase-9 cleaves and activates pro-caspase-3, -6 and -7 to produce effector caspases-3, -6 and -7 which are accountable for cellular substrate degradation, such as PARP-1 (Figure 1.5) (Green and Reed, 1998, Green and Kroemer, 2004).

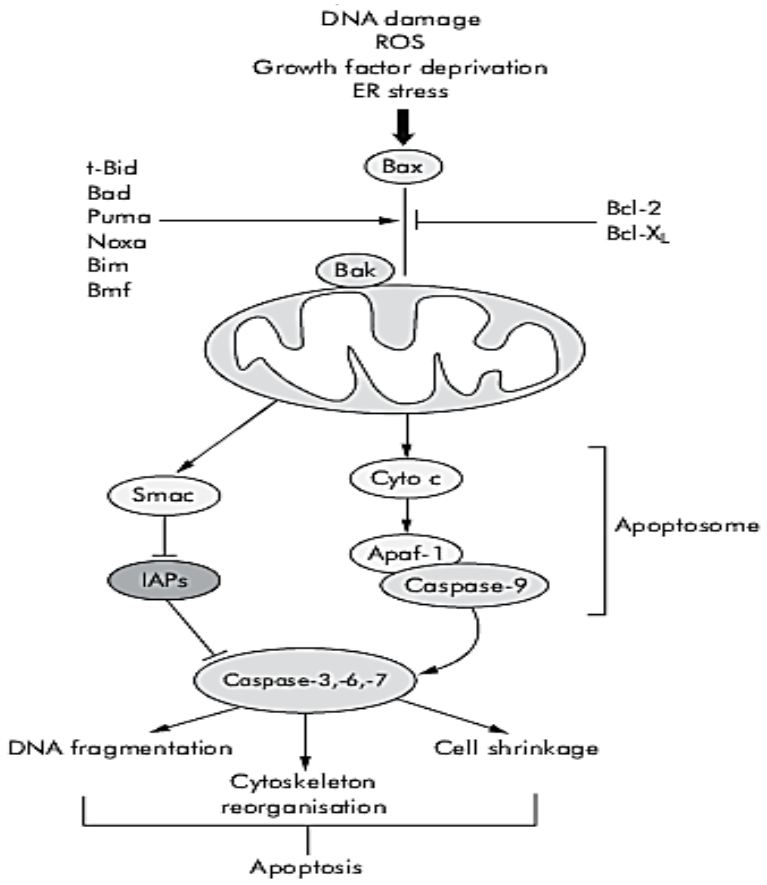

Figure 1.5: Intrinsic apoptotic pathway. Mitochondrial-mediated cell death pathway triggered by intracellular stressors which result in the oligomerisation of Bax and release of pro-apoptotic proteins from the mitochondria. These events trigger a caspase-cascade which ultimately result in apoptosis (Image adapted from Guicciardi and Gores, 2005).

1.3.4.3 Extrinsic apoptotic pathway: death receptor-mediated

The extrinsic apoptotic pathway is initiated at the cell membrane subsequent to the engagement of death receptors (e.g. tumour necrosis factor related apoptosis inducing ligand receptors 1 and 2 (TRAIL-R1 and TRAIL-R2), Fas/CD95 and tumour necrosis factor receptor 1 (TNF-R1), and by their associated ligands (TRAIL, Fas ligand (FasL)/CD95L and TNF-α). Binding of the receptor to the ligand induces receptor oligomerisation and adapter protein (TNF-R1 associated death domain protein (TRADD), Fas associated protein with death domain (FADD)) recruitment. This event leads to binding of the inactive pro-enzymes, initiator pro-caspase-8 and -10, to the intracellular domain of the death receptor to create a complex called death inducing signalling complex (DISC). Activated caspases at the DISC produce signals (due to the close proximity of a number of procaspase proteins) which lead to cell death by self-processing. Initiator caspases (active) can directly cleave and activate downstream effector caspases, or participate in the intrinsic apoptotic pathway. This can occur via cleavage and activation of Bid, the BH3 only protein, to form t-Bid (Figure 1.6) (Ashkenazi and Dixit, 1998).

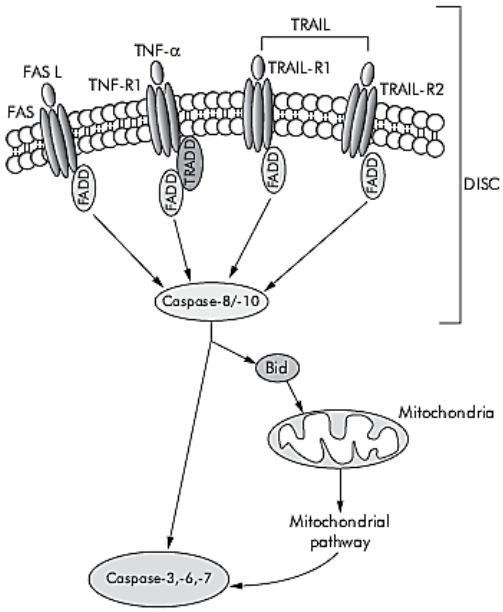

Figure 1.6: Extrinsic apoptotic pathway. The death receptor-mediated pathway involves the engagement of death receptors (e.g., Fas, TNFR1 and TRAIL-R) by their associated ligands (e.g., FasL, TNF and TRAIL), which induce recruitment of adapter proteins, procaspase-8 and -10 at the intracellular domain of the receptor to form a DISC. The signal generated at the DISC by activated caspases results in cell death (Image adapted from Guicciardi and Gores, 2005).

1.3.4.4 Bcl-2 family of proteins

The Bcl-2 family proteins regulate apoptosis by regulating the OMM. Based on Bcl-2 homology (BH) domains and protein function, Bcl-2 family proteins are divided into anti- and pro-apoptotic proteins. Anti-apoptotic proteins have BH1, BH2, BH3 and BH4 domains, e.g. Bcl-x_L and Bcl-2. Pro-apoptotic proteins are further subdivided into two groups: proteins containing BH1, BH2 and BH3 domains, e.g. Bax and Bak; proteins containing only BH3 domains, e.g. Bad and Bin. There is also an exceptional pro-apoptotic protein called Bcl-x_S which contains BH3 and BH4 domains (Harris and Thompson, 2000).

Bax (21 kDa protein) is a naturally occurring monomer localised in the cytoplasm and has also been shown to be localised on the OMM. Upon apoptotic stimulus, a change in pH or Bid interaction causes Bax to change its conformation and become a pro-apoptotic oligomer which translocated to the OMM. This oligomerisation of Bax can cause cytochrome *c* release from mitochondria into the cytoplasm. This occurs via interaction with voltage-dependent anion channels (VDACs) to from large pores in the OMM and increasing its permeability (Figure 1.7). The conformational change in Bax exposes its N-terminal domain and C-terminal transmembrane domain. The C-terminal sequence functions as a signal anchor which targets Bcl-2 to the mitochondria, hence, in response to cellular stress, Bax changes its conformation and lodges into the OMM, where it forms channels and becomes permeable to release cytochrome *c* and other pro-apoptotic proteins (Gross *et al.*, 1998, Desagher *et al.*, 1999, Harris and Thompson, 2000).

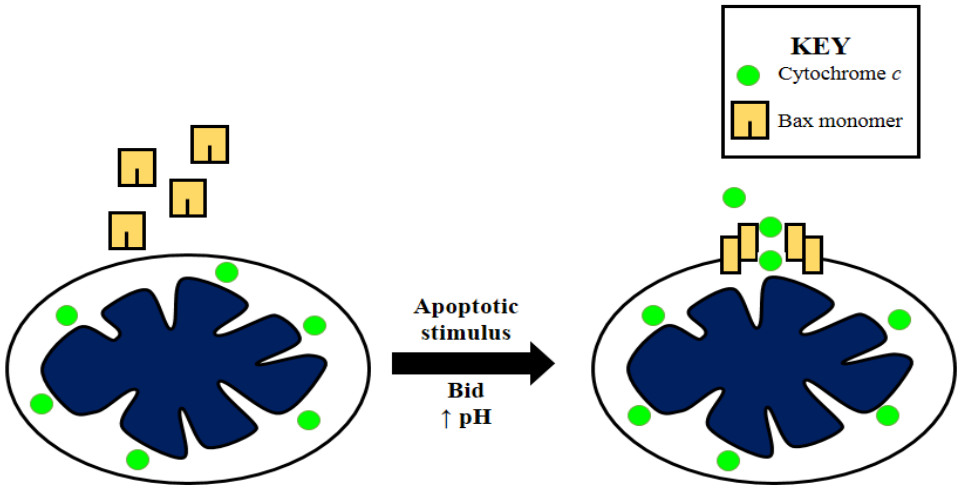

Figure 1.7: Bax oligomerises to allow cytochrome *c* release from mitochondria. Increased pH or Bid interactions due to apoptotic stimulus lead to oligomerisation of Bax to form channels in the OMM (Prepared by Author).

Bcl-2 is localised in the membranes of the mitochondria, nucleus and endoplasmic reticulum (ER). Bax and Bcl-2 are similar proteins with contrasting effects on the living state of cells, since Bax accelerates apoptosis while Bcl-2 prolongs cell survival (Reed, 1994). Bcl-2 regulates apoptosis by inhibiting translocation of Bax to the mitochondria, and also thereby inhibits all downstream effects of Bax, such as mt membrane depolarisation induced by Bax, and cytochrome *c* release. Bcl-2 may displace Bax by sequestering the site at which Bax inserts itself into the OMM. As mentioned, the exposure of the C-terminal of Bax causes Bcl-2 to target the mitochondria. Bax translocation may be inhibited by Bcl-2 by binding to this C-terminal (Murphy *et al.*, 2000).

1.3.4.5 Mitochondrial membrane potential & ATP production

The principal function of mitochondria is the production of ATP via oxidative phosphorylation reactions that occur in the ETC on the IMM. Mitochondria regulate apoptosis, ROS formation

and elimination, cellular Ca^{2+} content, metabolite anabolism and catabolism, and translocation of organelles. In healthy and functional mitochondria, energy is transduced within the mt matrix via an ATPase complex embedded in the IMM membrane which requires protons (H^+) generated from the ETC also within the IMM (Figure 1.8). This energy is stored as an electronegative chemical gradient across the mt membrane, allowing for the retention of membrane potential which is necessary for ATP production in the inner mt membrane (IMM). The membrane is regarded as polarised. Dysfunctional mitochondria have collapsed membrane potentials due to a disrupted chemical gradient, which results in depolarisation of the mt membrane. Since ATP production is necessary for cell survival and a maintained mt membrane potential is necessary for ATP synthesis, mt depolarisation is regarded as a pro-apoptotic event (Brand and Nicholls, 2011).

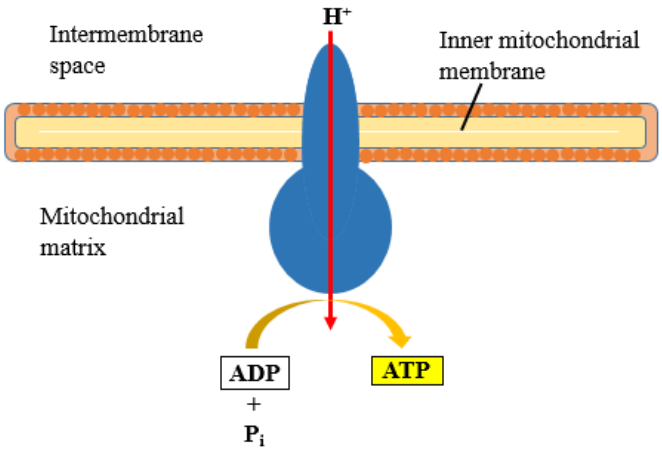

Figure 1.8: ATP synthase complex in IMM. ATP is synthesised in the mt matrix driven by a proton (H^+) gradient (Prepared by Author).

1.3.4.6 Inhibitor of apoptosis proteins and Smac/DIABLO

Inhibitor of apoptosis (IAP) proteins are anti-apoptotic proteins that were initially discovered in 1993 due to their capacity to suppress cell death (Crook *et al.*, 1993). IAP proteins belong to a family of five proteins associated with immunity, migration, cell cycle, cell death and inflammation. These proteins are characterised based on the presence of baculovirus IAP repeats (BIR domains) and contain Zn-finger-like motifs. Human IAP family of proteins comprise of eight members: normal-molecular-weight IAP (NIAP) which contains BIRC1; cellular IAP proteins (c-IAPs) form part of the TNFR2 complex, c-IAP1 contains BIRC2 and c-IAP2 contains BIRC3; X-chromosome-linked IAP (XIAP) contains BIRC4; survivin contains BIRC5; Apollon/Bruce contains BIRC6; livin or ML-IAP contains BIRC7 and ILP-2 contains BIRC8. The IAP proteins which directly regulate apoptosis include XIAP, c-IAP1, c-IAP2 and ML-IAP (de Almagro and Vucic, 2012).

The extrinsic apoptotic pathway is regulated by c-IAP1 and c-IAP2 via ubiquitin ligation. The intrinsic pathway is regulated by XIAP which binds and inhibits caspase-3/7 and -9 activities (Figure 1.9). XIAP, on the other hand, is inhibited by Smac/DIABLO and HtrA2 (serine protease with an IAP-binding motif (IBM), AVPS) (de Almagro and Vucic, 2012). Regions on the N-terminal side of BIRC2 of XIAP (Ala-Thr-Pro-Phe) interact with the catalytic site of the caspase to inhibit its activity (Vaux and Silke, 2003).

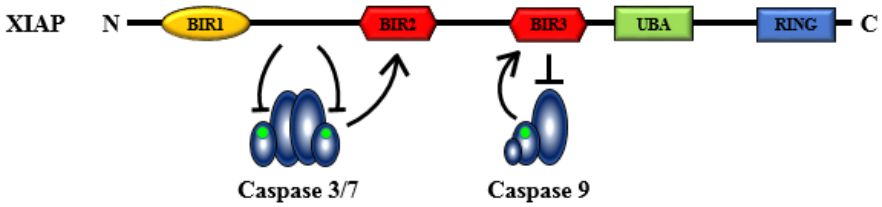

Figure 1.9: XIAP inhibits caspase-3/7 and caspase -9. The sequence between the BIR1 and BIR2 domains sequester the catalytic site of caspase-3/7, thereby inhibiting substrate entry. The BIR2 domain interacts with the exposed IBM of active caspase-3/7 (presented in green). Active caspase-9 (with an exposed IBM) binds to BIR3 of XIAP, inhibiting caspase-9 dimerisation required for caspase-9 activity (Prepared by Author).

Smac/DIABLO is an intracellular, pro-apoptotic IAP protein inhibitor which is localised in the IMS of the mitochondria and released into the cytoplasm during apoptosis. Smac/DIABLO is a dimer which competitively binds to IAP proteins, namely, c-IAP1, c-IAP2, XIAP and survivin, to prevent binding and inhibition of caspase-3/7 and -9 (Chai *et al.*, 2000). Smac/DIABLO binds BIRC2 and BIRC3 (simultaneously) on the N-terminal IBM containing the first four amino acid residues, AVPI (Ala–Val–Pro–Ile), on XIAP (Vaux and Silke, 2003, de Almagro and Vucic, 2012). Smac/DIABLO is initially synthesised as a precursor molecule containing 239 amino acid residues. The N terminal which contains 55 residues is a mt targeting sequence, which is degraded subsequent to import. Mature Smac/DIABLO only consists of 184 amino acid residues and naturally exists as an oligomer. The relationship between Smac/DIABLO and IAP proteins play an important role in the tight regulation of apoptosis (Chai *et al.*, 2000).

1.3.4.7 Poly (ADP-ribose) polymerase-1 activity

PARP-1 is a DNA-binding Zn-finger endonuclease that catalyses the degradation of internucleosomal DNA and is associated with the biochemical alterations that occur during apoptosis. PARP-1 is a 113 kDa protein and has 6 domains, which when cleaved, forms an 89 kDa and a 24 kDa fragment. The 89 kDa fragment is relatively stable containing the complete and intact carboxyl terminus; it lacks the Zn-finger domains (Zn1, 2 and 3) but contains the catalytic domain (helical subdomain and ADP-ribosyl transferases) and automodification domains (BRCA1-terminus). This fragment is covalently altered by a derivative of NAD^+ which is degraded by a poly (ADP-ribose)-specific enzyme and is responsible for NAD^+ consumption in late stage apoptosis. The 24 kDa fragment contains the Zn-finger DNA-binding domain and the amino terminus. Chelation of the Zn-fingers would desensitise the 89 kDa fragment to activation by nicked DNA, preventing DNA repair (Kaufmann *et al.*, 1993, Langelier *et al.*, 2012).

In response to DNA damage (DNA single or double stranded breaks), PARP-1 converts NAD^+ to nicotinamide as well as protein-linked ADP-ribose polymers, and catalyses the transfer of these polymers from NAD^+ to several molecules such as chromatin. PARP-1 is rather inactive in normal, healthy cells until it becomes activated by single or double stranded DNA breaks. When PARP-1 recognises interruptions in DNA strands, it binds to the damaged DNA via one of its two Zn-finger domains which are located near the amino terminus of the protein.

Thereafter, PARP-1 undergoes conformational changes and is activated. This activation of PARP-1 consumes NAD^+ which is consistent with cellular consumption of NAD^+ during apoptosis. Poly (ADP-ribosyl)ation of several nuclear proteins is catalysed by activated PARP-1, which aids protein release from damaged strands of DNA and allows DNA repair enzymes to interact with single strand DNA disruptions that are inhibited by unmodified PARP-1 (Kaufmann *et al.*, 1993).

PARP-1 is capable of interacting with RNA to inhibit transcription. The translocation of AIF from the mitochondrion to the nucleus is dependent on PARP-1. Deficiencies of PARP-1 result in aneuploidy and chromosomal instability since more and more chromosomes pair up. This means that poly (ADP-ribosyl)ation maintains genome integrity (Kaufmann *et al.*, 1993).

The protease responsible for PARP-1 cleavage is caspase-3/7. Caspase-3/7 recognises and cleaves a tetrapeptide carboxyl cleavage site on PARP-1, Asp-Glu-Val-Asp (DEVD), located between Gly215 and Asp214, to produce 24- and 89-kDa polypeptides (Germain *et al.*, 1999, Herceg and Wang, 1999). Zinc is essential to allow for the binding of PARP-1 to DNA strand breaks as Zn inhibits PARP-1 cleavage. This is achieved by Zn inhibition of the catalytic function of caspase 3 by interaction with either or both of the conserved sites, Cys-285 and His-237. This is another mechanism by which Zn chelation would allow for PARP-1 cleavage by caspase-3/7 to occur (Perry *et al.*, 1997).

CHAPTER 2

Materials and Methods

2.1 Materials

SNO cells were purchased from Highveld Biologicals (Johannesburg, South Africa (SA)). Cell culture reagents were purchased from Lonza Biotechnology (Basel, Switzerland). Western blot reagents were obtained from Bio-Rad (Hercules, CA, United States of America (USA)) and all antibodies sourced from Cell Signalling Technology. All other reagents were obtained from Merck (Darmstadt, Germany) unless otherwise stated.

2.2 Fusaric acid (FA) preparation

FA (*Gibberella fujikuroi*) (F6513) was obtained from Sigma Aldrich (St Louis, MO, USA). A stock solution (20 mg/ml) was prepared in 0.1 M phosphate-buffered saline (PBS) and diluted to 1 mg/ml stocks prior to each treatment for biochemical assays. Stock solutions were stored at 4°C.

2.3 Cell culture

SNO cells were cultured (37°C, 5% CO_2) in sterile 25 cm^3 cell culture flasks in complete culture medium (CCM) comprising of Eagle's minimum essential medium (EMEM) supplemented with 10% fetal calf serum, 1% L-glutamine and 1% penicillin-streptomycin-fungizone until 90% confluency (Wilson and Walker, 2010). The 3-(4,5-dimethylthiazol-2-yl)-2,5-diphenyltetrazolium bromide, or methylthiazol tetrazolium (MTT) assay was conducted to determine an IC_{50} value (concentration that produced half the maximum inhibition) for FA; which was used in all subsequent assays.

2.4. Methylthiazol tetrazolium (MTT) assay

2.4.1 Introduction

The MTT salt is a water-soluble tetrazolium yellow dye which is reduced by metabolically active cells to a water-insoluble purple formazan product (Figure 2.1). As only cells with functional mitochondria can cleave the tetrazolium ring, this assay is used to determine cell viability. Reducing enzymes that catalyse the transfer of electrons to an oxidant compound in the presence of reducing equivalents - flavin adenine dinucleotide ($FADH_2$) and nicotinamide adenine dinucleotide (NADH); catalyse the reaction. Both $FADH_2$ and NADH are derived from the tricarboxylic acid (TCA) cycle (Figure 2.2). The intensity of the formazan product is therefore, directly proportional to cellular metabolic activity which can be measured using a spectrophotometer (Mosmann, 1983, Riss *et al.*, 2013).

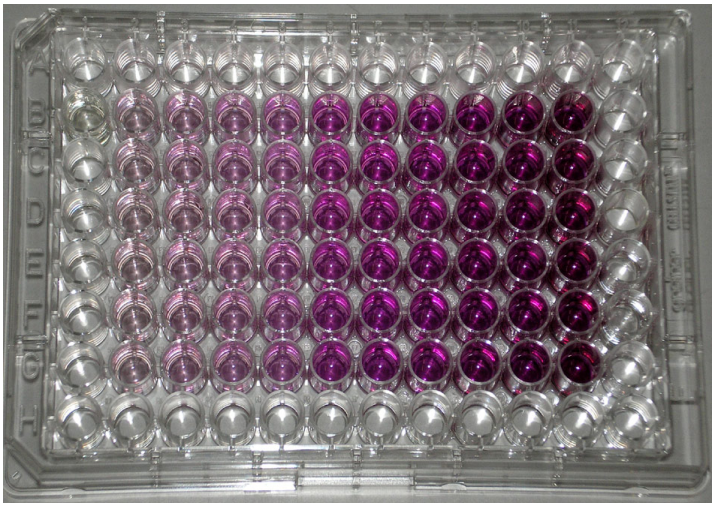

Figure 2.1: The purple formazan product following the reduction of the yellow tetrazolium MTT salt which is an indication of increased metabolic output (Image adapted from Stockert *et al.*, 2012).

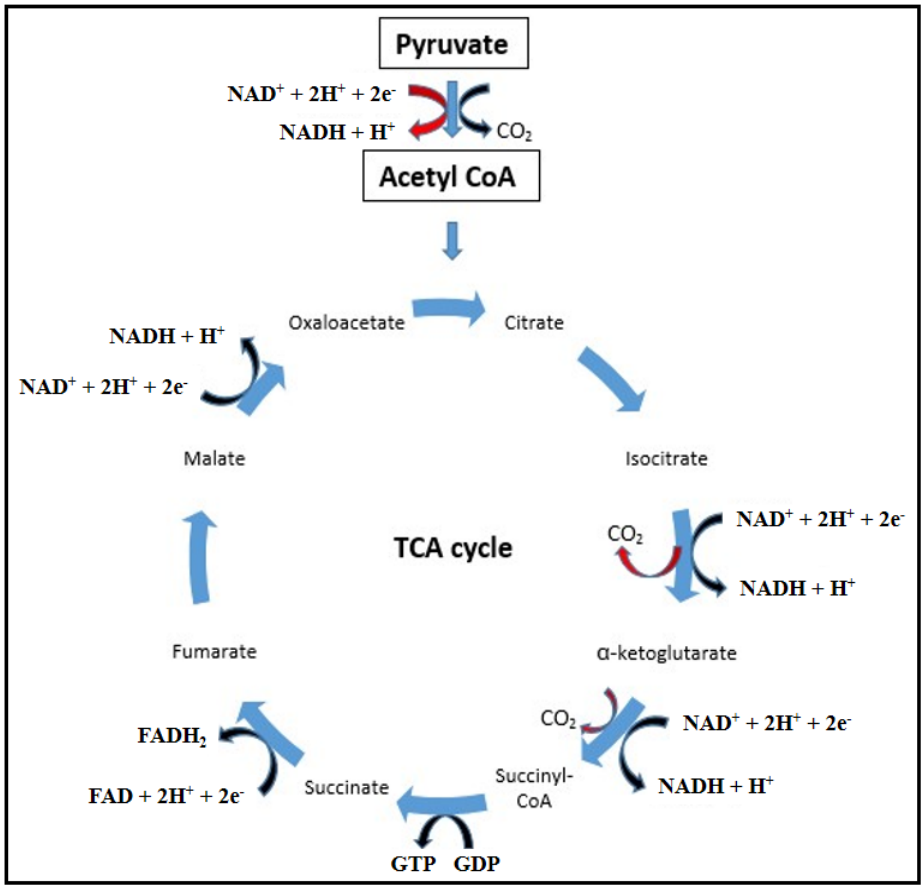

Figure 2.2: NADH and $FADH_2$ production in the TCA cycle (Prepared by Author).

2.4.2 Protocol

The cytotoxicity of FA on SNO cells was determined via the colorimetric MTT assay. SNO cells were seeded into a 96-well microtitre plate at an inoculation density of 15,000 cells/well in triplicate. Cells were incubated with a range of FA concentrations (0; 25; 50; 100; 250; 350 and 500 µg/ml) at 37°C for 24 h. Thereafter, the cells were incubated with MTT salt solution (5 mg/ml in 0.1 M PBS) and CCM at 37°C for 4 h. The supernatants were then aspirated and 100 µl dimethyl sulphoxide (DMSO) was added to each well and incubated at 37°C for 1 h to solubilise the formazan crystals. The optical density (OD) was measured using an enzyme-linked immunosorbent assay (ELISA) plate reader (Bio-Tek µQuant) at 570/690 nm. The percentage cell viability of the samples (refer to equation below) and a concentration-response curve was plotted using GraphPad Prism v5.0 software relative to the control. The concentration of FA that produced half the maximum inhibition (IC_{50}) had been calculated via linear extrapolation. Two independent experiments were conducted to verify the IC_{50}. For subsequent assays, SNO cells were treated FA at a concentration equal to its IC_{50}.

$$\% \text{ Cell viability} = \frac{\text{FA treated cells (mean OD)}}{\text{Control cells (mean OD)}} \times 100$$

2.5 ATP quantification assay

2.5.1 Introduction

ATP is a coenzyme that transports chemical energy throughout the cell and is required for metabolism. ATP is produced through substrate level phosphorylation in the TCA cycle, glycolysis and oxidative phosphorylation in the ETC during cellular respiration (Figure 2.3). The levels of intracellular ATP are indicative of respiratory capacity and mitochondrial function (Bergman, 1999).

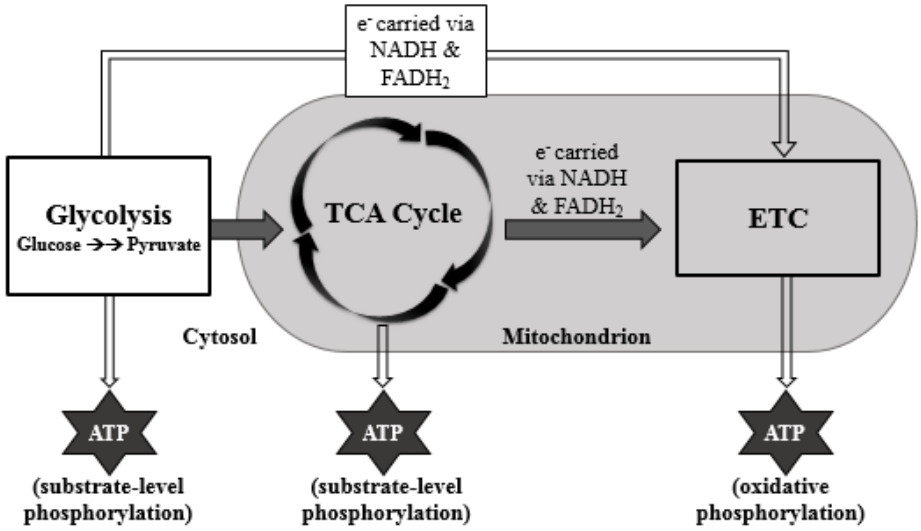

Figure 2.3: The sequential processes that lead to intracellular ATP production, namely glycolysis, the TCA cycle and the ETC. ATP production in the ETC is driven by electron transfer via reducing equivalents (Prepared by Author).

Intracellular ATP levels were quantified using a CellTiter-Glo® assay (Promega, Madison, Wisconsin, USA). The assay uses bioluminescence to determine intracellular ATP levels. Bioluminescence is the generation and emission of light by an organism due to a chemical reaction whereby chemical energy is transformed into light energy and the outcome is chemiluminescence (visible light) (Hastings, 2014). The assay is based on the luciferin-luciferase reaction that occurs in the firefly. Luciferase is the enzyme that catalyses the mono-oxygenation of D-luciferin in the presence of magnesium, ATP and oxygen, producing inactive oxyluciferin (Figure 2.4). The intensity of light that is produced by this reaction is directly proportional to the concentration of intracellular ATP (Hastings, 2014).

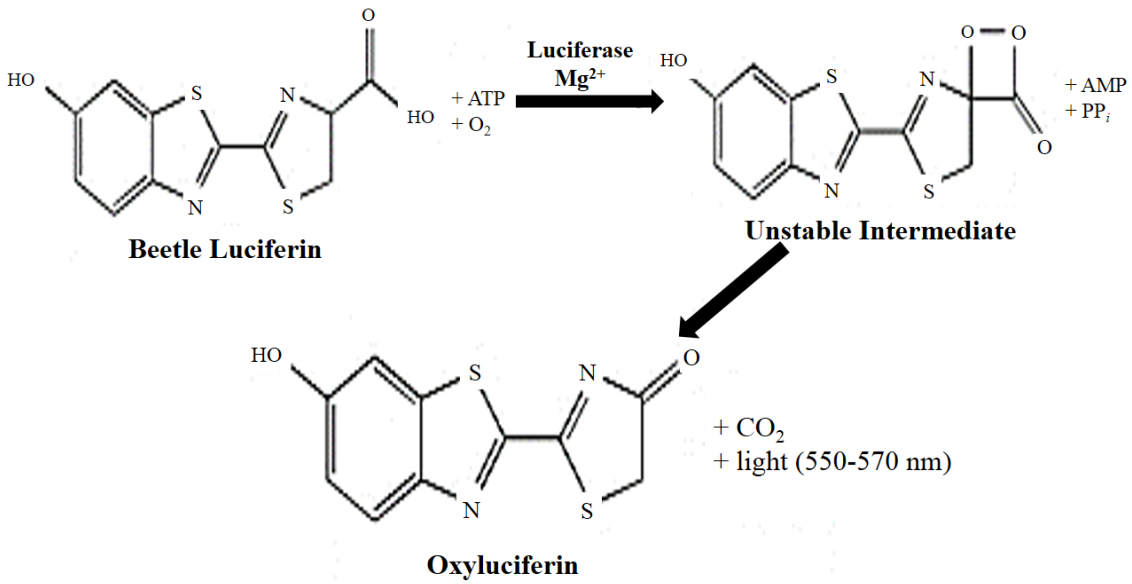

Figure 2.4: The luciferin-luciferase reaction. Mono-oxygenation of luciferin is catalysed by luciferase enzyme in the presence of magnesium ions, ATP and oxygen. This reaction gives of CO_2 and light as by products (Prepared by Author).

2.5.2 Protocol

For the CellTitre-Glo® assay, 50 µl of cell suspension (20,000 cells/well in 0.1 M PBS) was seeded into a white, opaque 96-well luminometer plate in triplicate. Thereafter, 20 µl of reagent was added into each well followed by incubation of the plate in the dark for 30 minutes (min) at room temperature (RT) to allow for the luciferin-luciferase reaction to occur. Luminescence, which is proportional to the level of intracellular ATP, was then detected using a Modulus™ microplate luminometer (Turner Biosystems, Sunnyvale, USA). The level of ATP was expressed as relative light units (RLU).

2.6 Glutathione assay

2.6.1 Introduction

Endogenous antioxidant defence systems combat excessive levels of ROS thus dampening ROS-associated toxicity. The most abundant endogenous antioxidant which functions in cellular defence and detoxification is glutathione. Glutathione exists predominantly in its biologically active form, reduced glutathione (GSH). In the presence of ROS, GSH acts as an electron donor and is oxidised to form GSSG. Oxidation of GSH results in a decreased ratio of GSH: GSSG. The recycling of GSH and GSSG are carried out by glutathione-S-transferase (GST) and GSH peroxidase (GPx) (Figure 2.5) (Circu and Aw, 2008).

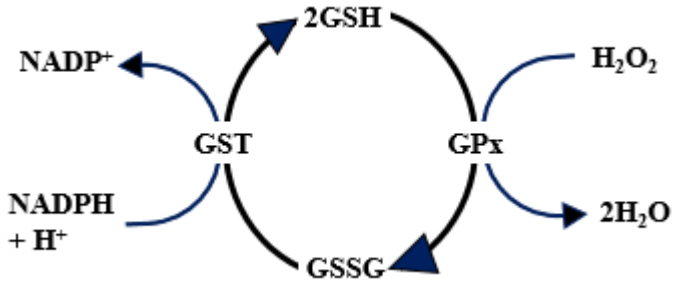

Figure 2.5: Reactions associated with the interconversion of the two different forms of glutathione. Detoxification of H_2O_2 by GPx requires GSH to generate water and GSSG, while regeneration of GSH from GSSG by GST requires NADPH as a cofactor (Prepared by Author).

The GSH luminometric assay is also based on the luciferin-luciferase reaction, where Luciferin-NT is converted to Luciferin by GST. This reaction consumes GSH and gives off ATP and oxygen as by-products. Thereafter, Luciferin is converted by Luciferase to produce light which is detected by a luminometer (Hastings, 2014).

2.6.2 Protocol

Intracellular glutathione (GSH) levels were quantified using the GSH-Glo™ assay (Promega, Madison, USA). Briefly, 50 µl of cell suspension (20,000 cells/well in 0.1 M PBS) were seeded into a white, opaque 96-well luminometer plate in triplicate. A 5 mM stock diluted in 0.1 M PBS was used to make GSH standards ranging from 0-50 µM. Subsequently, 50 µl per GSH standard and 50 µl of 2× GSH-Glo™ Reagent were added into each well and incubated for 30 min in the dark at RT. Thereafter, 50 µl of Reconstituted Luciferin Detection Reagent was added into each well and incubated for 15 min at RT. Luminescence was measured on a Modulus™ microplate luminometer. The data was expressed as relative fold change.

2.7. Thiobarbituric acid reactive substances (TBARS) assay

2.7.1 Introduction

Quantification of endogenous ROS is challenging as ROS have short half-lives. By-products of ROS are often used to quantify the extent of oxidative damage. Lipid peroxidation, the oxidation of polyunsaturated fatty acids in lipids by ROS, is a common biomarker for oxidative stress (Figure 2.6). The double bond and ethylene bridges in polyunsaturated fatty acids contain highly reactive hydrogen atoms which can readily interact with ROS (Fernández *et al.*, 1997).

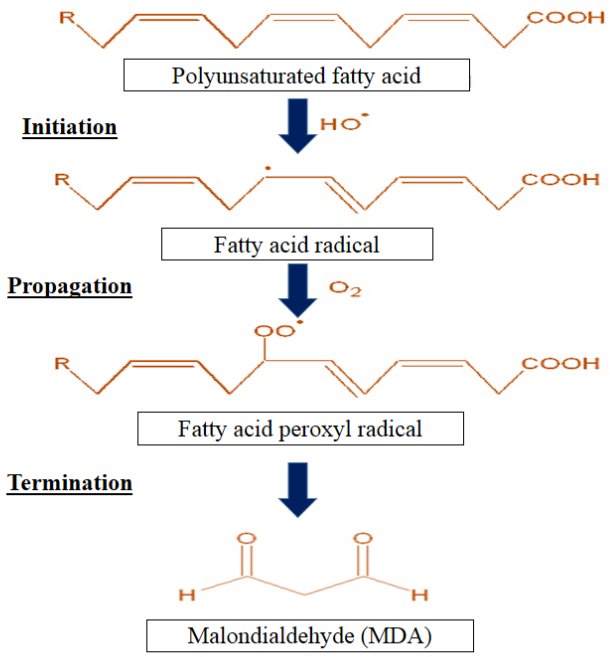

Figure 2.6: Free radical chain reaction of lipid peroxidation. Initiation involves the reaction of a free radical with a polyunsaturated fatty acid, forming a fatty acid radical. Propagation refers to the reaction of oxygen with the fatty acid radical to produce a fatty acid peroxyl radical. Termination entails the formation of the end product of lipid peroxidation, malondialdehyde (MDA) (Prepared by Author).

The Thiobarbituric Acid (TBA) Reactive Substances (TBARS) assay measures the concentration of the end product of lipid peroxidation, MDA (Asakawa and Matsushita, 1979). The principle of this assay is based on the ability of two molecules of TBA to condense with one molecule of MDA at a high temperature and low pH to form a red pigment that absorbs light at 532 nm. MDA reacts with the methylene group of TBA to form adducts. The colour intensity is proportional to the concentration of MDA which is measured using a spectrophotometer (Fernández *et al.*, 1997).

2.7.2 Protocol

Approximately 200 µl of supernatant per control/treatment was added into appropriately labelled, clean glass test tubes containing 200 µl of 2% phosphoric acid (H_3PO_4). This acidifies the samples so that any interfering proteins or enzymes become dysfunctional. Experimental assurance was accounted for by preparation of a negative control (3 mM HCl) and positive control (1 µl MDA). Thereafter, 200 µl of 7% H_3PO_4 was added to each of the tubes followed by 400 µl of TBA/Butylated hydroxytoluene (BHT) solution to every sample except the blank. BHT is an antioxidant which minimises artefact oxidation during the heating process, hence, BHT is used in conjunction with TBA as TBA is unspecific and can react with several other substances to form TBARS (Asakawa and Matsushita, 1979).

Each tube was briefly vortexed and the pH of each sample was adjusted using 1 M HCl to pH 1.5. The tubes were subsequently boiled in a water bath for 15 min at 100°C to allow for optimal hydrolysis of MDA-adducts. After the samples were allowed to cool to RT, 1500 µl of butanol was added to each tube in order to extract MDA by separating the solution into phases. The tubes were then vortexed and allowed to stand for the two phases to become distinct. A volume of 500 µl of the upper butanol phase was transferred to sterile 1500 µl micro-centrifuge tubes. This was followed by centrifugation (2500xg; 24°C; 6 min) and 100 µl of each sample was transferred to a 96-well microtitre plate in triplicate. The absorbance was measured at 532 nm with a reference wavelength of 600 nm using a Bio-Tek µQuant spectrophotometer. The average of 3 replicates were calculated and divided by the absorption coefficient, 156 mM^{-1} to determine the average concentration of MDA (µM). MDA levels were represented as relative fold change.

2.8 Lactate dehydrogenase cytotoxicity detection assay

2.8.1 Introduction

Lactate dehydrogenase (LDH) is an oxidoreductase which catalyses the interconversion of pyruvate and lactate during glycolysis and is localised in the cytosol. Upon cellular damage, the cell membrane integrity becomes compromised. Consequently, cellular contents, including cytosolic LDH leaks from the cytosol into the extracellular matrix (Watanabe *et al.*, 1995). The LDH cytotoxicity detection kit (11644793001) (Roche, Mannheim, Germany) was used to quantify cell damage and this was measured using colorimetric analysis. The assay consists of two serial enzymatic reactions. First, nicotinamide adenine dinucleotide (NAD^+) is reduced to $NADH/H^+$ via conversion of lactate to pyruvate. Subsequently, an oxidase (diaphorase enzyme) catalyses the transfer of H/H^+ from $NADH/H^+$ to a tetrazolium salt, iodonitrotetrazolium (INT) to produce a purple formazan product (Figure 2.7) (Watanabe *et al.*, 1995).

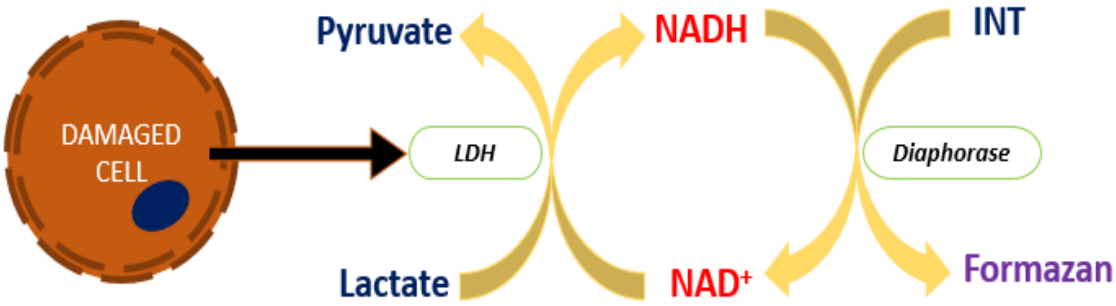

Figure 2.7: Intracellular lactate dehydrogenase (LDH) is released into the extracellular matrix when cell membrane integrity is compromised. Extracellular LDH is detected and measured by means of the oxidation of lactate with attendant reduction of NAD to NADH which is then used to produce a coloured substrate quantifiable via colorimetric analysis. INT: iodonitrotetrazolium (Prepared by Author).

2.8.2 Protocol

To quantify the level of extracellular LDH, 100 µl of supernatant per sample was added into a 96-well microtitre plate in triplicate. Thereafter, 100 µl of solution from the kit containing dye solution (INT/sodium lactate) and catalyst (diaphorase/NAD^+) was transferred to each well. This was followed by incubation in the dark for 25 min at RT. Absorbance was measured at 500 nm using a spectrophotometer (Bio-Tek µQuant). The OD values of replicates were averaged and LDH levels was expressed as mean OD.

2.9 Assessment of caspase activity

2.9.1 Introduction

Caspases are cysteine-aspartate proteases that are involved in the initiation (caspase-8 and -9) and execution (caspase-3/7) of apoptosis (Fan *et al.*, 2005). The luminometric assay used to assess caspase activity is based on the cleavage of the luciferin substrate which is specific to caspases. This reaction produces light which is directly proportional to caspase activity (Figure 2.8) (Hastings, 2014).

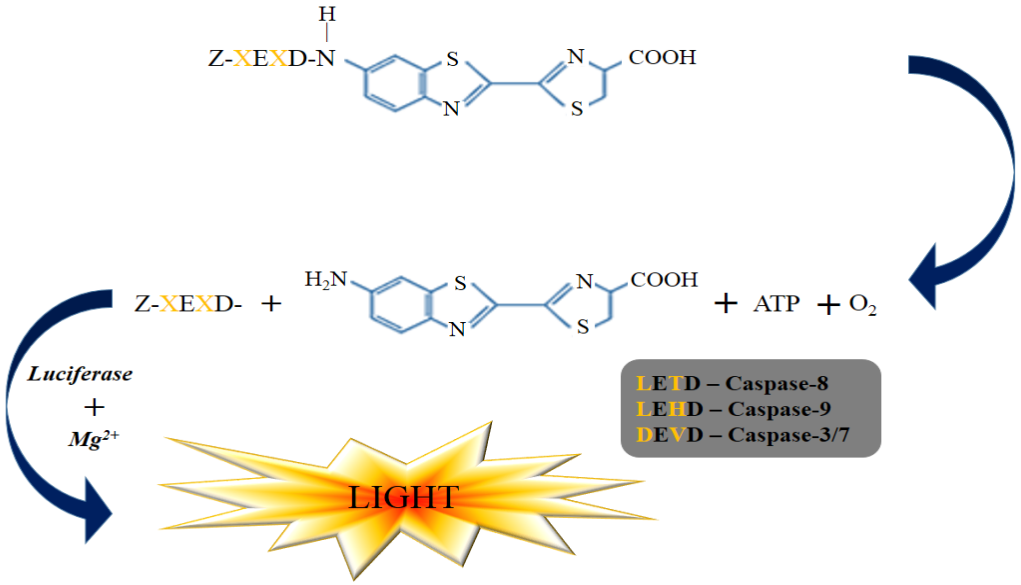

Figure 2.8: Reaction underlying the principle of the luminometric assay which quantifies caspase activity. Specific binding sequences of each caspase is cleaved by luciferin in the presence of ATP and O_2, and is converted by the enzyme, Luciferase, in the presence of magnesium (Mg^{2+}) to produce light (Prepared by Author).

2.9.2 Protocol

The activities of caspase-3/7, -8 and -9 were detected with Caspase-Glo® assay (Promega, Madison, USA). Briefly, 50 µl of cell suspension (20,000 cells/well in 0.1 M PBS) were seeded into a white, opaque 96-well microtitre plate in triplicate. As per manufacturer's guidelines, Caspase-Glo®-3/7, -8 and -9 reagents were reconstituted and 20 µl was added into each well. Thereafter, the plate was incubated in the dark (30 min, RT). Luminescence was detected using a Modulus™ microplate luminometer and expressed as relative fold change.

2.10 Western blotting

2.10.1 Introduction

Western blotting is a technique used to detect and quantify the expression of specific proteins in a homogenous sample. This is achieved by separating proteins through a gel, based on their molecular weight. Distinct proteins are transferred to a firm membrane which is probed by antibodies (Abs) that bind to specific proteins. Chemiluminescent detection of the protein of interest is achieved by developing the membrane using a substrate that binds to an enzyme attached to the Ab. Proteins are represented as bands and the band width is proportional to the quantity of the respective protein (Mahmood and Yang, 2012).

2.10.2 Protocol

Protein isolation & preparation-

Initially, protein is isolated from cell lysates. Total protein was extracted using Cytobuster™ reagent (catalog no. 710093, Novagen, San Diego, CA, USA), supplemented with protease and phosphotase inhibitor (Roche, Germany, 05892791001 and 04906837001 respectively), as per manufacturer's instructions. Cytobuster reagent (200 µl) was added to cells in a 25 cm^3 flask and left on ice for 30 min. The cells were lysed mechanically, aspirated and centrifuged to isolate the crude protein extract (4°C, 10 min, 10,000xg).

Crude protein samples were then quantified using the bicinchoninic acid (BCA) assay (Sigma, Germany). The colorimetric BCA assay is based on the Biuret reaction which measures the production of Cu^+, when peptide bonds in the sample react with Cu^{2+} under alkaline conditions. The Cu^+ chromophore then reacts with 2 BCA molecules to produce a purple chromophore (562 nm, 37°C). The colour produced is a result of the interaction between BCA and Cu^{2+} with amino acid residues (tryptophan, tyrosine and cysteine) in the protein sample (Bainor *et al.*, 2011). Bovine serum albumin (BSA) was used to make protein standards (0, 0.2, 0.4, 0.6, 0.8, 1 mg/ml) to determine the concentrations of the samples. Both the standards and samples were incubated with a working solution (BCA and $CuSO_4$) at 37°C for 30 min and the OD was measured using a µQuant Biotek ELISA plate reader (562 nm). A standard curve was generated using the OD values obtained for the standards to determine the concentrations of the crude protein samples. The samples were subsequently standardised to a concentration of 1.5 mg/ml in Cytobuster. Protein quantification is required to standardise samples to the same concentration to allow for comparison of protein expression between treated samples.

Sodium dodecyl sulphate-polyacrylamide gel electrophoresis (SDS-PAGE)-

Standardised protein samples were then boiled in Laemmli buffer [dH_2O, 0.5 M Tris-HCl (pH 6.8), 3% glycerol, 10% SDS, 12% β-mercaptoethanol, 2% bromophenol blue dye] (1:4, 20 min) to denature protein. Water (dH_2O) was used as a solvent to homogenise the sample. Glycerol was used to add density to the sample to facilitate sample loading in the well and prevents mixing of samples. Tris-HCl was used to buffer the sample and provide negatively charged chloride ions to the sample. Chloride ions migrate quicker through the electric field than glycerol, forming an ion front moving before glycerol. The overall charge of samples was adjusted by the anionic detergent, SDS: this prevents side chains with positive charges from influencing migration toward the positive electrode. SDS surrounds proteins, forming micelles, giving proteins a negative charge and ensuring protein migration as a result of repulsion by SO_4^- molecules (Figure 2.9). The reducing agent, β-mercaptoethanol, was used to break disulphide peptide bonds to allow for distinct separation of bands based on protein size and not protein configuration. The tracking dye, bromophenol blue, was used to visualise protein migration during electrophoresis (Yang and Ma, 2009).

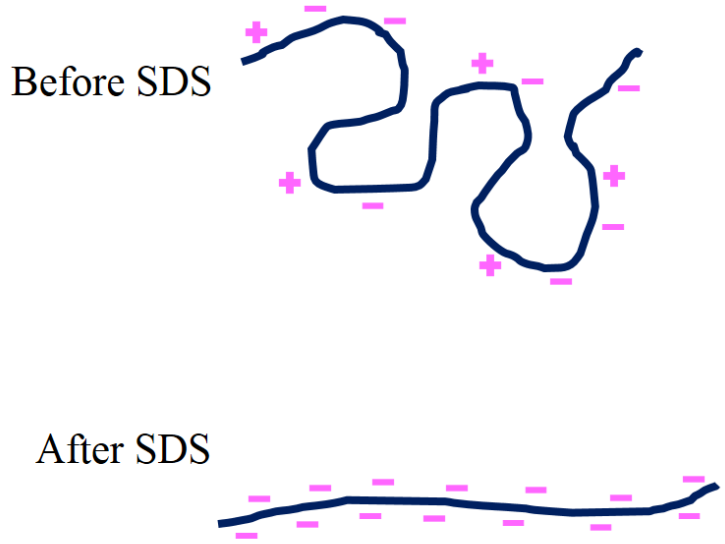

Figure 2.9: The charge of proteins before and after application of SDS. Proteins naturally have positively and negatively charged R-groups; SDS is an anion which alters the charge of proteins to negative, regardless of its previous charge (Prepared by Author).

Denatured protein samples were then separated via SDS-PAGE (Figure 2.10). Firstly, 7.5% resolving gel was prepared [dH_2O, 1.5 M Tris, 10% SDS, Bis/acrylamide, 10% ammonium persulphate (APS), tetramethylene diamine (TEMED)] and allowed to polymerise (1 h). The decomposition catalyst, TEMED, initiates the addition of monomers to Bis/acrylamide, a cross-linking agent, in a head-to-tail fashion. The free radical donor, APS, catalyses the polymerisation which creates a porous gel matrix for protein migration. Thereafter, 4% stacking gel was prepared (dH_2O, 0.5 M Tris, 10% SDS, Bis/acrylamide, 10% APS, TEMED) and added on top of the resolving gel (1 h). The percentage of the resolving gel is higher (more cross-linking) as the gel will have smaller pores to yield more distinct bands, especially for low molecular weight proteins. Protein samples were then subjected to an electric field (150 V, 1 h) using a Bio-Rad compact power supply. To facilitate the electric field by providing conducting ions, 1 x running (electrode) buffer (dH_2O, Tris, glycine, SDS, 4°C) was used during electrophoresis (Yang and Ma, 2009).

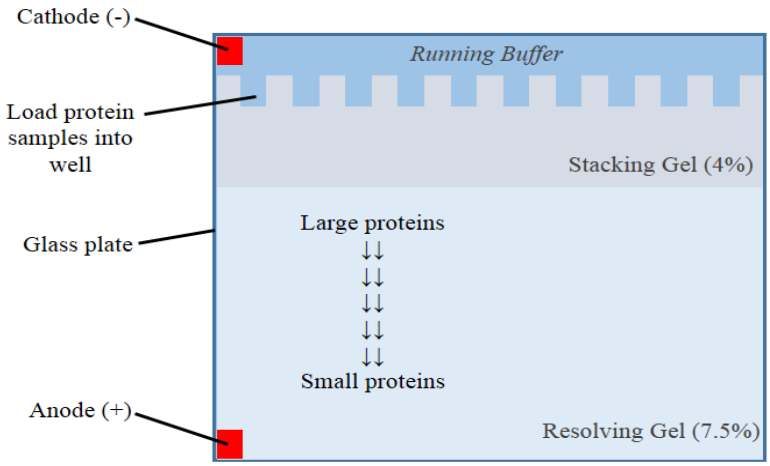

Figure 2.10: The setup of the electrophoresis apparatus. Migration of proteins through a gel subject to an electric field to allow for separation of proteins based on size (Prepared by Author).

Electrotransfer-

Electrophoresed protein bands were then electro-transferred from the gel to a nitrocellulose membrane. Electrotransfer involves equilibrating the membranes, fibre pads and gels in transfer buffer (dH_2O, Tris, glycine, methanol, pH 8.3, 4°C) for 10 min. This is followed by sandwiching the gel against the membrane enclosed in fibre pads and sponges and immersion in transfer buffer subject to a current (400 mA, 1 h) (Figure 2.11) (Yang and Ma, 2009).

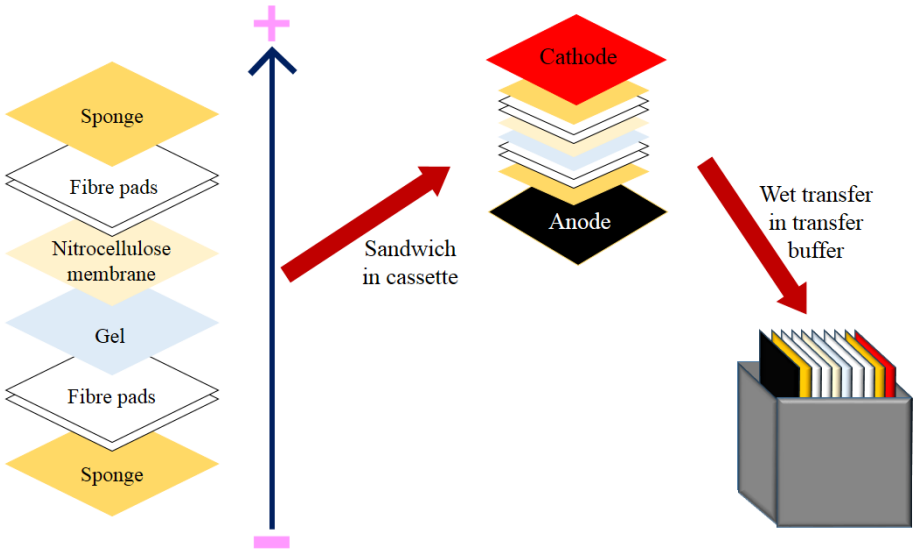

Figure 2.11: Preparation of protein transfer. Assembly of sandwich comprising of the gel and membrane covered in sponges and fibre pads to allow for transfer of proteins from gel to membrane as current moves from the negative to positive electrode (Prepared by Author).

Immunoprobing-

Upon completion of protein transfer to a membrane, the target protein was immunoprobed using specific Abs (Figure 2.12). Prior to immune-probing, it was necessary to block the membranes where the protein did not bind to prevent non-specific binding of antibodies. The membrane was submerged in 5% BSA in Tris-buffered saline [dH_2O, Tris-HCl (pH 7.4), NaCl] containing 0.5% Tween20 (TTBS) for 1 h (RT). Thereafter, the membranes were incubated with primary (1°) Abs [Bax (610982), Bcl-2 (2827), Smac/DIABLO (110291), Cleaved PARP-1 (9541); 1:1,000] for 1 h at RT and then at 4°C overnight, to allow for binding of the antibody to its specific target protein. The membranes were then equilibrated to RT and subsequently washed for ~1 h (5 washes, 10-15min each) with TTBS to wash off excess Abs that did not bind to target proteins (Yang and Ma, 2009).

This was followed by immunodetection probing with a secondary (2°) Ab to the 1° Ab. The 2° Ab is conjugated to an enzyme, which is usually horse radish peroxidase (HRP) or alkaline phosphatase, to allow for detection of the protein which the Ab has bound to. The membranes were exposed to HRP-conjugated 2° Ab [goat anti-rabbit (7076S) Bax, Bcl-2, Smac/DIABLO (1:5,000), cleaved-PARP-1 (1:10,000)] for 1 h on the shaker, at RT. The membranes were washed again for ~1 h (5 washes, 10-15min each) with TTBS. The next part of immunodetection involved developing the membrane by adding a substrate that HRP recognises (Yang and Ma, 2009). The Clarity Western Enhanced Chemiluminescence (ECL) Substrate (catalog no. 1705061, Bio-Rad) was used to detect the reaction (Figure 2.13), in the Alliance 2.7 Image Documentation System (UViTech). Protein expression was analysed using UviBand Advanced Image Analysis software v12.14 (UViTech).

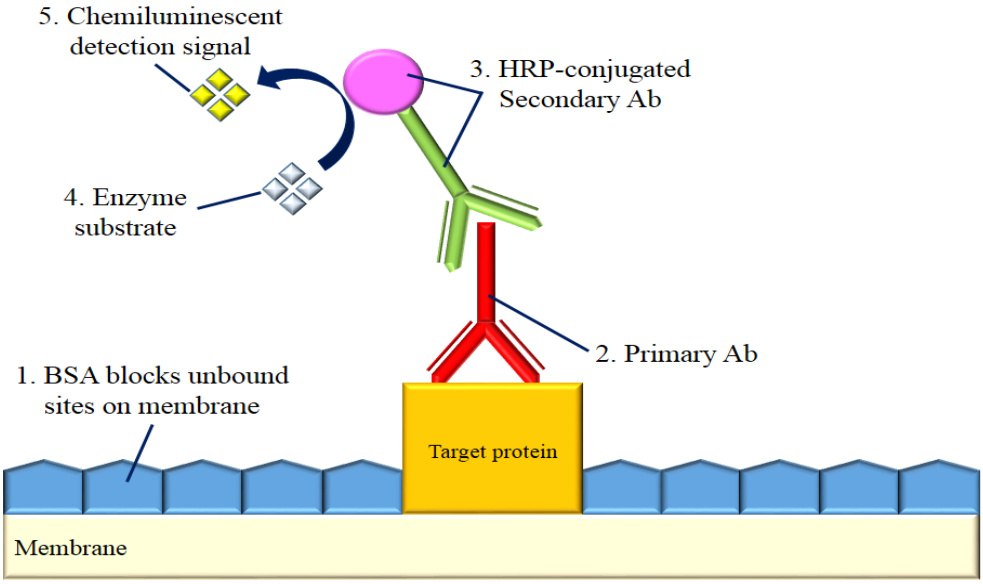

Figure 2.12: Principle of immunoprobing and immunodetection. Unoccupied sites on the membrane are blocked followed by 1° Ab binding to a specific target protein. An enzyme-conjugated 2° Ab then binds to the 1° Ab. The enzyme is developed by a substrate to allow for chemiluminescence detection (Prepared by Author).

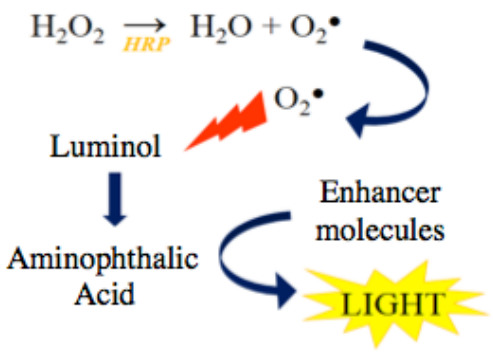

Figure 2.13: Reactions defining immunodetection using the ECL substrate. HRP catalyses the conversion of H_2O_2 to form water and $O_2^{\bullet}$. Luminol is oxidised by $O_2^{\bullet}$ to form aminophthalic acid, which reacts with enhancer molecules to produce detectable light (Prepared by Author).

The membranes were washed using TTBS (3 washes, 10 min each), quenched using 5 ml H_2O_2 (30 min, 37°C) and washed again (3 washes, 10 min each) before blocking in 5% BSA (1 h). Thereafter, the membranes were re-probed with a housekeeping protein, HRP-conjugated-anti-β-actin [(A3854, 1:5,000) Sigma, St Louis, Missouri, USA] for 1 h at RT to normalise protein expression and control for loading error (Liu *et al.*, 2014). Data was expressed as mean relative band density (RBD) and fold change, relative to the control and housekeeping protein.

2.11 Comet assay

2.11.1 Introduction

The Comet, or single cell gel electrophoresis (SCGE), assay is used to detect DNA fragmentation in individual cells. DNA fragmentation is a late characteristic of apoptosis, a result of the chain reaction that occurs due to the caspase cascade. Healthy, undamaged DNA maintains a highly organised, supercoiled structure within the nucleus whilst damaged DNA loses its structural organisation and migrates out of the nucleus when subjected to an electric field. This principle forms the basis of the Comet assay (Figure 2.14). When an electric field is applied to cells embedded in agarose gel, DNA migration out of the nucleus forms a 'comet', where the head contains intact, undamaged DNA and the tail contains damaged, fragmented DNA. The Comet assay utilises fluorescence to visualise the presence and extent of DNA damage (Singh *et al.*, 1988).

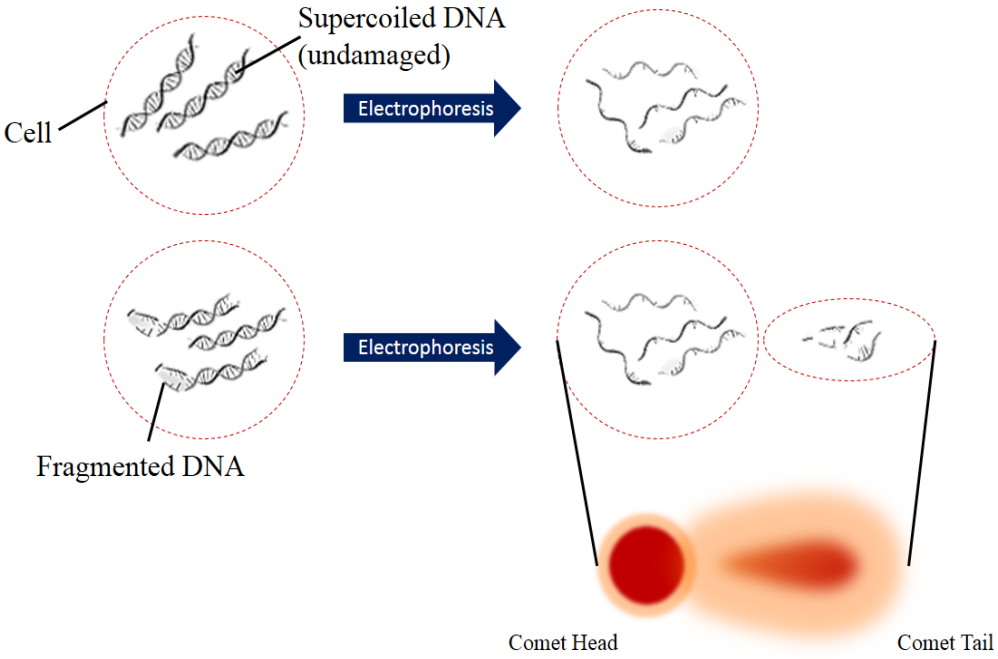

Figure 2.14: Principle of the Comet assay. Electrophoresis of intact DNA results in uncoiling of DNA, whilst that of fragmented DNA results in migration of damaged DNA out of the nuclear cavity forming a comet (Prepared by Author).

2.11.2 Protocol

Cells were encapsulated in low melting point agarose (LMPA). Briefly, three microscope slides with frosted ends per control and treatment were prepared: the first layer contained 1% LMPA (400 µl, 37°C) which was incubated for 10 min at 4°C; the second layer contained cell suspension (20,000 cells in 25 µl 0.1 M PBS), GelRed™ nucleic acid gel stain (1µl) (Biotium, California, cat. no. 41003) and 0.5% LMPA (175 µl, 37°C) which solidified in 10 min at 4°C; the third layer contained 0.5% LMPA (200 µl, 37°C) which was incubated for 10 min at 4°C. The layered gels were covered with coverslips (Singh *et al.*, 1988).

The subsequent step involved lysing the cell membranes to allow for permeation of fragmented DNA out of the cell. Coverslips were removed and solidified gels were submerged in cold cell lysis buffer [100 mM EDTA, 2.5 M NaCl, 1% Triton X-100, 10% DMSO, and 10 mM Tris (pH 10)] and incubated (1 h, 4°C, dark). Thereafter, the slides were submerged in electrophoresis buffer [1 mM Na_2EDTA (pH 13) and 300 mM NaOH] for 20 min at RT to allow for equilibration prior to electrophoresis (300 mA, 25 V, 35 min, RT) using a Bio-Rad compact power supply (Singh *et al.*, 1988).

The slides were rinsed three times (5 min each) (0.4 M Tris, pH 7.4) to neutralise the samples prior to replacement of coverslips. The slides were then viewed using a fluorescent microscope (Olympus IX51 inverted microscope, excitation: 510-560 nm; emission 590 nm). Images of 50 cells and comets were captured in total from three slides per control/treatment. Lengths of cells and comet tails were measured using Soft imaging system (Life Science - ©Olympus Soft Imaging Solutions v5) and reported in µm as average tail lengths (Singh *et al.*, 1988).

2.12 Hoechst Assay

2.12.1 Introduction

Hoechst 33342 is a water soluble and cell permeable dye that fluoresces blue (Figure 2.15). The dye binds to minor grooves of double stranded (ds) nucleic acids, specifically the adenine-thymine (AT)-rich regions. Hoechst likewise binds to guanine-cytosine (GC)-rich regions on DNA, but fluorescence is enhanced by two-fold when bound to AT-rich regions of dsDNA. Binding affinity of the dye is also higher to AT-rich regions rather than GC-rich regions. Hoechst fluorescence (excitation- 350 nm, emission- 461 nm) is sensitive to the conformation of DNA and chromatin structures; hence it can detect the extent of damaged nuclear components. In a cell undergoing apoptosis, the Hoechst dye is used to visualise apoptotic bodies, fragmented DNA and hypercondensed chromatin (Vekshin, 2011).

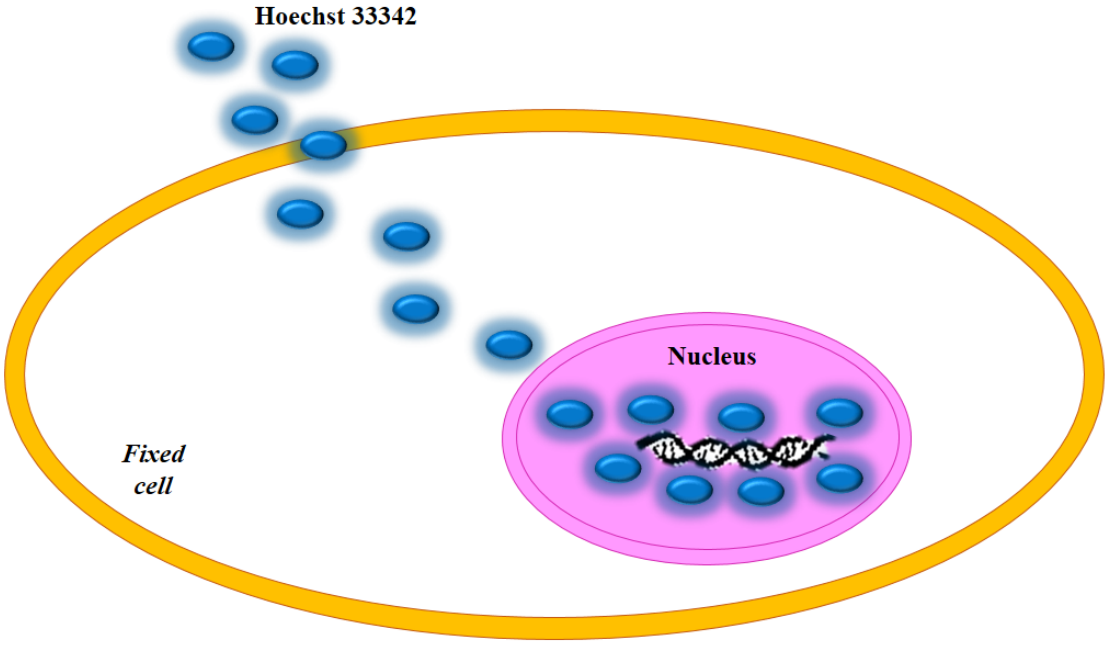

Figure 2.15: Hoechst 33342 staining of nucleus. Hoechst dye permeates the cell membrane and enters the nucleus where it binds to dsDNA and fluoresces blue (Prepared by Author).

2.12.2 Protocol

Nuclear structure and cellular morphology was assessed in SNO cells treated with FA by staining with Hoechst 33342 (H3570) (Invitrogen™, Eugene, Oregon, USA). Cells were seeded (500,000 cells) into a 6-well plate and treated in triplicate for 24 h. Cells were thereafter washed three times (0.1 M PBS) and fixed in 10% paraformaldehyde (PFA) (5 min) to preserve the cells. The cells were washed again (0.1 M PBS) to remove excess PFA. Hoechst working solution (5 µg/ml in 0.1 M PBS) was added and incubated (15 min, 37°C). Prior to viewing, cells were washed to remove any dye that did not bind to nucleic acids in the sample. Images were captured using a fluorescent microscope (excitation- 350 nm, emission- 450 nm). Ten images per treatment replicate were captured at magnifications 10x and 20x (Vekshin, 2011).

2.15 Statistical analysis

Statistical analyses were carried out using GraphPad Prism v5.0 software (GraphPad Software Inc., La Jolla, USA). The concentration-response-inhibition equation produced an IC_{50} for MTT assay. The statistical significances were determined by unpaired t-test with Welch's correction (results reported as mean ± standard deviation (SD)) and a 95% confidence interval with a *p* value of less than 0.05.

CHAPTER 3

Results

3.1 Metabolic activity & cell viability

3.1.1 Methylthiazol tetrazolium (MTT) assay

The MTT assay was used to measure FA toxicity in SNO cells over 24 h. Serial dilutions of FA (0-500 µg/ml) was used to determine a dose response (Addendum A). Analysis of the dose response curve revealed that a concentration of 78.81 µg/ml was sufficient to cause 50% of SNO toxicity (IC_{50}) and this concentration of FA was used in all subsequent assays (Figure 3.1).

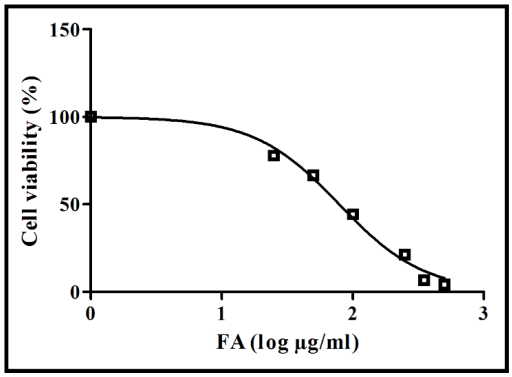

Figure 3.1: FA induced a dose-dependent decrease in SNO cell viability following treatment for 24 h. Data represented as a percentage of viable cells relative to the untreated control. Higher concentrations showed increased cell death rates.

3.1.2 ATP quantification

The concentration of ATP in SNO cells was assessed via luminometry. The ATP levels were significantly reduced by FA with a 1.16-fold decrease (3,628,000 ± 79,920 RLU) compared to the control (4,212,000 ± 120,900 RLU; $p = 0.006$) (Figure 3.2).

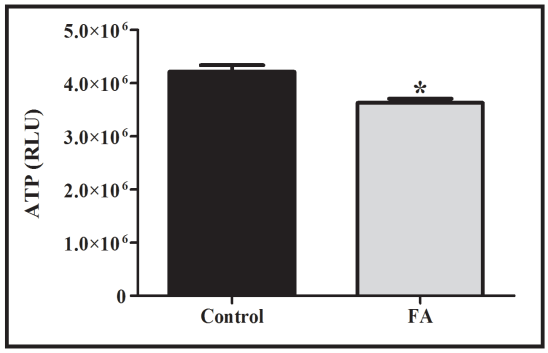

Figure 3.2: Levels of ATP in control vs FA treated SNO cells. FA significantly decreased ATP levels ($p = 0.006$) after 24 h. RLU: relative light units. *$p < 0.05$ relative to control.

3.2 Oxidative stress

3.2.1 Lipid peroxidation

Lipid peroxidation induced by ROS was measured by quantifying the extracellular MDA, i.e. the end product of lipid peroxidation, as an indicator of oxidative stress. FA increased levels of extracellular MDA by a significant 1.23-fold (1.242 ± 0.03 µM) compared to that of control cells (1.007 ± 0.003 µM, $p = 0.0166$) (Figure 3.3).

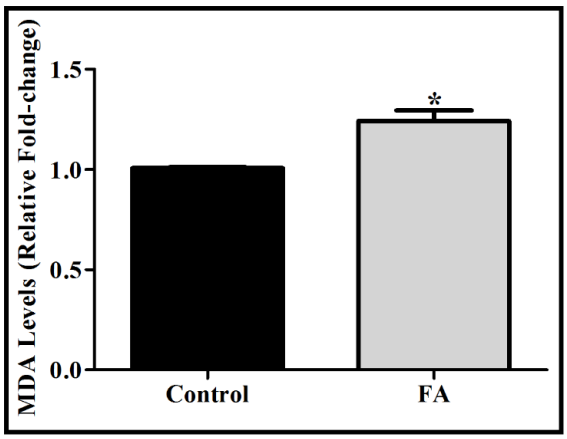

Figure 3.3: FA increased levels of extracellular MDA. MDA: malondialdehyde. *$p < 0.05$ relative to control.

3.2.2 Antioxidant response

Reduced glutathione (GSH) levels were measured as an indicator of endogenous antioxidant capacity. Lipid peroxidation was concomitant with decreased levels of intracellular GSH (1.62-fold) in FA treated SNO cells (0.617 ± 0.006 µM) compared to that of the control (1.01 ± 0.006 µM, $p < 0.0001$) (Figure 3.4).

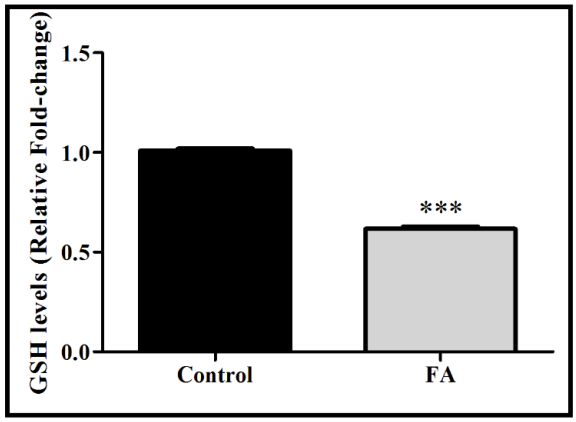

Figure 3.4: FA significantly reduced levels of intracellular GSH ($p < 0.0001$). GSH: reduced glutathione. ***$p < 0.0001$ relative to control.

3.3 Reduced membrane integrity

3.3.1 Increased extracellular LDH

Extracellular LDH levels were quantified using the LDH cytotoxicity detection kit. FA induced significant SNO cell membrane damage when compared to control SNO cells as measured by increased extracellular LDH levels (control: 1.849 ± 0.018 OD; FA: 2.122 ± 0.004 OD, p = 0.002) (Figure 3.5).

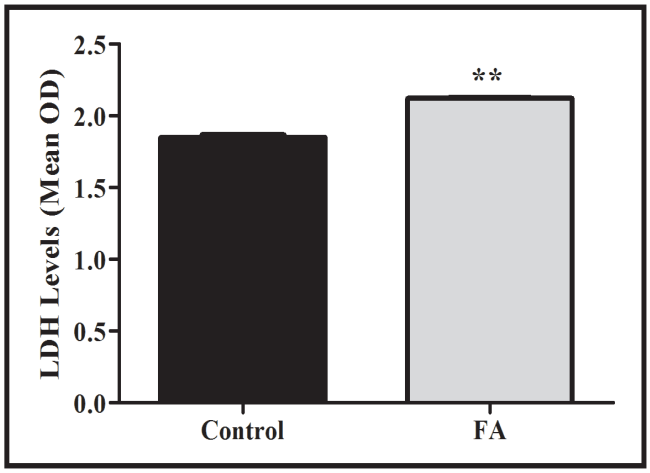

Figure 3.5: FA significantly increased LDH leakage in SNO cells indicative of membrane damage. FA is cytotoxic to SNO cells. LDH: lactate dehydrogenase, OD; optical density. **p < 0.005 relative to control.

3.4 Apoptotic induction

3.4.1 Protein expression of Bax, Bcl-2, Smac/DIABLO and cleaved-PARP-1

Expression of pro- and anti-apoptotic proteins were measured via Western blotting. FA induced a significant 1.08-fold increase in Bax expression (0.0726 ± 0.0008 RBD vs. control: 0.0675 ± 0.0005 RBD, p = 0.0138) [Figure 3.6 (A)]; a 1.02-fold increase in Smac/DIABLO expression (1.026 ± 0.0287 RBD vs. control: 1.003 ± 0.003 RBD) [Figure 3.6 (C)]; a significant 1.24-fold decrease in Bcl-2 expression (0.8131 ± 0.0176 RBD vs. control: 1.010 ± 0.0058 RBD, p = 0.0087) [Figure 3.6 (B)], and a significant 1.53-fold increase in the 24 kDa fragment of PARP-1 (2.02 ± 0.077 RBD vs. control: 1.325 ± 0.1117 RBD, p = 0.0143), indicating DNA damage [Figure 3.6 (D)].

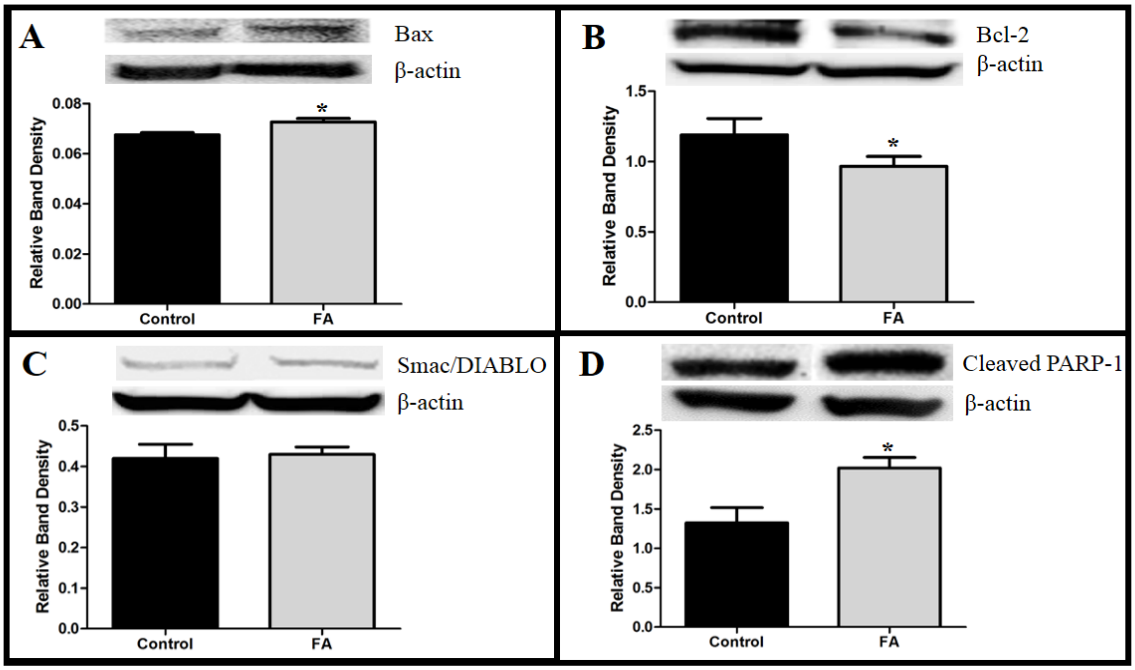

Figure 3.6: FA regulates protein expression of **A.** Bax ($p < 0.05$), **B.** Bcl-2 ($p < 0.05$), **C.** Smac/DIABLO and **D.** cleaved PARP-1 ($p < 0.05$) in SNO cells after treatment for 24 h. Pro-apoptotic protein expression was upregulated (Bax) with the same protein expression of Smac/DIABLO in treated and untreated cells, while anti-apoptotic protein expression was reduced (Bcl-2), indicating apoptotic induction. Increased expression of the 24 kDa fragment of PARP-1 showed that DNA strand breaks were not repaired by the PARP-1 enzyme resulting in DNA fragmentation. *$p < 0.05$ relative to the control.

3.5 Caspase activation

3.5.1 Initiator and executioner caspase activation

The activity of caspase-3/7, -8 and -9 were assessed via luminometry. FA significantly increased the activity of all caspases measured: caspase-3/7 by 1.17-fold ($p = 0.0306$) [Figure 3.7 (C)]; caspase-8 by 1.34-fold ($p = 0.013$) [Figure 3.7 (A)] and caspase-9 by 1.24-fold ($p = 0.0059$) in SNO cells [Figure 3.7 (B)]. FA induced caspase-dependent apoptosis in SNO cells after 24 h.

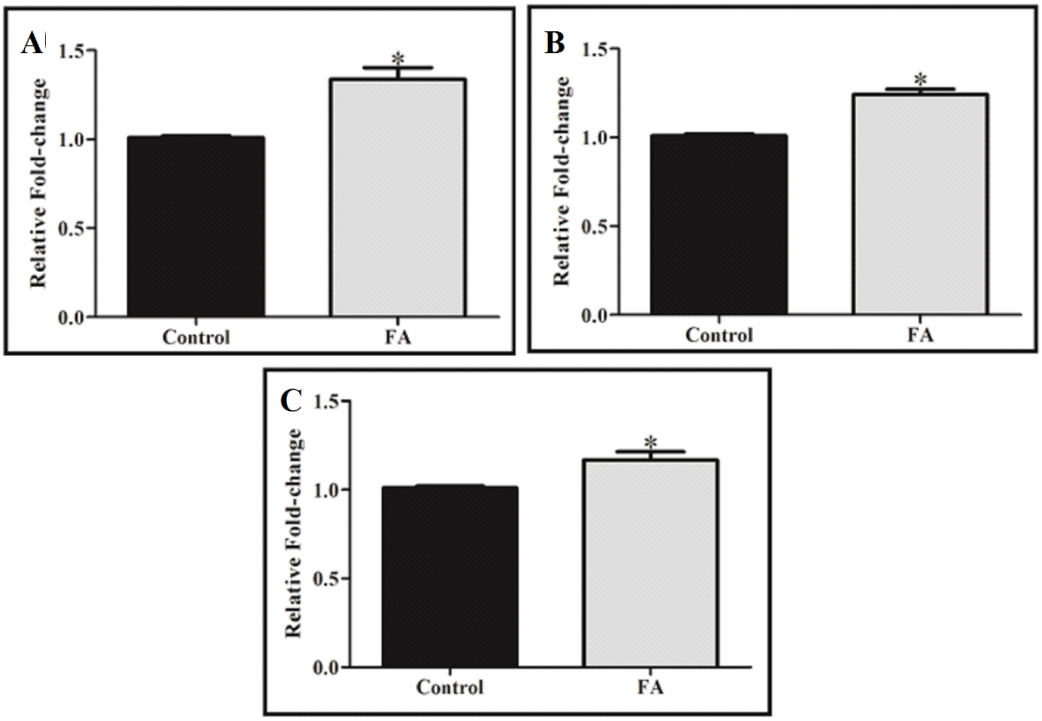

Figure 3.7: FA significantly influenced caspase activity. Activity of **A.** initiator caspase-8 and **B.** caspase-9, as well as **C.** executioner caspase-3/7 were significantly elevated in FA treated SNO cells ($p < 0.05$) compared to the control. *$p < 0.05$ relative to the control.

3.6 Late stages of apoptosis

Late stages of apoptosis are characterised by hypercondensed nuclei, apoptotic body formation and DNA fragmentation. Hoechst staining showed higher cell density and healthy cells undergoing various stages of mitosis in the untreated control [Figure 3.8 (A)], while FA induced nuclear condensation, apoptotic body formation and DNA fragmentation in SNO cells after 24 h [Figure 3.8 (B)].

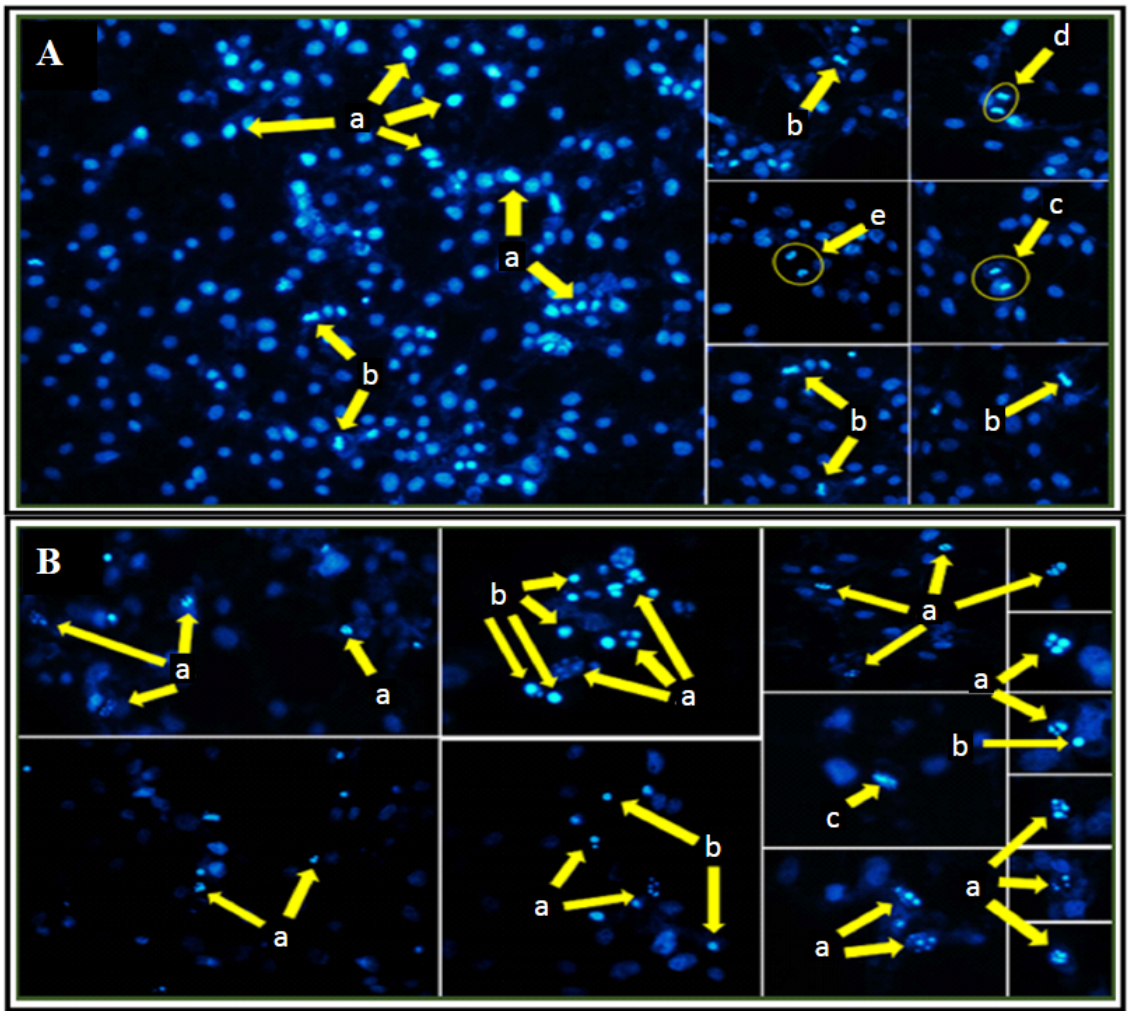

Figure 3.8: Nuclear morphology of untreated SNO cells vs FA treated SNO cells. **A.** Uptake of Hoechst 33324 stain by untreated SNO cells showing (a) early prophase, (b) metaphase, (c) late anaphase, (d) early telophase and (e) late telophase. **B.** FA induced (a) apoptotic body formation, (b) chromatin condensation, (c) DNA fragmentation and reduced SNO cell density as compared to control (20x).

3.7 Damage of nuclear components

3.7.1 DNA damage

The comet assay was used to detect fragmented DNA in SNO cells, where longer comet tails indicate a greater extent of DNA fragmentation. Figure 3.9 (B) shows significantly longer comet tails in FA treated cells (5.926 ± 0.0795 µm) compared to control cells (3.092 ± 0.2102 µm, $p < 0.0001$) [Figure 3.9 (A)].

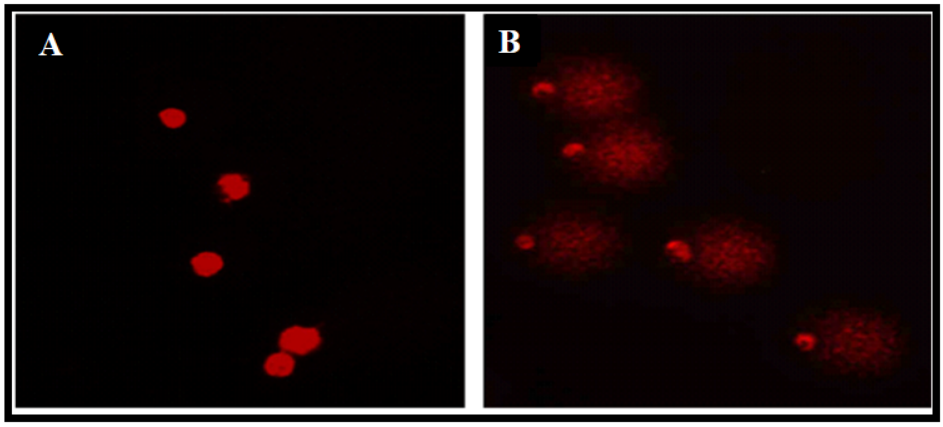

Figure 3.9: DNA damage induced by FA. DNA fragmentation was increased in **B.** FA treated cells with longer comet tails (***) compared to **A.** control cells with larger comet heads containing intact DNA (40x). ***$p < 0.0001$ relative to control.

CHAPTER 4

4.1 Discussion

FA, a mycotoxin produced by the ubiquitous soil fungus, *Fusarium heterosporum*, is a major contaminant of maize and maize products (Bacon *et al.*, 1996). Consumption of mycotoxin-contaminated maize as a staple may contribute to the high incidence of OC worldwide, and especially among black South African men. FA is known to have low to moderately toxic effects in plants and has been suggested as a causative agent of OC (Nedělník, 2002), however the effects of FA in humans has not yet been conclusively explored. It was hypothesised that FA induces cytotoxic effects on SNO cancer cells upon acute exposure.

The mitochondrion is a major metabolic cellular organelle performing several key functions including aerobic respiration which is responsible for generating cellular energy. The MTT assay measures metabolic activity of the mt respiratory chain by quantifying the ratio of reducing equivalents to oxidising equivalents in the cell (Mosmann, 1983). FA revealed a dose-dependent decrease in cellular metabolic activity and viability in SNO cells as observed by the MTT assay (Figure 3.1). Reduced metabolic activity may be due to a decrease in the rate of the Kreb's cycle that leads to a decreased output of reducing equivalents and ATP (Telles-Pupulin *et al.*, 1998). These reducing equivalents are required by the mt respiratory chain within the mt membrane, as well as for MTT salt reduction to generate a formazan product (Mossmann, 1983).

The disruption of the mt respiratory chain leads to a disruption of the mt membrane proton gradient, which is essential for functioning of ATPase to generate ATP. The butyl tail of FA impairs the activity of cytochrome *c* oxidase, resulting in slow movement of electrons and uncoupling of the respiratory chain from ATP synthesis (Gäumann, 1958). FA also decreases the activity of succinate dehydrogenase and α-ketoglutarate dehydrogenase in the Kreb's cycle, further contributing to dissipation of the proton gradient (Telles-Pupulin *et al.*, 1998). Thus, the alteration in the cellular NADH/NADPH reductase system corresponds with the significant decrease in ATP by FA in SNO cells (Figure 3.2). Recent work by Sheik Abdul *et al*. proposed that FA induced oxidative and mitochondrial stress in the hepatocellular carcinoma $HepG_2$ cell line (Sheik Abdul *et al.*, 2016).

Mitochondria are also major ROS producing organelles and are prone to oxidative damage. Limited electron transfer as a result of mt membrane disruption leads to excessive production of ROS. Increased ROS, coupled with a decrease in the endogenous antioxidant GSH leads to oxidative stress, accompanied by the oxidation of DNA and lipids (Circu and Aw, 2010). FA significantly increased the level of ROS-induced lipid peroxidation (Figure 3.3) and simultaneously decreased levels of GSH, compared to control cells (Figure 3.4). FA thereby disrupts the mt membrane of SNO cells and processes that occur within it, leading to oxidative stress.

Lipid peroxidation disrupts cellular membrane integrity. Membrane disintegration may be accentuated by damage caused by the lipid-soluble butyl tail of FA as it penetrates through the cell membrane (Dowhan, 1997, Fernández-Pol, 1998). FA also has the ability to chelate divalent cations between the N atom of the pyridine ring and the carboxyl radical (Gäumann, 1958). Divalent cations, particularly Ca^{2+} and Zn^{2+}, interact with membranous phospholipids to allow for the essential process of signal transduction (Träuble and Eibl, 1974). Furthermore, these cations are referred to as protective molecules of the membrane, as they prevent alterations in

membrane permeability subsequent to breach by toxins. Therefore, this chelating effect contributes to cell membrane damage (Bashford *et al.*, 1986).

To assess the integrity of the cell membrane, extracellular levels of LDH were measured, since LDH is exclusively found in the cytoplasm and only exits the cell through damaged membranes (Watanabe *et al.*, 1995). The significant increase in extracellular LDH levels (Figure 3.5) confirmed that FA disrupts the cellular membrane of SNO cells. Thus both the mt membrane and cell membrane of SNO cells are affected by FA.

Since FA affected the mt membrane, the expression of mt proteins were analysed. The Bcl-2 family of proteins, particularly Bax and Bcl-2 are important in apoptosis, as MPTPs in the mt membrane consist of and are regulated by Bax and Bcl-2. Bax, a pro-apoptotic protein which is inhibited by Zn^{2+}, induces the formation of MPTPs by interacting with lipids in the OMM (Ganju and Eastman, 2003). FA significantly increased Bax protein expression [Figure 3.6 (A)]. This suggests a role of FA in Zn^{2+} chelation, as this would allow for Bax activation. Bcl-2 is an anti-apoptotic protein and inhibitor of Bax (Hockenbery *et al.*, 1990). FA caused a significant decrease in Bcl-2 expression [Figure 3.6 (B)], thus preventing its inhibitory effect on Bax activation.

Upon formation of MPTPs, mt pro-apoptotic proteins such as Cyt *c* and Smac/DIABLO are released into the cytoplasm. Cyt *c* binds to Apaf-1, which recruits pro-caspase-9 to form an ATP-requiring apoptosome. This apoptosome cleaves pro-caspase-9 to form active caspase-9, the initiator caspase of the intrinsic pathway. Caspase-9 activates executioner caspase-3/7, which mediates proteolysis of apoptotic cells. Caspase-8, the initiator caspase of the extrinsic pathway, activates Bid which activates Bax. The pro-apoptotic protein, Smac/DIABLO, functions to inhibit the activity of IAPs, which inhibit caspase-3/7 and -9 (Ashkenazi and Dixit, 1998, Green and Reed, 1998, Guicciardi and Gores, 2005). Levels of Smac/DIABLO were the same in control and FA-treated cells [Figure 3.6 (C)]. FA significantly increased the activation of caspases -3/7, -8 and -9 (Figure 3.7) in SNO cells, compared to control cells.

Active caspase-3/7 cleaves the 75 kDa subunit of complex I of the ETC disrupting electron transport and mt membrane permeability (Ricci *et al.*, 2004), further increasing ROS production, ATP depletion and mt damage.

PARP-1, an ATP-dependent Zn-finger endonuclease, is activated by caspase-3/7 and binds to breaks of internucleosomal DNA. PARP-1 is a 113 kDa protein, which when cleaved, forms an 89 kDa and a 24 kDa fragment. PARP-1 also contains a Zn-finger domain which can be chelated by FA, which causes PARP-1 cleavage and renders PARP-1 ineffective in its DNA binding and repair activity (Kaufmann *et al.*, 1993). Zn inhibits PARP-1 cleavage and is therefore essential to allow for the binding of PARP-1 to DNA strand breaks. This is achieved by Zn inhibition of the catalytic function of caspase-3/7 by interaction with either or both of the conserved sites, Cys-285 and His-237. This is another mechanism by which Zn chelation would allow for PARP-1 cleavage to occur (Perry *et al.*, 1997). A significant increase in the expression of the 24 kDa fragment of PARP-1 indicates that PARP-1 is cleaved by FA and contributes to DNA damage [Figure 3.6 (D)]. This result may be due to the chelating effect of FA on Zn and hence the significant increase in caspase-3/7 activity.

DNA damage was assessed which showed FA treated cells had fragmented DNA as longer tails [Figure 3.9 (B)] compared to intact DNA in the control cells [Figure 3.9 (A)]. Other late stages of apoptosis include condensation and damage of nuclear components followed by formation of apoptotic bodies (Edinger and Thompson, 2004). Figure 3.8 (B) shows that FA induced

hypercondensation of nuclei, DNA fragmentation and resulted in the formation of a substantial amount of apoptotic bodies in SNO cells, compared to the untreated control [Figure 3.8 (A)].

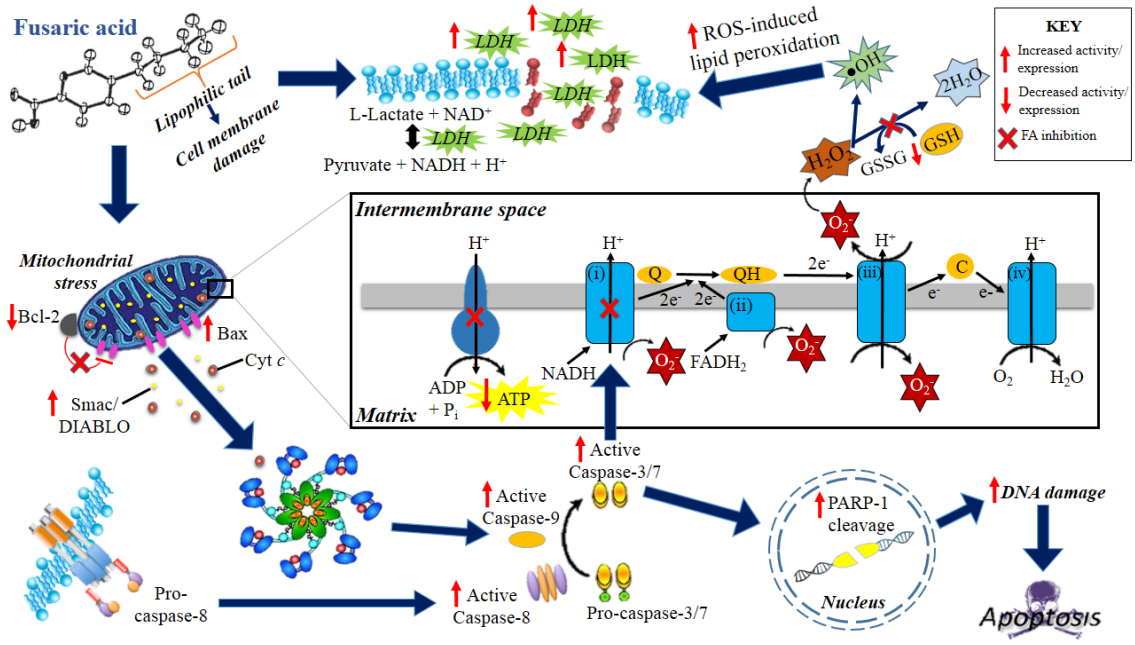

Figure 4: Schematic overview of the biochemical effects of FA on membrane integrity, oxidative stress and apoptosis in human cancerous oesophageal SNO cells (Prepared by Author).

4.2 Conclusion and Recommendations

FA is a major contaminant of maize and has been suggested as an aetiological agent of OC. However, the mechanism by which FA causes cytotoxicity in oesophageal cells has not been elucidated. In this study, the cytotoxic effects in the SNO cell line were determined (Figure 4).

Results showed that FA induced oxidative stress by increasing the level of ROS-induced lipid peroxidation and concomitantly reducing antioxidant response, which simultaneously resulted in membrane damage. Disruption of mt activity was associated with decreased output of reducing equivalents and low ATP levels. Collectively, these events triggered the recruitment of apoptotic machinery which compromised DNA integrity and averted its repair, leading to cell death via both intrinsic and extrinsic apoptosis. Taken together, FA is a cytotoxic agent to human oesophageal SNO cells. Understanding the mechanism of toxicity of FA in humans may aid in preventing and treating the outcomes of consuming FA-contaminated agricultural produce.

Chelation by FA was not tested in this study as the assay was not entirely optimised for the SNO cell line. Based on present findings, further studies are required to determine if the chelating effects of FA are associated with the outcomes of this study, particularly the effect of Zn chelation on Zn-finger proteins such as PARP-1, p53, SOD and IAP. The consistency of FA in other cell lines (including normal oesophageal cells) must be established as this study serves as a preliminary study. Further studies on the effects of FA are needed using an *in vivo* laboratory animal model.

REFERENCES

Asakawa, T. and Matsushita, S. (1979). Thiobarbituric acid test for detecting lipid peroxides. *Lipids* 14(4): 401-406.

Ashkenazi, A. and Dixit, V. M. (1998). Death receptors: signaling and modulation. *Science* 281(1): 1305-1308.

Bachmann, E. (1956). The influence of fusaric acid on the water permeability of plant protoplasts. Diss. Natural Sciences. Switzerland, ETH Zürich. Doctoral dissertation.

Bacon, C. W., Porter, J. K., Norred, W. P. and Leslie, J. F. (1996). Production of fusaric acid by *Fusarium* species. *Applied and Environmental Microbiology* 62(11): 4039-4043.

Bainor, A., Chang, L., McQuade, T. J., Webb, B. and Gestwicki, J. E. (2011). Bicinchoninic acid (BCA) assay in low volume. *Analytical Biochemistry* 410(2): 310-312.

Ballo, R. M. and Millikan, K. W. (2015). Esophageal Cancer. Common Surgical Diseases. New York, Springer 133-135.

Bashford, C. L., Alder, G. M., Menestrina, G., Micklem, K. J., Murphy, J. J. and Pasternak, C. C. (1986). Membrane damage by hemolytic viruses, toxins, complement, and other cytotoxic agents. A common mechanism blocked by divalent cations. *Journal of Biological Chemistry* 261(20): 9300-9308.

Bergman, J. (1999). ATP: The perfect energy currency for the cell. *Creation Research Society Quarterely* 36(1): 2-9.

Betteridge, D. J. (2000). What is oxidative stress? *Metabolism* 49(2): 3-8.

Bey, E., Alexander, J., Whitcutt, J. M., Hunt, J. A. and Gear, J. H. S. (1976). Carcinoma of the esophagus in Africans: Establishment of a continuously growing cell line from a tumor specimen. *In Vitro* 12(2): 107-114.

Brand, M. D. and Nicholls, D. G. (2011). Assessing mitochondrial dysfunction in cells. *Biochemical Journal* 435(1): 297-312.

Bravi, F., Edefonti, V., Randi, G., Garavello, W., La Vecchia, C., Ferraroni, M., Talamini, R., Franceschi, S. and Decarli, A. (2012). Dietary patterns and the risk of esophageal cancer. *Annals of Oncology* 23(3): 765–770.

Cathcart, R., Schwiers, E., Saul, R. L. and Ames, B. N. (1984). Thymine glycol and thymidine glycol in human and rat urine: a possible assay for oxidative DNA damage. *Proceedings of the National Academy of Sciences* 81(18): 5633-5637.

Chai, J., Du, C., Wu, J., Kyin, S., Wang, X. and Shi, Y. (2000). Structural and biochemical basis of apoptotic activation by Smac/DIABLO. *Nature Reviews Cancer* 406(1): 855-862.

Circu, M. L. and Aw, T. Y. (2008). Glutathione and apoptosis. *Free Radical Research* 42(8): 689-706.

Circu, M. L. and Aw, T. Y. (2010). Reactive Oxygen Species, Cellular Redox Systems and Apoptosis. *Free Radical Biological Medicine* 48(6): 749-762.

Cousin, M. A., Riley, R. T., and Pastka, J. J. (2005). Foodborne mycotoxins: Chemistry, Biology, Ecology, and Toxicology. *Caister Academic Press* 163-226.

Crook, N. E., Clem, R. J. and Miller, L. K. (1993). An apoptosis-inhibiting baculovirus gene with a zinc finger-like motif. *Journal of Virology* 67(4): 2168-2174.

Dalle-Donne, I., Giustarini, D., Colombo, R., Rossi, R. and Milzani, A. (2003). Protein carbonylation in human diseases. *Trends in Molecular Medicine* 9(1): 169-176.

Dar, N. A., Islami, F., Bhat, G. A., Shah, I. A., Makhdoomi, M. A., Iqbal, B., Rafiq, R., Lone, M. M., Abnet, C. C. and Boffetta, P. (2013). Poor oral hygiene and risk of esophageal squamous cell carcinoma in Kashmir. *British Journal of Cancer* 109(5): 1367-1372.

de Almagro, M. C. and Vucic, D. (2012). The inhibitor of apoptosis (IAP) proteins are critical regulators of signaling pathways and targets for anti-cancer therapy. *Experimental Oncology* 34(3): 200-211.

Desagher, S., Osen-Sand, A., Nichols, A., Eskes, R., Montessuit, S., Lauper, S., Maundrell, K., Antonsson, B. and Martinou, J. C. (1999). Bid-induced conformational change of Bax is responsible for mitochondrial cytochrome *c* release during apoptosis. *The Journal of cell biology* 144(5): 891-901.

Dowhan, W. (1997). Molecular basis for membrane phospholipid diversity: Why are there so many lipids? *Annual review of biochemistry* 66(1): 199-232.

Edinger, A. L. and Thompson, C. B. (2004). Death by design: apoptosis, necrosis and autophagy. *Current Opinion in Cell Biology* 16(1): 663-669.

Evan, G. I. and Vousden, K. H. (2001). Proliferation, cell cycle and apoptosis in cancer. *Nature* 411(1): 342-347.

Fan, T., Han, L., Cong, R. and Liang, J. (2005). Caspase Family Proteases and Apoptosis. *Acta Biochimica et Biophysica Sinica* 37(11): 719-727.

Fernández-Pol, J. A. (1998). Antiviral Agent. U.S. Patent and Trademark Office. Washington, DC. 5,767,135: 1-13.

Fernández, J., Pérez-Álvarez, J. A. and Fernández-López, J. A. (1997). Thiobarbituric acid test for monitoring lipid oxidation in meat. *Food Chemistry* 59(3): 345-353.

Ganju, N. and Eastman, A. (2003). Zinc inhibits Bax and Bak activation and cytochrome *c* release induce by chemical inducers of apoptosis but not by death-receptor-initated pathways. *Cell Death and Differentiation* 10(6): 652-661.

Gäumann, E. (1958). The mechanism of fusaric acid injury. *Phytopathology* 48(1): 670-686.

Gerber, D. E. (2008). Targeted therapies: A new generation of cancer treatments. *American Family Physician* 77(3): 311-319.

Germain, M., Affar, E. B., D'Amours, D., Dixit, V. M., Salvesen, G. S. and Poirier, G. G. (1999). Cleavage of automodified poly(ADP-ribose) polymerase during apoptosis. *The Journal of Biological Chemistry* 274(40): 28379–28384.

Grant, R. S., Coggan, S. E. and Smythe, G. A. (2009). The physiological action of picolinic acid in the human brain. *International Journal of Tryptophan Research* 2(1): 71-79.

Green, D. R. and Kroemer, G. (2004). The pathophysiology of mitochondrial cell death. *Science* 305(1): 626-629.

Green, D. R. and Reed, J. C. (1998). Mitochondria and apoptosis. *Science* 281(5381): 1309-1312.

Gross, A., Jockel, J., Wei, M. C. and Korsmeyer, S. J. (1998). Enforced dimerization of BAX results in its translocation, mitochondrial dysfunction and apoptosis. *The EMBO Journal* 17(14): 3878-3885.

Guicciardi, M. E. and Gores, G. J. (2005). Apoptosis: a mechanism of acute and chronic liver injury. *Gut* 54(7): 1024-1033.

Gutteridge, J. M. C. (1995). Lipid peroxidation and antioxidants as biomarkers of tissue damage. *Clinical Chemistry* 41(1): 1819-1828.

Hamanaka, R. B. and Chandel, N. S. (2010). Mitochondrial reactive oxygen species regulate cell signaling and dictate biological outcomes. *Trends in Biochemical Sciences* 35(9): 505-513.

Hanahan, D. and Weinberg, R. A. (2011). Hallmarks of cancer: The next generation. *Cell* 144(1): 646-674.

Harris, M. H. and Thompson, C. B. (2000). The role of the Bcl-2 family in the regulation of outer mitochondrial membrane permeability. *Cell Death and Differentiation* 7(12): 1182-1191.

Hastings, J. W. (2014). The chemistry of bioluminescence. Current Topics in Bioenergetics. Sanadi, D. R. Boston, Massachusetts, Elsevier. 3.

Herceg, Z. and Wang, Z. (1999). Failure of poly(ADP-ribose) polymerase cleavage by caspases leads to induction of necrosis and enhanced apoptosis. *Molecular and Cellular Biology* 19(7): 5124-5133.

Hockenbery, D., Nunez, G., Milliman, C., Schreiber, R. D. and Korsmeyer, S. J. (1990). Bcl-2 is an inner mitochondrial membrane protein that blocks programmed cell death. *Nature* 348(1): 334-336.

Ježek, P. and Hlavatá, L. (2005). Mitochondria in homeostasis of reactive oxygen species in cells, tissues and organism. *The International Journal of Biochemistry & Cell Biology* 37(12): 2478-2503.

Jiao, J., Sun, L., Zhou, B., Gao, Z., Hao, Y., Zhu, X. and Liang, Y. (2014). Hydrogen peroxide production and mitochondrial dysfunction contribute to the fusaric acid-induced programmed cell death in tobacco cells. *Journal of Plant Physiology* 171(19): 1197-1203.

Kasai, H. (1997). Analysis of a form of oxidative DNA damage, 8-hydroxy-2'-deoxyguanosine, as a marker of cellular oxidative stress during carcinogenesis. *Mutation Research* 387(1): 147-163.

Kaufmann, S. H., Desnoyers, S., Ottaviano, Y., Davidson, N. E. and Poirier, G. G. (1993). Specific proteolytic cleavage of poly(ADP-ribose) polymerase: An early marker of chemotherapy-induced apoptosis. *Cancer Research* 53(1): 3976-3985.

Kelly, F. J. (2003). Oxidative stress: its role in air pollution and adverse health effects. *Occupational and Environmental Medicine* 60(8): 612-616.

Kerr, J. F., Wyllie, A. H. and Currie, A. R. (1972). Apoptosis: a basic biological phenomenon with wide-ranging implications in tissue kinetics. *British Journal of Cancer* 26(4): 239-257.

Langelier, M., Planck, J. L., Roy, S. and Pascal, J. M. (2012). Structural basis for DNA damage–dependent poly(ADP-ribosyl)ation by human PARP-1. *Science* 336(1): 728-732.

Liu, Z., Mahmood, T. and Yang, P. C. (2014). Western blot: technique, theory, and trouble shooting. *North American Journal of Medical Sciences* 6(3): 160.

Mahmood, T. and Yang, P. (2012). Western Blot: Technique, Theory, and Trouble Shooting. *North American Journal of Medical Sciences* 4(9): 429-434.

Masella, R., Di Benedetto, R., Vari, R., Filesi, C. and Giovannini, C. (2005). Novel mechanisms of natural antioxidant compounds in biological systems: Involvement of glutathione and glutathione-related enzymes. *Journal of Nutritional Biochemistry* 16(1): 577-586.

Mosmann, T. (1983). Rapid colorimetric assay for celullar growth and survival: Application to proliferation and cytotoxicity assays. *Journal of Immunological Methods* 65(1-2): 55-63.

Mqoco, T. S. and Marais, S. (2010). Influence of estradiol analogue on cell growth, morphology and death in esophageal carcinoma cells. *Biocell* 34(3): 113-120.

Murphy, J. J., Ranganathan, V., Farnsworth, M. L., Kavallaris, M. and Lock, R. B. (2000). Bcl-2 inhibits Bax translocation from cytosol to mitochondria during drug-induced apoptosis of human tumor cells. *Cell Death and Differentiation* 7(1): 102-111.

Nedělník, J. (2002). Damage to Corn by Fungi of the Genus *Fusarium* and the Presence of Fusariotoxins. *Plant Protection Science* 38(2): 46-54.

Oda, T., Xu, J. K. U., Nakazawa, T. and Namikoshi, M. (2010). 12˙-Hydroxyl group remarkably reduces Roridin E cytotoxicity. *Mycoscience* 51(4): 317-320.

Ogata, S., Inoue, K., Iwata, K., Okumura, K. and Taguchi, H. (2001). Apoptosis induced by picolinic acid-related compounds in HL-60 cells. *Bioscience, Biotechnology, and Biochemistry* 65(10): 2337-2339.

Oliveira, P. A., Colaço, A., Chaves, R., Guedes-Pinto, H., De-La-Cruz P., L. E. and Lopes, C. (2007). Chemical carcinogenesis. *Annals of the Brazilian Academy of Sciences* 79(4): 593-616.

Omar, H. E. D. M. (2013). Mycotoxins-induced oxidative stress and disease. Mycotoxin and food safety in developing countries. Makun, H. A., InTech. 3**:** 63-92.

Pal, M., Gizaw, F., Abera, F., Shukla, P. K. and Hazarika, R. A. (2015). Mycotoxins: A growing concern to human and animal health. *Beverage & Food World* 42(5): 42-50.

Pan, J., Hong, M. and Ren, J. (2009). Reactive oxygen species: A double-edged sword in oncogenesis. *World Journal of Gastroenterology* 15(14): 1702-1707.

Perry, D. K., Smyth, M. J., Stennicke, H. R., Salvesen, G. S., Duriez, P., Poirier, G. G. and Hannun, Y. A. (1997). Zinc is a potent inhibitor of the apoptotic protease, caspase-3. *The Journal of Biological Chemistry* 272(30): 18530-18533.

Pitot, H. C. (1993). The molecular biology of carcinogenesis. *Cancer* 72(1): 962-970.

Qian, Y., Kachroo, A. H., Yellman, C. M., Marcotte, E. M. and Johnson, K. A. (2014). Yeast cells expressing the human mitochondrial DNA polymerase reveal Correlations between polymerase fidelity and human disease progression. *The Journal of Biological Chemistry* 289(1): 5970-5985.

Reed, J. C. (1994). Bcl-2 and the regulation of programmed cell death. *The Journal of Cell Biology* 124(1-2): 1-6.

Ricci, J., Munoz-Pinedo, C., Fitzgerald, P., Bailly-Maitre, B., Perkins, G. A., Yadava, N., Scheffler, I. E., Ellisman, M. H. and Green, D. R. (2004). Disruption of Mitochondrial Function during Apoptosis Is Mediated by Caspase Cleavage of the p75 Subunit of Complex I of the Electron Transport Chain. *Cell* 117(6): 773-786.

Riss, T. L., Moravec, R. A., Niles, A. L., Benink, H. A., Worzella, T. J., Minor, L., Storts, D. and Reid, Y. (2013). Cell Viability Assays. Assay Guidance Manual. Sittampalam, G. S., Coussens, N. P., Nelson, H., Arkin, M., Auld, D., Austin, C., Bejcek, B., Glicksman, M., Inglese, J., Iversen, P. W., Li, Z., McGee, J., McManus, O., Minor, L., Napper, A., Peltier, J. M., Riss, T., Trask, O. J. J. and Weidner, J., Eli Lilly & Company and the National Center for Advancing Translational Sciences: 1-23.

Shahbaz Sarwar, C. M., Luketich, J. D., Landreneau, R. J. and Abbas, G. (2010). Esophageal cancer: An update. *International Journal of Surgery* 8(1): 417-422.

Sheik Abdul, N., Nagiah, S. and Chuturgoon, A. A. (2016). Fusaric acid induces mitochondrial tress in human hepatocellular carcinoma (HepG2) cells. *Toxicon* 119(1): 336-344.

Siegel, R. L., Miller, K. D. and Jemal, A. (2016). Cancer Statistics, 2016. *CA: A Cancer Journal for Clinicians* 66(1): 7-30.

Sies, H. (1985). Oxidative Stress: introductory remarks. Oxidative stress. Sies, H. London, Academic Press**:** 1-8.

Sies, H. (2015). Oxidative stress: a concept in redox biology and medicine. *Redox Biology* 4(1): 180-183.

Singh, N. P., McCoy, M. T., Tice, R. R. and Schneider, E. L. (1988). A simple technique for quantitation of low levels of DNA damage in individual cells. *Experimental Cell Research* 175(1): 184-191.

Singh, V. K. and Upadhyay, R. S. (2014). Fusaric acid induced cell death and changes in oxidative metabolism of *Solanum lycopersicum* L. *Botanical Studies* 55(1): 66-76.

Stack, B. C., Hansen, J. P., Ruda, J. M., Jaglowski, J., Shvidler, J. and Hollenbeak, C. S. (2004). Fusaric acid: a novel agent and mechanism to treat HNSCC. *Otolaryngology--Head and Neck Surgery* 131(1): 54-60.

Stack, B. C., Ye, J., Willis, R., Hubbard, M. and Hendrickson, H. P. (2014). Determination of oral bioavailability of fusaric acid in male sprague-dawley rats. *Drugs in R&D* 14(2): 139-145.

Stadtman, E. R. (2004). Role of oxidant species in aging. *Current Medicinal Chemistry* 11(9): 1105-1112.

Stockert, J. C., Blázquez-Castro, A., Cañete, M., Horobin, R. W. and Villanueva, Á. (2012). MTT assay for cell viability: Intracellular localization of the formazan product is in lipid droplets. *Acta Histochemica* 114(8): 785-796.

Streit, E., Schwab, C., Sulyok, M., Naehrer, K., Krska, R. and Schatzmayr, G. (2013). Multi-mycotoxin screening reveals the occurrence of 139 different secondary metabolites in feed and feed ingredients. *Toxins* 5(3): 504-523.

Surai, P. F., Mezes, M., Melnichuk, S. D. and Fotina, T. I. (2008). Mycotoxins and animal health: From oxidative stress to gene expression. *Krmiva* 50(1): 35-43.

Telles-Pupulin, A. R., Salgueiro-Pagadigorria, C. L., Bracht, A. and Ishii-Iwamoto, E. L. (1998). Effects of fusric acid on rat liver mitochondria. *Comparative Biochemistry and Physiology Part C: Pharmacology, Toxicology and Endocrinology* 120(1): 43-51.

Träuble, H. and Eibl, H. (1974). Electrostatic Effects on Lipid Phase Transitions: Membrane Structure and Ionic Environment. *Proceedings of the National Academy of Sciences* 71(1): 214-219.

Vaux, D. L. and Silke, J. (2003). Mammalian mitochondrial IAP binding proteins. *Biochemical and Biophysical Research Communications* 304(1): 499-504.

Vekshin, N. (2011). Binding of Hoechst with nucleic acids using fluorescence spectroscopy. *Journal of Biophysical Chemistry* 2(4): 443-447.

Voss, K. A., Porter, J. K., Bacon, C. W., Meredith, F. I. and Norred, W. P. (1999). Fusaric acid and modifications of the subchronic toxicity to rats of fumonisins in *F. moniliforme* culture material. *Food and Chemical Toxicology* 37(8): 853-861.

Wang, T., Zhang, Y., Wang, Y. and Pei, Y. H. (2007). Anti-tumor effects of Rubratoxin B on cell toxicity, inhibition of cell proliferation, cytotoxic activity and matrix metalloproteinase-2, 9. *Toxicology in vitro* 21(4): 646-650.

Watanabe, W., Sudo, K., Asawa, S., Konno, K., Yokota, T. and Shigeta, S. (1995). Use of lactate dehydrogenase to evaluate the anti-viral activity against influenza A virus. *Journal of Virological Methods* 51(2): 185-191.

Wilson, K. and Walker, J. (2010). Principles and techniques of biochemistry and molecular biology, New York, Cambridge University Press.

Yabuta, T., Kambe, K. and Hayashi, T. (1937). Biochemistry of the bakanaefungus. I. Fusarinic acid, a new product of the bakanae fungus. *Journal of the Agricultural Chemical Society of Japan* 10(1): 1059–1068.

Yang, Y. and Ma, H. (2009). Western blotting and ELISA techniques. *Researcher* 1(2): 67-86.

Ye, J., Montero, M. and Stack, B. C. (2013). Effects of fusaric acid treatment on HEp2 and docetaxel-resistant HEp2 laryngeal squamous cell carcinoma. *Chemotherapy* 59(1): 121-128.

APPENDICES

Appendix A

Cell Viability Raw Data

SNO cells were treated with a range of FA concentrations (0 – 500 µg/ml) over a 24 h period. The MTT assay revealed a dose-dependent decrease in SNO cell viability and an IC_{50} of 78.81 µg/ml was determined (Appendix Table 1).

Table 1: SNO cell viability treated with a range of FA concentrations (0 – 500 µg/ml) for 24 h.

FA concentration (µg/ml)	Log [FA]	Mean Absorbance ± SD	% Viability
0	0	0.605 ± 0.056	100
25	1.398	0.471 ± 0.013	77.796
50	1.699	0.402 ± 0.041	66.501
100	2	0.268 ± 0.011	44.353
250	2.398	0.129 ± 0.053	21.322
350	2.544	0.040 ± 0.004	6.612
500	2.699	0.024 ± 0.002	4.022

SD: Standard deviation.

Appendix B

Table 1: Formulation of Eagle's Minimum Essential Medium

Component		Concentration (µg/L)
Amino acids	L-arginine-HCl	126
	L-Cystine • 2HCl	31.3
	L-Histidine-HCl • H_2O	42
	L-Isoleucine	52
	L-Leucine	52
	L-Lysine • HCl	72.5
	L-Methionine	15
	L-Phenylalanine	32
	L-Threonine	48
	L-Tryptophan	10
	L-Tyrosine • 2Na • $2H_2O$	51.9
	L-Valine	46
Inorganic salts	$CaCl_2$ • $2H_2O$	200
	KCl	400
	$MgSO_4$ (anhydrous)	97.7
	NaCl	6800
	NaH_2PO_4 (anhydrous)	122
Vitamins	Choline chloride	1
	D-Pantothenate • ½Ca	1
	Folic acid	1
	myo-Inositol	2
	Niacinamide	1
	Pyridoxal • HCl	1
	Riboflavin	0.1
	Thiamine • HCl	1
Other	Glucose	1000
	Phenol red • Na	11

Appendix C

Raw data- Caspase Activity, ATP levels, LDH levels

Table 1: Caspase activity, ATP levels and LDH levels in SNO cells following FA treatment.

		Absorbance (RLU)			Mean RLU	Relative fold change ± SD
		A	**B**	**C**		
Caspase-8	Control	316787	257096	254571	276151	1.34 ± 0.064
	FA	325192	346962	439446	324863	
Caspase-9	Control	284530	340268	285561	303453	1.24 ± 0.029
	FA	360877	356767	411209	353555	
Caspase-3/7	Control	7016.4	6738.2	7474.7	7440.7	1.17 ± 0.048
	FA	7802.9	8077.1	8889.8	8256.6	

		Absorbance (RLU)			Mean RLU ± SD
		A	**B**	**C**	
ATP	Control	4351040	4128210	4158210	4212487 ±120924
	FA	3716890	3605480	3561930	3628100 ± 79918

		Absorbance (OD)			Mean OD ± SD
		A	**B**	**C**	
LDH	Control	1.861	1.858	1.829	1.849 ± 0.018
	FA	2.119	2.124	1.966	2.122 ± 0.004

LDH: Lactate dehydrogenase, OD: Optical density, RLU: Relative light units, SD: Standard deviation.

Appendix D

Protein quantification and standardisation using bovine serum albumin (BSA)

Table1: Absorbance values of serially diluted concentrations of BSA used as standards.

BSA standards (mg/ml)	OD1	OD2	OD3	Mean OD	SD
0	0.095	0.09	0.09	0.092	0.003
0.2	0.445	0.427	0.429	0.434	0.01
0.4	0.607	0.62	0.616	0.614	0.007
0.6	0.854	0.806	0.767	0.809	0.044
0.8	1.079	0.928	0.954	0.987	0.081
1	1.127	1.077	1.193	1.132	0.058

BSA: Bovine serum albumin, OD: Optical density, SD: Standard deviation.

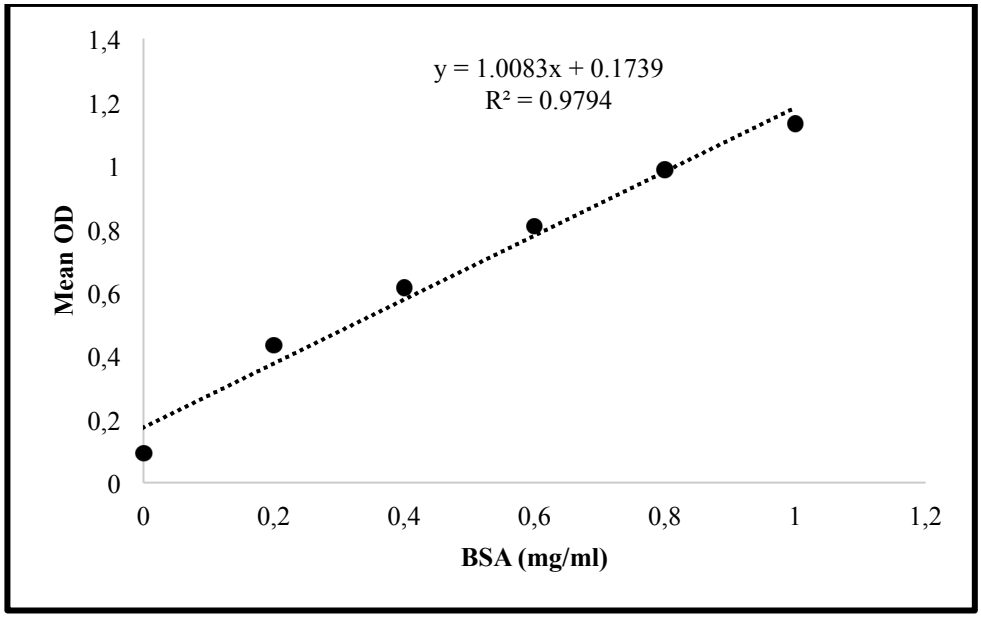

Figure 1: Standard curve using known concentrations of BSA. Equation of the line was used to determine the concentration of control and treatment protein samples via the BCA assay. BSA: Bovine serum albumin, OD: Optical density.

Table 2: Standardisation of protein samples (control & FA) to 1.5 mg/ml using standard curve of BSA concentrations.

Sample	Mean OD	Protein (mg/ml)	C_2 (mg/ml)	V_2 (µl)	V_1 (µl)
Control	2.317	2.125	1.5	200	141.18
FA	1.671	1.586	1.5	200	189.16

OD: Optical density, C_2: Final concentration, V_1: Initial volume, V_2: Final volume.

Appendix E

Glutathione (GSH) Assay- Raw data

Table 1: Absorbance values (RLU) of serially diluted GSH used as standards.

GSH standards (µM)	Absorbance (RLU)			Mean RLU
	A	B	C	
0	52707	54025.7	67614.7	58115.8
3.125	768442	778701	631743	726295.3
6.25	1225850	1154050	767117	1189950
12.5	1455670	1608900	197537	1532285
25	1698740	2029640	340.006	1864190
50	2688090	2658140	406.008	2673115

GSH: reduced glutathione, RLU (Relative light units).

Table 2: Absorbance values of samples (RLU)

Sample	Absorbance (RLU)			Mean RLU
	A	B	C	
Control	1016610	989729	1031060	1012466
FA	875122	848530	858431	860694.3

RLU: Relative light units.

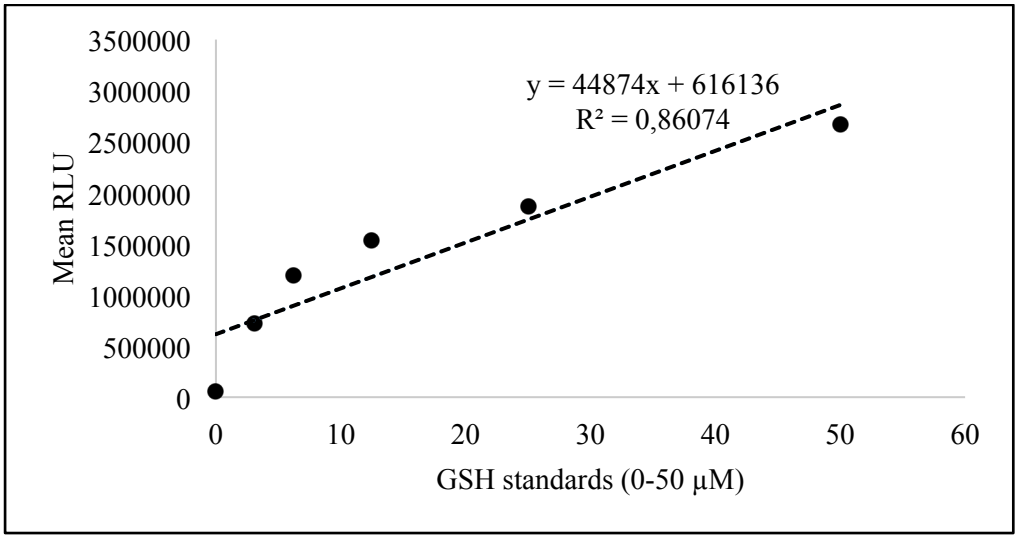

Figure 1: Standard curve representing mean absorbance values of GSH concentrations. RLU: Relative light units.

Appendix F

Comet Assay- Raw data

Table 1: Comet tail lengths of control and FA treated SNO cells

	Control (µm)	FA (µm)
1	2.71	6.32
2	2.06	6.71
3	1.55	6.19
4	1.16	5.29
5	1.03	6.06
6	1.29	6.58
7	1.42	5.93
8	1.68	6.42
9	1.55	6.8
10	1.29	6.58
11	1.81	6.06
12	1.55	5.68
13	1.81	5.03
14	1.68	5.03
15	1.29	6.19
16	1.16	5.8
17	1.03	5.03
18	1.16	5.93
19	1.42	5.93
20	0.90	6.19
21	1.55	5.93
22	4.84	5.93
23	4.84	6.06
24	4.19	5.16
25	4.84	7.09
26	4.51	6.32
27	4.19	6.06
28	4.84	6.71
29	3.55	5.29
30	4.84	5.8
31	4.84	5.42
32	3.55	5.93
33	4.19	6.06
34	4.51	4.9
35	4.51	6.06
36	4.51	5.42
37	3.55	5.03
38	4.84	6.32
39	4.19	7.22
40	4.19	6.32
41	2.58	6.32

42	3.22	5.03
43	2.9	6.06
44	4.19	6.29
45	4.19	5.65
46	4.84	5.29
47	4.84	6.09
48	4.84	5.93
49	4.19	5.29
50	4.19	5.58
Mean	**3.09**	**5.93**

Appendix G

Additional Data

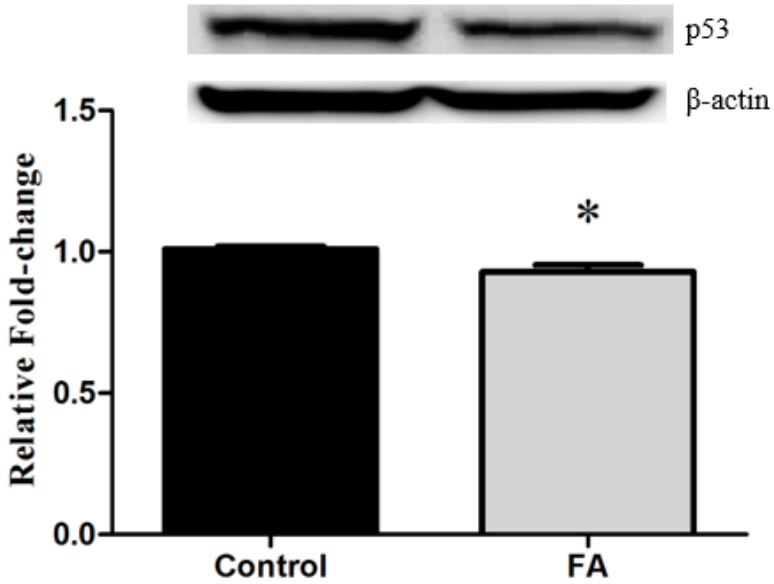

Figure 1: FA induced a significant decrease in protein expression of p53 (p = 0.0334).

The tumour suppressor protein, p53 contains Zn-finger domains. FA is a chelator of divalent metal cations, including Zn. FA induced a significant 1.09-fold decrease in p53 protein expression. Normally, upregulation of p53 signals for cell cycle arrest and DNA repair. However, the damage to DNA caused by FA was not repaired due to reduced expression of p53, thus the excessive amount of DNA damage observed. The Zn-chelation property of FA may have explained the reduced expression of p53, however, chelation was not tested in this study.

This result indicates that FA induced p53-independent apoptosis in SNO cells after 24 h of treatment.

Appendix H

Published Manuscript in Toxicon (TOXCON-D-16-00468)

http://dx.doi.org/10.1016/j.toxicon.2016.12.006

Toxicon 126 (2017) 4e11

Contents lists available at ScienceDirect

Toxicon

journal homepage: www.elsevier.com/locate/toxicon

Fusaric acid induces oxidative stress and apoptosis in human cancerous oesophageal SNO cells

Nikita Devnarain, Charlette Tiloke, Savania Nagiah, Anil A. Chuturgoon *

Discipline of Medical Biochemistry, University of KwaZulu-Natal, South Africa

article info

Article history:
Received 12 October 2016
Received in revised form 6
December 2016 Accepted 8
December 2016
Available online 9 December 2016

Keywords:
Fusaric acid
Apoptosis
Oxidative stress
SNO oesophageal cancer cells
Caspases-3/7, -8, -9

abstract

Oesophageal cancer (OC) is a global problem incrementally incident among black South African males. The high incidence of OC may be due to the consumption of corn as a staple, often contaminated with mycotoxins. Fusaric acid (FA), a neglected mycotoxin, is known to disrupt mitochondrial energy meta-bolism, chelates divalent metal cations and induces cell death in plants. This study investigated FA-induced cytotoxicity and apoptotic induction in the SNO OC cell line. Cells were treated with FA (IC_{50} ¼ 78.81 mg/mL; 24 h; MTT assay) and assayed for oxidative stress and membrane damage (TBARS, LDH cytotoxicity and glutathione), apoptotic induction (ATP levels, caspase-8, -9, -3/7 activities) (Luminometry), single strand DNA and nuclear fragmentation (Comet and Hoechst assay). Additionally, relative expression of pro- and anti-apoptotic proteins were determined (Western Blotting). Significant antioxidant depletion was consistent with a concomitant increase in ROS-induced lipid peroxidation and extracellular LDH levels. FA induced apoptosis by significantly increasing Bax expression and caspase-8, -9 and -3/7 activities whilst decreasing ATP levels and Bcl-2 expression. Further, FA significantly increased comet tail lengths, PARP-1 expression and late stage apoptotic body formation in SNO cells. This study shows that FA is cytotoxic and induces increased apoptosis in SNO cells.

1. Introduction

Cancer is a major public health issue worldwide (Siegel et al., 2016). Oesophageal cancer (OC) is the sixth most common cause of cancer-related deaths worldwide and the second most common cancer among black South African men. The incremental incidence of OC is especially due to an increase in cancer-causing behaviours, particularly excessive smoking and alcohol consumption (Ballo and Millikan, 2015). This high OC incidence can also be attributed to the staple diet of corn (often heavily contaminated with fungi and mycotoxins) consumed by the majority South African black popu-lation (Nedelník, 2002). Not only is corn consumed directly, but heavily contaminated corn is fermented to produce home brewed alcohol which contains a potent cocktail of mycotoxins (Cousin et al., 2005) and may contribute to the high incidence of OC in black South African men who consume excessive amounts of the brewed alcohol.

Since the oesophagus is the second organ in the digestive tract, the oesophagus becomes highly susceptible to exposure to contaminated food which may be carcinogenic. The human oeso-phageal epithelial carcinoma (SNO) cell line which was initially derived from a well-differentiated squamous cell carcinoma explanted from a 62-year old African male in July 1972, is suitable as a transfection host and a good model for in vitro oesophageal toxicity testing (Bey et al., 1976).

Mycotoxins, low molecular mass metabolites of fungi, that have the ability to damage cell membranes. The membrane-active properties of mycotoxins determine their toxicity, as these prop-erties enhance their mycological pathogenicity and self-defences. Mycotoxin contamination of corn is a global problem (Surai et al., 2008). Fusaric acid (FA, 5-butylpicolinic acid), a mycotoxin pro-duced by Fusarium heterosporum (Yabuta et al., 1937), is reported to have a mean volume of 643 mg/kg in feed samples (Streit et al., 2013).

FA induces several biological effects in animal and humans; FA inhibits tyrosine hydroxylase and dopamine b-hydroxylase, which result in elevated levels of serum melatonin, tyrosine, dopamine and 5-hydroxytrypamine; FA induces peripheral arteriolar dilation

* Corresponding author. Discipline of Medical Biochemistry and Chemical Pa-thology, School of Laboratory Medicine and Medical Sciences, Howard College Campus, University of KwaZulu-Natal, George Campbell Building, Durban, 4041, South Africa.

E-mail address: chutur@ukzn.ac.za (A.A. Chuturgoon).

http://dx.doi.org/10.1016/j.toxicon.2016.12.006 0041-0101/

which causes peripheral vascular resistance and consequential antihypertensive effects (Voss et al., 1999).
FA, a metabolite of tryptophan and picolinic acid, contains a pyridine ring (Stack et al., 2004) that allows for the chelation of divalent metal cations (Gaumann,€ 1958). Chelation of divalent metal cations from catalytic DNA-associated metalloproteins pre-vents DNA repair and synthesis, resulting in DNA damage (Stack et al., 2004). FA contains an n-butyl aliphatic side chain in the b-position which accentuates its lipophilic properties to freely penetrate into the cell membrane and cause damage (Fernandez-Pol, 1998). FA being a weak acid, will affect mitochondrial (mt) polarity and inhibit oxidative phosphorylation (Bachmann, 1956).

Membrane disruption and the inhibition of oxidative phos-phorylation by FA (Telles-Pupulin et al., 1998) will contribute to a highly oxidative environment. Oxidative stress is defined as 'an imbalance between oxidants and antioxidants in favour of the ox-idants, leading to a disruption of redox signalling and control and/ or molecular damage' (Sies, 1985). Highly volatile reactive oxygen species (ROS) are natural by-products of cellular processes, including mt respiration and are necessary for normal physiological functions such as apoptosis, cell signalling and immunity. However, oxidation of nucleic acids, proteins and carbohydrates by excessive ROS causes structural and functional alterations in cells such as lipid peroxidation, protein carbonyl formation, DNA mutations/le-sions (Jezek and Hlavata, 2005). ROS are neutralized through endogenous antioxidants (Gutteridge, 1995).

Chronic high ROS to antioxidant ratio can lead to deleterious effects in the cell and eventual cell death (Circu and Aw, 2010). Apoptosis involves an intrinsically regulated mechanism for death essential for the maintenance of tissue homeostasis, immune function, growth and development. It allows for the rapid removal of redundant, senescent, damaged or genetically mutated cells (Kerr et al., 1972). Apoptosis can occur via the extrinsic or intrinsic pathway, the endpoint of which is the activation of caspases to degrade specific cellular proteins and other constituents. Caspases regulate both the intrinsic and extrinsic pathways of apoptosis by proteolysis of cellular proteins (Fan et al., 2005).

This study investigated the cytotoxic effects of FA in the SNO cell line upon acute exposure.

2. Methods

2.1. Materials

SNO cells were purchased from Highveld Biologicals (Johan-nesburg, South Africa (SA)). Cell culture reagents were purchased from Whitehead Scientific (Johannesburg, SA). Western blot re-agents were obtained from Bio-Rad (Hercules, CA, USA) and all antibodies from Cell Signalling Technology. All other reagents were obtained from Merck (Darmstadt, Germany). FA (Gibberella fuji-kuroi) (F6513) was obtained from Sigma Aldrich.

2.2. Cell culture and FA treatment

The SNO cells were cultured (37 C, 5% CO_2) in sterile 25 cm^3 culture flasks in complete culture medium (CCM) comprising of Eagle's minimum essential media (10% foetal calf serum, 1% L-glutamine, 1% penicillin-streptomycin-fungizone) until 90% con-fluency was reached (Wilson and Walker, 2010). Treatments were made from 1 mg/ml stocks of FA diluted in 0.1 M phosphate-buffered saline (PBS).

2.3. Cell viability assay

The cell viability and cytotoxicity of FA in SNO cells were determined via the MTT assay. SNO cells (15,000 cells) were seeded into a 96-well microtitre plate in triplicate. Cells were incubated with FA concentrations (0e500 mg/mL) at 37 C for 24 h. Thereafter, the cells were incubated with MTT salt solution (5 mg/mL in 0.1 M PBS) and CCM (37 C, 4 h). The supernatants were then aspirated and 100 mL dimethyl sulphoxide (DMSO) was added and incubated (37 C, 1 h). Optical density was measured using a microplate reader (Bio-Tek mQuant) at 570/690 nm. The concentration of FA that produced half the maximum inhibition (IC_{50}) had been calculated via linear extrapolation. Two independent experiments were con-ducted to verify the IC_{50} which was used in all subsequent assays. All subsequent assays are representations of two experiments.

2.4. ATP quantification assay

Intracellular ATP levels were quantified using a CellTiter-Glo® kit (Promega, Madison, USA). Briefly, 50 mL of cell suspension (20,000 cells/well in 0.1 M PBS) were seeded into a microtitre plate in triplicate. Thereafter, 20 mL of reagent was added followed by incubation (dark, 30min, room temperature (RT)). Luminescence, which was proportional to the level of intracellular ATP, was then detected using a Modulus™ microplate luminometer (Turner Bio-systems, Sunnyvale, USA) and expressed as relative light units (RLU).

2.5. Glutathione assay

Intracellular glutathione (GSH) levels were quantified using the GSH-Glo™ assay (Promega, Madison, USA). Briefly, 50 mL of cell suspension (20,000 cells/well in 0.1 M PBS) were seeded into a microtitre plate in triplicate. A 5 mM stock diluted in PBS was used to make GSH standards (0e50 mM). Subsequently, 50 mL per stan-dard and 50 mL of 2 GSH-Glo™ Reagent were added and incu-bated (30 min, dark, RT). Thereafter, 50 mL of Reconstituted Luciferin Detection Reagent was added and incubated (15 min, RT). Luminescence was measured using a Modulus™ microplate luminometer and expressed as relative fold change.

2.6. TBARS assay

The extent of lipid peroxidation was measured using the Thio-barbituric Acid Reactive Substance (TBARS) assay which measures the level of malondialdehyde (MDA), a by-product of lipid peroxi-dation and an indicator of oxidative stress (Fernandez et al., 1997). Supernatants per control/treatment were added into test tubes containing 2% H_3PO_4 (200 mL), 7% H_3PO_4 (200 mL) and TBA/Butyl-ated hydroxytoluene solution (400 mL) (Asakawa and Matsushita, 1979). Subsequently, MDA (1 mL) was added to the positive con-trol and hydrochloric acid (HCl) (400 mL) to the blank. Each was adjusted to pH 1.5. Samples were boiled (15 min) then allowed to cool to RT prior to the addition of butanol (1,500 mL). Each tube was vortexed and allowed to separate into two phases. The butanol phase was then transferred to sterile tubes and centrifuged (2,500g; 24 C; 6 min). Thereafter, each sample (100 mL) was transferred to a microtitre plate in triplicate. The absorbance was measured at 532/600 nm by means of a Bio-Tek mQuant spectrophotometer.

2.7. LDH cytotoxicity detection assay

Extracellular LDH levels were quantified using a Cytotoxicity Detection Kit (11644793001) (Roche, Mannheim, Germany). Briefly, supernatants (100 mL) were added into a microtitre plate in tripli-cate. Thereafter, dye solution (INT/sodium lactate) (100 mL) and catalyst (diaphorase/NAD^b) (100 mL) were added, followed by

incubation (dark, 25min, RT). Absorbance was measured at 500 nm using a spectrophotometer (Bio-Tek mQuant).

2.8. Assessment of caspase activity

The activities of caspase-3/7, -8 and -9 were detected with Caspase-Glo® assay (Promega, Madison, USA). Briefly, 50 mL of cell suspension (20,000 cells/well in 0.1 M PBS) were seeded into a microtitre plate in triplicate. As per manufacturer's guidelines, Caspase-Glo®-3/-7, -8 and -9 reagents were reconstituted and added (20 mL). Thereafter, the plate was incubated (dark, 30 min, RT). Luminescence was detected using a Modulus™ microplate luminometer and expressed as relative fold change.

2.9. Western Blotting

Western blotting was used to determine protein expression of Bax, Bcl-2, Smac/DIABLO and cleaved poly(ADP-ribose) polymer-ase-1 (PARP-1). Total protein was extracted using Cytobuster™ reagent (Novagen, San Diego, CA, USA), supplemented with prote-ase and phosphatase inhibitor (Roche, Germany, 05892791001 and 04906837001 respectively), as per manufacturer's instructions. Protein was quantified via the bicinchoninic acid assay (Sigma, Germany) (Bainor et al., 2011) and standardized to 1.5 mg/mL. Samples were boiled in Laemmli buffer [dH_2O, 0.5 M Tris-HCl (pH 6.8), 3% glycerol, 10% SDS, 12% b-mercaptoethanol, 2% bromophenol blue] (1:4, 20min) (Yang and Ma, 2009). Protein samples were separated using sodium dodecyl sulphate-polyacrylamide gel electrophoresis (4% stacking, 7% resolving) (1 h, 150 V) using a Bio-Rad compact power supply. Thereafter, the separated proteins were electro-transferred to a nitrocellulose membrane (400 mA; 1 h) and then blocked (1 h) in 5% bovine serum albumin in Tris-buffered saline containing 0.5% Tween20 (TTBS). Membranes were subse-quently immune-probed with primary antibody [Bax (610982), Bcl-2 (2827), Smac/DIABLO (110291), Cleaved PARP-1 (9541); 1:1000] (4 C, overnight). Membranes were then washed with TTBS and then exposed to secondary antibody [Bax, Bcl-2, Smac/DIABLO [rabbit (7076S), 1:5000]; Cleaved-PARP-1 (1:10,000)] (1 h, RT). Membranes were washed again with TTBS and b-actin (A3854, 1:5000) was utilised to normalise protein expression. The Clarity Western ECL Substrate (Bio-Rad) detection reagents were used to detect chemiluminescent signal on the Alliance 2.7 image docu-mentation system (UViTech). Protein expression was analysed us-ing UviBand Advanced Image Analysis software v12.14 (UViTech). Data was expressed as relative band density (RBD) and fold change.

2.10. SCGE (comet) assay

The Comet assay was used to detect DNA damage (Singh et al., 1988). Three slides per treatment/control were prepared: the first layer contained 1% low melting point agarose (LMPA, 400 mL) (37 C); the second layer contained cell suspension (20,000 cells in 25 mL) in 0.5% LMPA (175 mL) and GelRed™ nucleic acid gel stain (1 mL) (Biotium, California, cat. no. 41003) (37 C); the third layer contained 0.5% LMPA (200 mL) (37 C). Solidified gels were sub-merged in cold cell lysis buffer (100 mM EDTA, 2.5 M NaCl, 1% Triton X-100, 10% DMSO, and 10 mM Tris (pH 10)) and then incubated (1 h, 4 C). Thereafter, the slides were laid in electrophoresis buffer (1 mM Na_2EDTA (pH 13) and 300 mM NaOH) (20min, RT) and then subjected to electrophoresis (25 V, 35 min, RT) using a Bio-Rad compact power supply. Using neutralisation buffer (0.4 M Tris (pH 7.4)), the slides were rinsed (three times, 5 min) and then viewed using a fluorescent microscope (Olympus IXSI inverted microscope, excitation: 510e560 nm; emission 590 nm). Images of 50 cells and comets were captured in total from three slides per control/treatment. Lengths of cells and comet tails were measured using Soft imaging system (Life Science - ©Olympus Soft Imaging Solutions v5) and reported in mm.

2.11. Hoechst staining assay

To assess nuclear structure and cellular morphology, SNO cells were stained with Hoechst 33342 (H3570) (Invitrogen™, Eugene, Oregon, USA). Cells were seeded (500,000 cells) into a 6 well plate and treated in triplicate. Cells were thereafter washed (0.1 M PBS), fixed (10% paraformaldehyde, 5min) and washed again (0.1 M PBS). Hoechst working solution (10 mg/mL, Molecular Probes, Eugene, OR) was added and incubated (15 min, 37 C). Images were captured using a fluorescent microscope (350 nm excitation, 450 nm emission). Ten images per treatment replicate were captured at magnifications 10 and 20 .

2.12. Statistical analysis

Statistical analyses were carried out using GraphPad Prism v5.0 software (GraphPad Software Inc., La Jolla, USA). The concentration-response-inhibition equation produced an IC_{50} for MTT assay. The statistical significances were determined by unpaired t-test with Welch's correction (results reported as mean ± standard deviation (SD)) and a 95% confidence interval with a p value of less than 0.05.

3. Results

3.1. Cell viability

The MTT assay was used to measure FA cytotoxicity in SNO cells and an IC_{50} of 78.81 mg/mL was calculated and used in all subse-quent assays (Fig. 1).

3.2. ATP quantification

The concentration of ATP in SNO cells was assessed via lumin-ometry. The ATP levels were significantly reduced by FA with a 1.16-fold decrease (3,628,000 ± 79,920 RLU) compared to the control (4,212,000 ± 120,900 RLU; p ¼ 0.006) (Fig. 2).

3.3. Oxidative stress

Lipid peroxidation by ROS was measured by quantifying the level of MDA, the end product of lipid peroxidation. Levels of extracellular MDA in FA treated cells (1.242 ± 0.03 mM) were

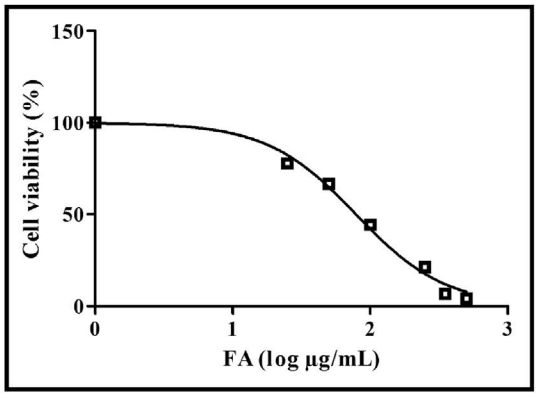

Fig. 1. FA induced a dose-dependent decrease in SNO cell viability (0e500 mg/mL) with higher concentrations showing increased cell death rates.

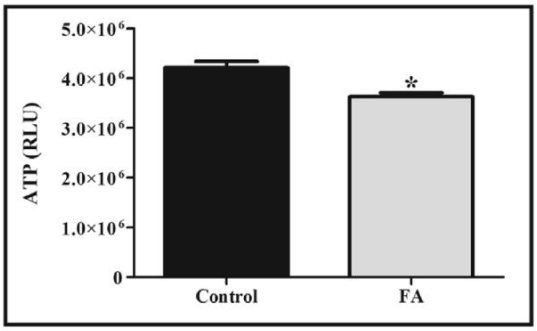

Fig. 2. Levels of ATP in control vs FA treated SNO cells. FA significantly decreased ATP levels (p ¼ 0.006). RLU: relative light units. *p < 0.05 relative to control.

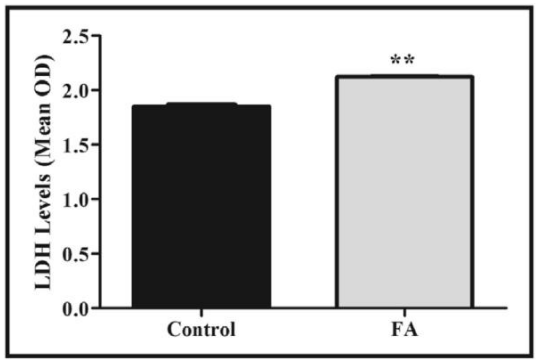

Fig. 4. FA significantly increased LDH leakage in SNO cells indicative of membrane damage. LDH: lactate dehydrogenase, OD; optical density. **p < 0.005 relative to control.

significantly increased by 1.23-fold compared to that of control cells (1.007 ± 0.003 mM, p ¼ 0.0166) (Fig. 3a). There was a significant decrease in GSH levels (-1.62-fold) in FA treated SNO cells (0.6171 ± 0.006 mM) compared to that of the control (1.010 ± 0.006 mM, p < 0.0001) (Fig. 3b).

3.4. Extracellular LDH levels

FA induced significant SNO cell membrane damage when compared to control SNO cells as measured by increased extracel-lular LDH levels (control: 1.849 ± 0.018 Optical density (OD); FA: 2.122 ± 0.004 OD, p ¼ 0.002) (Fig. 4).

3.5. Caspase activation

The activity of caspases-3/7, -8 and -9 were assessed via luminometry (Fig. 5). FA significantly increased the activity of all caspases measured: caspase-3/7 by 1.17-fold (p ¼ 0.0306); caspase-8 by 1.34-fold (p ¼ 0.013) and caspase-9 by 1.24-fold (p ¼ 0.0059) in SNO cells.

3.6. Western blot analysis

Western Blotting was used to determine the effect of FA on relative protein expression of pro-apoptotic proteins Bax, Smac/ DIABLO and anti-apoptotic protein Bcl-2 (Fig. 6). FA induced a significant 1.08-fold increase in Bax expression (0.0726 ± 0.0008 RBD vs. control: 0.0675 ± 0.0005 RBD, p ¼ 0.0138); a 1.02-fold in-crease in Smac/DIABLO expression (1.026 ± 0.0287 RBD vs. control: 1.003 ± 0.0033 RBD) and a significant -1.24-fold decrease in Bcl-2 expression (0.8131 ± 0.0176 RBD vs. control: 1.010 ± 0.0058 RBD, p ¼ 0.0087). Subsequent to caspase-3/7 activation, PARP-1 is cleaved to produce a 24 kDa and 89 kDa fragment. FA significantly increased (1.53-fold) 24 kDa fragment of PARP-1 (2.021 ± 0.0771 RBD vs. control: 1.325 ± 0.1117 RBD, p ¼ 0.0143) (Fig. 6).

3.7. DNA damage

The comet assay was used to assess DNA damage by FA in SNO cells. FA induced DNA damage in SNO cells with significantly increased comet tail lengths (Fig. 7a) as compared to control cells (5.926 ± 0.0795 mm vs. control: 3.092 ± 0.2102 mm, p < 0.0001) (Fig. 7b).

3.8. Hoechst staining assay

Late stages of apoptosis are characterized by nuclear conden-sation, apoptotic body formation and DNA fragmentation. Hoechst staining showed increased cell density and healthy cells undergo-ing various stages of mitosis in the untreated control (Fig. 8a), while FA induced nuclear condensation, apoptotic body formation and DNA fragmentation in SNO cells (Fig. 8b).

4. Discussion

There is a high incidence of OC among black South African men and thousands of people worldwide (Siegel et al., 2016). FA is known to have low to moderate toxic effects in plants and has been suggested as a causative agent of OC (Nedelník, 2002), however the effects of FA in humans has not yet been conclusively explored. This study assessed the acute toxicity of FA on human oesophageal epithelial carcinoma (SNO) cells.

Increased ROS, coupled with a decrease in the endogenous

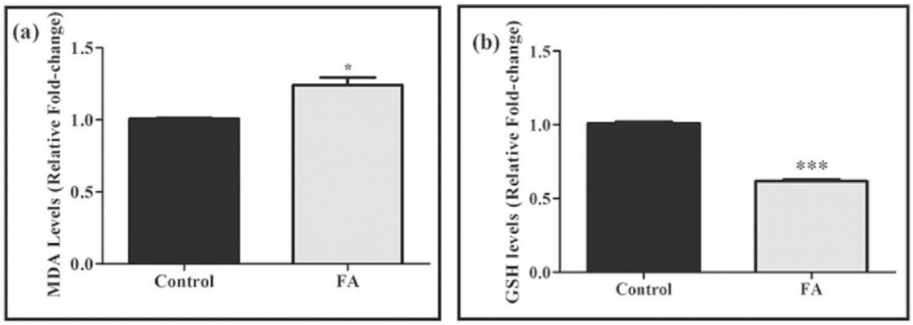

Fig. 3. Oxidative stress induced by FA in SNO cells. FA significantly increased levels of MDA (a by-product of lipid peroxidation) (p ¼ 0.0166) (a) with a corresponding decrease in levels of intracellular GSH (p < 0.0001) (b). GSH: glutathione; MDA: malondialdehyde. *p < 0.05, ***p < 0.0001 relative to control.

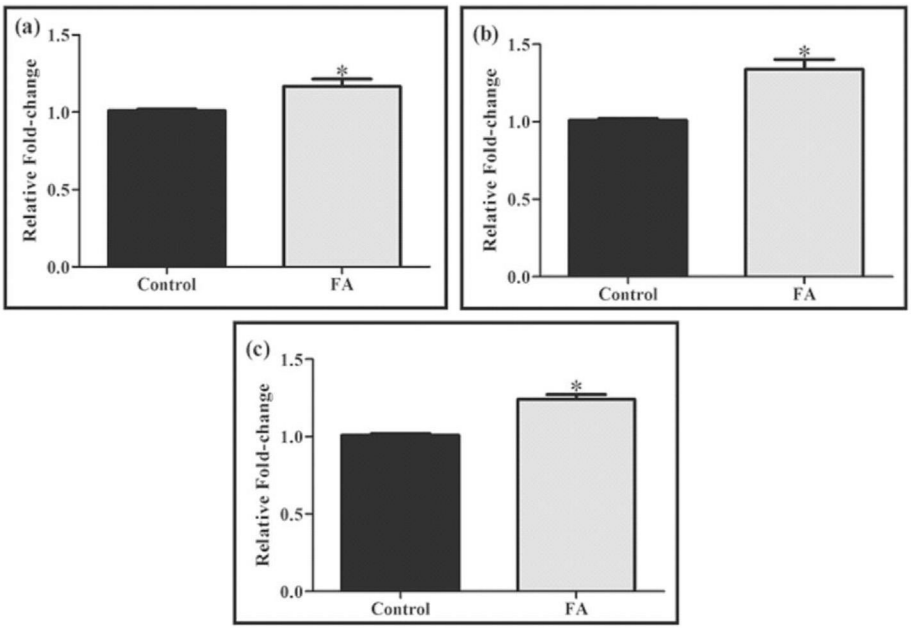

Fig. 5. Caspase activity was significantly influenced by FA. Activity of initiator caspase-8 (b) and -9 (c), as well as executioner caspase-3/7 (a) were significantly elevated in FA treated SNO cells. *p < 0.05 relative to control.

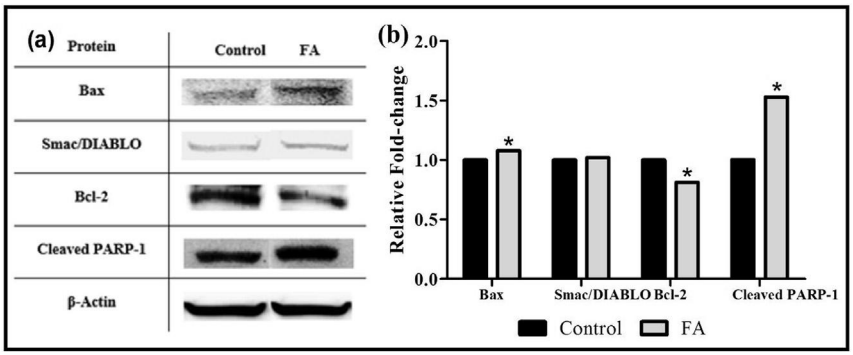

Fig. 6. FA regulates relative protein expression of Bax, Smac/DIABLO, Bcl-2 and the 24 kDa fragment of PARP-1 in SNO cells after treatment for 24 h.

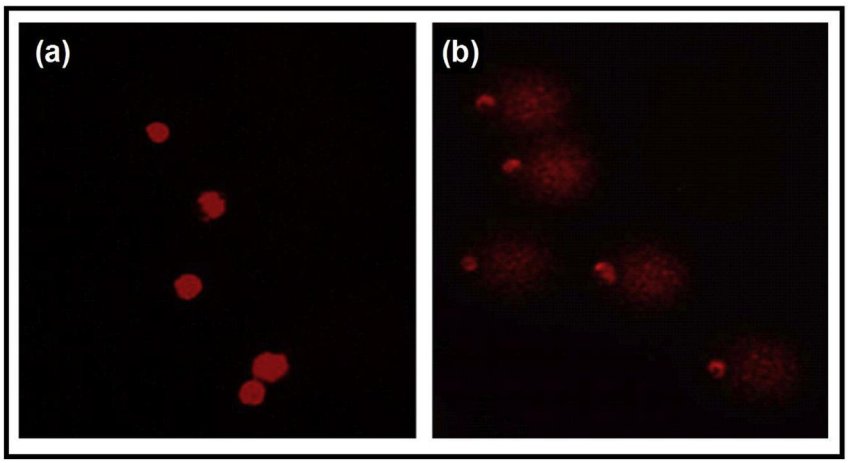

Fig. 7. Comet assay images of FA treated SNO cells (a) and untreated cells (b) for 24 h. Comet tail lengths were increased in FA treated SNO cells (b) compared to control cells (a) (40 , ***p < 0.0001).

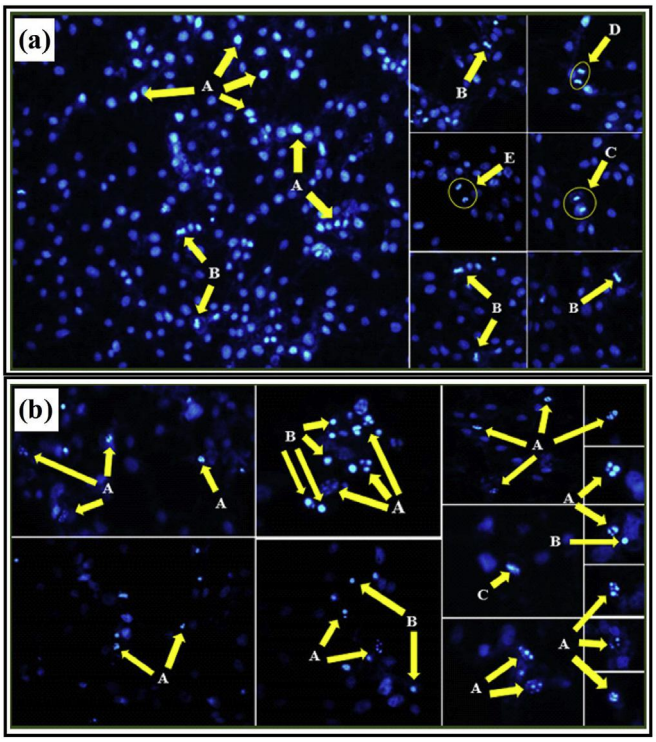

Fig. 8. (a). Uptake of Hoechst 33324 stain by untreated SNO cells (20). Diagram represents: (A-early prophase, B- metaphase, C- late anaphase, D-early telophase, E-late telophase (cytokinesis)); (b). Uptake of Hoechst 33324 stain by FA treated SNO cells (20). FA induced apoptosis (A-apoptotic body formation, B- chromatin condensation, C- DNA fragmentation and reduced SNO cell density as compared to control).

antioxidant GSH lead to oxidative stress, accompanied by the oxidation of DNA and lipids (Circu and Aw, 2010). FA significantly increased the levels of ROS-induced lipid peroxidation (Fig. 3a) and simultaneously significantly decreased levels of GSH, compared to control cells (Fig. 3b) leading to oxidative stress.

The lipophilic tail of FA causes damage to the lipid components of the cell membrane and compromises its integrity in the process (Dowhan, 1997; Fernandez-Pol, 1998). LDH is an enzyme found in the cytoplasm of healthy cells with intact cell membranes (Watanabe et al., 1995). An increase in extracellular LDH levels (Fig. 4) signifies cell membrane damage caused by lipid peroxida-tion and the FA lipophilic tail.

Further, FA may disrupt membrane integrity by chelating diva-lent cations. FA sequesters divalent metal cations between the N atom of its pyridine ring and the carboxyl radical in its a-position, creating a five-membered direct link (G€aumann, 1958). Divalent metal cations contribute to membrane integrity by stabilising the ordered state of membranes. Divalent cations react with negatively charged phospholipids in membranes which are essential for natural processes such as signal transduction (Tr€auble and Eibl, 1974). Divalent cations, especially calcium ($Ca^{2þ}$) and $Zn^{2þ}$ also inhibit permeability changes in membranes by blocking leakage at the site of lesion formation subsequent to binding of toxins to cells, and are known as membrane protective agents (Bashford et al., 1986).

The mitochondrion is known as the cellular metabolic hub since one of its most important functions is aerobic respiration. The MTT assay measures metabolic activity of the mt respiratory chain by quantifying the ratio of reducing equivalents to oxidising equiva-lents in the cell (Mosmann, 1983). FA revealed a dose-dependent decrease in cellular metabolic activity and viability in SNO cells as observed by the MTT assay (Fig. 1). Reduced metabolic activity may be due to a decline in the rate of the Kreb's cycle which leads to a decreased output of reducing equivalents required for MTT salt reduction to generate a formazan product. On the other hand, as indicated by the TBARS assay, the level of lipid peroxidation was significantly increased (Fig. 3a). Hence, both the cell membrane of SNO cells and the mitochondria are also affected by FA.

FA decreases the activity of succinate dehydrogenase and a-ketoglutarate dehydrogenase in the Kreb's cycle by influencing the mt proton gradient. This gradient is necessary for coupling of the ETC to oxidative phosphorylation in order to produce ATP (Telles-Pupulin et al., 1998). FA significantly decreased ATP levels in SNO cells (Fig. 2); also the lipophilic tail of FA may have impaired the activity of Cyt c oxidase resulting in uncoupling the ETC from ATP synthesis (Gaumann,€ 1958). Thus, the observed alterations in the cellular NADH/NADPH reductase system corresponds with the dose-dependent decrease in ATP levels. FA disrupts the integrity of the mt membrane and processes that occur within mitochondria of SNO cells. Recent work by Sheik Abdul et al. proposed that FA induced oxidative and mitochondrial stress in the hepatocellular carcinoma $HepG_2$ cell line (Sheik Abdul et al., 2016).

Since mt disruption and ATP depletion are early events in apoptosis (Telles-Pupulin et al., 1998), the expression and activities of apoptotic markers were analysed. The Bcl-2 family of proteins, particularly Bax and Bcl-2 are important in apoptosis. Mt perme-ability transition pores (MPTPs) in the mt membrane consist of and are regulated by Bax and Bcl-2. Bax, a pro-apoptotic protein, in-duces the formation of MPTPs by interacting with lipids in the outer mt membrane (OMM). FA significantly increased Bax protein expression (Fig. 6). This suggests a role of FA in $Zn^{2þ}$ chelation, since $Zn^{2þ}$ is an inhibitor of Bax and $Zn^{2þ}$ chelation would allow for Bax activation (Ganju and Eastman, 2003). Bcl-2 is an anti-apoptotic protein and inhibitor of Bax (Hockenbery et al., 1990). FA caused a significant decrease in Bcl-2 expression (Fig. 6), thus preventing its inhibitory effect on Bax activation.

Upon formation of MPTPs, mt pro-apoptotic proteins such as Cyt c and Smac/DIABLO are released into the cytoplasm. Cyt c binds to Apaf-1, which recruits pro-caspase-9 to form an ATP-requiring apoptosome. This apoptosome cleaves pro-caspase-9 to form active caspase-9, which is the initiator caspase of the intrinsic pathway. Caspase-9 activates executioner caspase-3/7, which me-diates proteolysis of apoptotic cells. Caspase-8, the initiator caspase of the extrinsic pathway, activates Bid which activates Bax. The pro-apoptotic protein, Smac/DIABLO, functions to inhibit the activity of inhibitor of apoptosis proteins (IAPs), which inhibit caspase-3/7 and -9 (Ashkenazi and Dixit, 1998; Green and Reed, 1998; Guicciardi and Gores, 2005). FA increased Smac/DIABLO levels (Fig. 6) and significantly increased the activation of caspases -3/7, -8 and -9 (Fig. 5) in SNO cells, compared to control cells.

Active caspase-3/7 cleaves the 75 kDa subunit of complex I of the ETC disrupting electron transport and mt membrane perme-ability (Ricci et al., 2004) and further increasing ROS production, ATP depletion and mt damage.

PARP-1, ATP-dependent Zn-finger endonuclease, is activated by caspase-3/7 and binds to breaks of internucleosomal DNA. PARP-1 is a 113 kDa protein, which when cleaved, forms an 89 kDa (carboxyl-terminus catalytic fragment) and a 24 kDa fragment (amino-terminus DNA-binding domain). PARP-1 also contains a Zn-finger domain which can be chelated by FA, which causes PARP-1 cleavage and renders PARP-1 ineffective in its DNA binding and repair activity (Kaufmann et al., 1993). Zn inhibits PARP-1 cleavage and is therefore essential to allow for the binding of PARP-1 to DNA strand breaks. This is achieved by Zn inhibition of the catalytic function of caspase-3/7 by interaction with either or both of the conserved sites, Cys-285 and His-237. This is another mechanism

by which Zn chelation would allow for PARP-1 cleavage to occur (Perry et al., 1997). A significant increase in the expression of the 24 kDa fragment of PARP-1 indicates that PARP-1 is cleaved by FA and contributes to DNA damage (Fig. 7b). This result may be due to the chelating effect of FA on Zn and hence the significant increase in caspase-3/7 activity.

Late stages of apoptosis include condensation and damage of nuclear components followed by the formation of apoptotic bodies. FA caused nuclear condensation (Fig. 8b), significant DNA damage (Figs. 6 and 7b) and resulted in the formation of a substantial amount of apoptotic bodies (Fig. 8b) in SNO cells. These results are consistent with caspase and PARP-1 activation, and confirms that FA is a potent inducer of apoptosis in SNO cells.

The results of this study are consistent with previous studies which showed that FA induced DNA damage and decreased the expression of Zn-finger proteins via chelation; significantly inhibited cellular proliferation; increased expression of caspases-3/ 7, -9, four anti-inflammatory cytokines and cleaved PARP-1; induced changes in the cell cycle and ultimately induced apoptosis. The data led to the conclusion that FA had tumouristatic and tumouricidal effects on HNSCC (Stack et al., 2004; Jaglowski and Stack Jr., 2006, Ruda et al., 2006; McCastlain et al., 2007; Ye et al., 2013).

5. Conclusion

FA increased oxidative stress and induced apoptosis via both the intrinsic and extrinsic pathways in SNO cells. Taken together, FA is a cytotoxic agent to human oesophageal SNO cells. Understanding the mechanism of toxicity of FA in humans may aid in preventing and treating the outcomes of consuming FA-contaminated agri-cultural produce. Additional studies need to determine the chelating effects of FA in other cell lines (including normal cells).

Ethics statement

We, Nikita Devnarian, Charlette Tiloke, Savania Nagiah and Anil A Chuturgoon, declare that all the work reported in the manuscript: Fusaric acid induces oxidative stress and apoptosis in human cancerous oesophageal SNO cells, meets with the highest ethical standards. We have not submitted this work to any other journal or had any aspect of the work published elsewhere. We also declare no conflict of interest and are in agreement with the contents of the manuscript. This study was a cell culture (in vitro) project and as such required no Institutional Ethical Approval.

Conflict of interest

The authors declared that there is no conflict of interest.

Funding

This research received no specific grant from any funding agency in the public, commercial, or not-for-profit sectors.

Acknowledgements

The authors would like to acknowledge the National Research Foundation (Grant UID: 94392) and the College of Health Sciences, UKZN for financial support during this study.

Transparency document

Transparency document related to this article can be found online at http://dx.doi.org/10.1016/j.toxicon.2016.12.006.

References

Asakawa, T., Matsushita, S., 1979. Thiobarbituric acid test for detecting lipid per-oxides. Lipids 14 (4), 401e406.
Ashkenazi, A., Dixit, V.M., 1998. Death receptors: signaling and modulation. Science 281 (1), 1305e1308.
Bachmann, E., 1956. The Influence of Fusaric Acid on the Water Permeability of Plant Protoplasts. ETH Zürich. PhD Thesis, Diss. Natural Sciences.
Bainor, A., Chang, L., McQuade, T.J., Webb, B., Gestwicki, J.E., 2011. Bicinchoninic acid (BCA) assay in low volume. Anal. Biochem. 410, 310e312.
Ballo, R.M., Millikan, K.W., 2015. Esophageal Cancer. Common Surgical Diseases. Springer, New York, pp. 133e135.
Bashford, C.L., Alder, G.M., Menestrina, G., Micklem, K.J., Murphy, J.J., Pasternak, C.C., 1986. Membrane damage by hemolytic viruses, toxins, complement, and other cytotoxic agents. A common mechanism blocked by divalent cations. J. Biol. Chem. 261 (20), 9300e9308.
Bey, E., Alexander, J., Whitcutt, J.M., Hunt, J.A., Gear, J.H.S., 1976. Carcinoma of the esophagus in Africans: establishment of a continuously growing cell line from a tumor specimen. In Vitro 12 (2), 107e114.
Circu, M.L., Aw, T.Y., 2010. Reactive oxygen species, cellular redox systems and apoptosis. Free Radic. Biol. Med. 48 (6), 749e762.
Cousin, M.A., Riley, R.T., Pastka, J.J., 2005. Foodborne Mycotoxins: Chemistry, Biology, Ecology, and Toxicology. Caister Academic Press, pp. 163e226.
Dowhan, W., 1997. Molecular basis for membrane phospholipid diversity: why are there so many lipids? Annu. Rev. Biochem. 66 (1), 199e232.
Fan, T., Han, L., Cong, R., Liang, J., 2005. Caspase family proteases and apoptosis. Acta Biochim. Biophys. Sinica 37 (11), 719e727.
Fernandez -Pol, J. A. (1998). Antiviral Agent. Washington, DC: U.S. Patent and Trademark Office.
Fernandez, J., Perez -Alvarez, J.A., Fernandez-Lopez, J.A., 1997. Thiobarbituric acid test for monitoring lipid oxidation in meat. Food Chem. 59 (3), 345e353. Ganju, N., Eastman, A., 2003. Zinc inhibits Bax and Bak activation and cytochrome c release induce by chemical inducers of apoptosis but not by death-receptor-initiated pathways. Cell Death Differ. 10 (6), 652e661.
Gaumann,€ E., 1958. The mechanism of fusaric acid injury. Phytopathology 48 (1), 670e686.
Green, D.R., Reed, J.C., 1998. Mitochondria and apoptosis. Science 281 (5391), 1309e1312.
Guicciardi, M.E., Gores, G.J., 2005. Apoptosis: a mechanism of acute and chronic liver injury. Gut 54 (7), 1024e1033.
Gutteridge, J.M.C., 1995. Lipid peroxidation and antioxidants as biomarkers of tissue damage. Clin. Chem. 41 (1), 1819e1828.
Hockenbery, D., Nunez, G., Milliman, C., Schreiber, R.D., Korsmeyer, S.J., 1990. Bcl-2 is an inner mitochondrial membrane protein that blocks programmed cell death. Nature 348 (1), 334e336.
Jaglowski, J., Stack Jr., B.C., 2006. Enhanced growth inhibition of squamous cell carcinoma of the head and neck by combination therapy of fusaric acid and paclitaxel or carboplatin. Cancer Lett. 243 (1), 58e63.
Jezek, P., Hlavata, L., 2005. Mitochondria in homeostasis of reactive oxygen species in cells, tissues and organism. Int. J. Biochem. Cell Biol. 37 (12), 2478e2503.
Kaufmann, S.H., Desnoyers, S., Ottaviano, Y., Davidson, N.E., Poirier, G.G., 1993. Specific proteolytic cleavage of poly(ADP-ribose) polymerase: an early marker of chemotherapy-induced apoptosis. Cancer Res. 53 (1), 3976e3985.
Kerr, J.F., Wyllie, A.H., Currie, A.R., 1972. Apoptosis: a basic biological phenomenon with wide-ranging implications in tissue kinetics. Br. J. Cancer 26 (4), 239.
McCastlain, K., Stack, B.C., Ye, J., Clarke, B.M., Spring, P.M., 2007. Effects of fusaric acid on squamous cell carcinoma. Otolaryngol. Head Neck Surg. 137 (2), 166.
Mosmann, T., 1983. Rapid colorimetric assay for cellular growth and survival: application to proliferation and cytotoxicity assays. J. Immunol. Methods 65, 55e63.
Nedelník, J., 2002. Damage to corn by fungi of the genus Fusarium and the presence of fusariotoxins. Plant Prot. Sci. 38 (2), 46e54.
Perry, D.K., Smyth, M.J., Stennicke, H.R., Salvesen, G.S., Duriez, P., Poirier, G.G., Hannun, Y.A., 1997. Zinc is a potent inhibitor of the apoptotic protease, caspase-3. J. Biol. Chem. 272 (30), 18530e18533.
Ricci, J., Munoz-Pinedo, C., Fitzgerald, P., Bailly-Maitre, B., Perkins, G.A., Yadava, N., Scheffler, I.E., Ellisman, M.H., Green, D.R., 2004. Disruption of mitochondrial function during apoptosis is mediated by caspase cleavage of the p75 subunit of complex I of the electron transport chain. Cell 117, 773e786.
Ruda, J.M., Beus, K.S., Hollenbeak, C.S., Wilson, R.P., Stack Jr., B.C., 2006. The effect of single agent oral fusaric acid (FA) on the growth of subcutaneously xenografted SCC-1 cells in a nude mouse model. Investig. New Drugs 24 (1), 377e381.
Sheik Abdul, N., Nagiah, S., Chuturgoon, A.A., 2016. Fusaric acid induces mito-chondrial stress in human hepatocellular carcinoma (Hepg2) cells. Toxicon 119, 336e344.
Siegel, R.L., Miller, K.D., Jemal, A., 2016. Cancer statistics, 2016. CA A Cancer J. Clin. 66 (1), 7e30.
Sies, H., 1985. Oxidative Stress: introductory remarks. Oxidative Stress 1e8. Singh, N.P., McCoy, M.T., Tice, R.R., Schneider, E.L., 1988. A simple technique for quantitation of low levels of DNA damage in individual cells. Exp. Cell Res. 1751, 184e191.
Stack, B.C., Hansen, J.P., Ruda, J.M., Jaglowski, J., Shvidler, J., Hollenbeak, C.S., 2004. Fusaric acid: a novel agent and mechanism to treat HNSCC. Otolaryngol.Head Neck Surg. 131 (1), 7

t, E., Schwab, C., Sulyok, M., Naehrer, K., Krska, R., Schatzmayr, G., 2013. Multi-mycotoxin screening reveals the occurrence of 139 different secondary me-tabolites in feed and feed ingredients. Toxins 5 (3), 504e523.

i, P.F., Mezes, M., Melnichuk, S.D., Fotina, T.I., 2008. Mycotoxins and animal health: from oxidative stress to gene expression. Krmiva 50 (1), 35e43.

ɛs-Pupulin, A.R., Salgueiro-Pagadigorria, C.L., Bracht, A., Ishii-Iwamoto, E.L., 1998. Effects of fusric acid on rat liver mitochondria. Comp. Biochem. Physiol. Part C Pharmacol. Toxicol. Endocrinol. 120 (1), 43e51.

ıuble, H., Eibl, H., 1974. Electrostatic effects on lipid phase transitions: membrane structure and ionic environment. Proc. Natl. Acad. Sci. 71 (1), 214e219.

ş, K.A., Porter, J.K., Bacon, C.W., Meredith, F.I., Norred, W.P., 1999. Fusaric acid and modifications of the subchronic toxicity to rats of fumonisims in F. moniliforme culture material. Food Chem. Toxicol. 37 (8), 853e861.

Watanabe, W., Sudo, K., Asawa, S., Konno, K., Yokota, T., Shigeta, S., 1995. Use of lactate dehydrogenase to evaluate the anti-viral activity against influenza A virus. J. Virol. Methods 51 (2), 185e191.

Wilson, K., Walker, J. (Eds.), 2010. Principles and Techniques of Biochemistry and Molecular Biology. Cambridge University Press.

Yabuta, T., Kambe, K., Hayashi, T., 1937. Biochemistry of the bakanaefungus. I. Fusarinic acid, a new product of the bakanae fungus. J. Agric. Chem. Soc. Jpn. 10 (1), 1059e1068.

Yang, Y., Ma, H., 2009. Western blotting and ELISA techniques. Research 1, 67e86. Ye, J., Montero, M., Stack Jr., B.C., 2013. Effects of fusaric acid treatment on HEp2 and docetaxel-resistant HEp2 laryngeal squamous cell carcinoma. Chemotherapy 59 (1), 121e128